ADAPTIVE THERMAL COMFORT ANALYSIS OF HISTORIC MOSQUE: THE CASE STUDY OF SALEPÇİOĞLU MOSQUE, İZMİR, TURKEY

A Thesis Submitted to
the Graduate School of Engineering and Science of
İzmir Institute of Technology
in Partial Fulfillment of the Requirements for the Degree of

MASTER OF SCIENCE

in Energy Engineering

by
Khaled .S .M BUGHRARA

October 2016
İZMİR

We approve the thesis of **Khaled .S .M BUGHRARA**

Examining Committee Members:

Dr. Zeynep DURMUŞ ARSAN
Department of Architecture, İzmir Institute of Technology

Prof. Dr. Gülden GÖKÇEN AKKURT
Department of Energy Systems Engineering, İzmir Institute of Technology

Assoc. Prof. Dr. Tahsin BAŞARAN
Department of Architecture, İzmir Institute of Technology

Prof. Dr. Türkan GÖKSAL ÖZBALTA
Department of Civil Engineering, Ege University

Assoc. Prof. Dr. İlker KAHRAMAN
Department of Architecture, Yaşar University

25 October 2016

Dr. Zeynep DURMUŞ ARSAN
Supervisor, Department of Architecture, İzmir Institute of Technology

Prof. Dr. Gülden GÖKÇEN AKKURT
Co-Supervisor, Department of Energy Systems Engineering, İzmir Institute of Technology

Prof. Dr. Gülden GÖKÇEN AKKURT
Head of the Department of Energy Systems Engineering

Prof. Dr. Bilge KARAÇALI
Dean of the Graduate School of Engineering and Sciences

ACKNOWLEDGMENTS

I would like to express my thanks to Inst. Dr. Zeynep DURMUŞ ARSAN for his kind supporting and advices. I would like to thank to Prof. Dr. Gülden GÖKÇEN AKKURT for beneficial contributions and sharing her precious experiences through my study.

I would also like to thank Prof. Dr. Alper BABA for his contributions about determination of the material construction of the building. Additionally, many thanks should be given to Izmir Institute of Technology, Center for Material Research for the precious support for experimental analysis of stone samples.

I would also like to thank The Prime Ministry Directorate General of Foundation, Republic of Turkey for the permission to take measurement in the Mosque and its co-operation. Additionally, many thanks should be given to the ENVAR Architecture and Engineering Inc. for the use of measured drawings in this study.

My gratitude also goes to Aaron BORANIAN for his supports about Energy Plus software, my appreciate also extends to my colleagues, Cem Doğan ŞAHİN, Turgay COŞKUN, Mümine GERÇEK and Gazi ÖZDEMİR for their supports and advices throughout this study.

Finally, I am deeply grateful to my parents, for their endless patience, encouragement and continuous support throughout my education. Without their presence, it would be more challenging to accomplish this study.

ABSTRACT

ADAPTIVE THERMAL COMFORT ANALYSIS OF HISTORIC MOSQUES: THE CASE STUDY OF SALEPÇİOĞLU MOSQUE, İZMİR, TURKEY

Mosques differ from other types of buildings by having intermittent operation schedule. Due to five prayer times per day throughout the year, mosques are fully or partially, yet periodically, occupied. Historic mosques, possessing cultural heritage value, need to be evaluated in terms of thermal comfort. The adaptive thermal comfort method presented by ASHRAE 55 is recommended to be used to analyze thermal comfort conditions of unconditioned buildings.

The aim of research is to analyze thermal comfort conditions of historic mosques throughout the year, and to conduct an adaptive comfort analysis. The selected Salepçioğlu Mosque was built in 1905 in Kemeraltı, İzmir, Turkey. The objective is to improve indoor thermal comfort levels by applicable interventions with specific attention to its heritage value. First, indoor and outdoor microclimate of Salepçioğlu Mosque was monitored from October 2014 to September 2015. The physical model of mosque was created via dynamic simulation modelling tool, DesignBuilder v4.2. The model was calibrated by comparing simulated and measured indoor air temperature within hourly error ranges defined by ASHRAE Guideline 14. Whole-year thermal comfort analysis was conducted on monthly basis by using adaptive thermal comfort model.

The adaptive comfort analysis of monitoring campaign shows that the Mosque does not satisfy acceptable comfort levels. Different scenarios were applied to better comfort levels. The best improvement is obtained with underfloor heating by which discomfort hours drop into 1369 hours by 31.34%, while it was 3760 hours by 86.08% in the baseline model.

ÖZET

TARİHİ CAMİLERİN UYARLANIR ISIL KONFOR ANALİZİ: SALEPÇİOĞLU CAMİSİ ALAN ÇALIŞMASI, İZMİR, TÜRKİYE

Camiler, aralıklı kullanım şekilleriyle diğer bina tiplerinden farklılaşır. Bütün bir yıl boyunca ve her gün kılınan beş vakit namaz dolayısıyla camiler tümüyle veya kısmi olsa da periyodik olarak kullanılır. Kültürel miras değerine sahip tarihi camiler, sağladıkları termal konfor ortamı ile incelenmelidir. ASHRAE 55'ce ortaya konan uyarlanabilir termal konfor metodu, iklimlendirilmeyen yapıların termal konfor şartlarının analizi için önerilmektedir.

Bu araştırmanın amacı, tarihi camilerin yıl boyu ısıl konfor koşullarını analiz etmek ve uyarlanabilir ısıl konfor analizi gerçekleştirmektir. Seçilen Salepçioğlu Cami, İzmir'in Kemeraltı semtinde 1905'te inşa edilmiş bir camidir. Hedef, iç ortam ısıl konfor düzeyini yapının miras değerine de özen göstererek uygulanabilir müdehalelerle iyileştirmektir. İlk olarak, Salepçioğlu Cami'nin iç ve dış ortam yerel iklim şartları Ekim 2014'den Eylul 2015'e kadar izlenmiştir. Ardından, DesignBuilder v4.2 dinamik benzetim modelleme aracı kullanılarak caminin dijital modeli yaratılmıştır. Model, ASHRAE 14 Rehberi'nde tanımlanan saatlik hata payı aralığında kalacak şekilde, ölçüm ve simulasyon sonucu iç ortam sıcaklık verileri kıyaslanarak kalibre edilmiştir. Yapının yıllık ısıl konfort analizi, ASHRAE 55'de sunulan uyarlanabilir ısıl konfor modeli kullanılarak aylık bazda gerçekleştirilmiştir.

Yerinde izleme çalışmasına dayanarak gerçektirilen analizler, yapının yeterli konfor şartlarını sağlamadığını ortaya koymuştur. Konfor düzeyini iyileştirmek için farklı senaryolar uygulanmıştır. En başarılı iyileştirme, temel modelde %86,08'lik oran ile 3760 saat olan konforsuz saati, %31,34'lük oran ve 1369 saate düşüren yerden ısıtmadan sağlanmıştır.

TABLE OF CONTENTS

APPENDICES

LIST OF FIGURES

LIST OF TABLES

LIST OF SYMBOLS

U value	Overall heat transfer coefficient (W/m².K)
HVAC	Heating, ventilation and air-conditioning
MBE	Mean bias error
RMSE	Root-mean-squared error
Temp	Temperature (ºC)
RH	Relative Humidity (%)
Min	Minimum
Max	Maximum
DB	DesignBuilder
ASHRAE	American Society of Heating, Refrigerating, and Air-Conditioning Engineers
2D	Two Dimensional
3D	Three Dimensional
T_{ma}	The average measured temperatures for N observations (ºC)
N	The number of observations
T_m	The measured hourly temperatures (ºC)
T_s	The simulated hourly temperatures (ºC)
T_{out}	The mean monthly outdoor air temperature in (ºC) or (ºF)
PMV	The Predicted Mean Vote
PPD	The Predicted Percentage of Dissatisfied

CHAPTER 1

INTRODUCTION

1.1. Problem Statement

Many studies have been conducted on thermal comfort analysis of buildings, due to the fact that people spend more than 90% of their lifetimes in controlled environments where the mechanical heating, cooling or ventilation systems are used (Sateri, 2004). Yet, few of them deals with the indoor comfort conditions of the historic buildings.

The required level of thermal comfort is needed for living in a building. Human can live and survive in very hot to cold conditions, that no absolute standard can be determined for thermal comfort (Darby and White, 2005). Thermal comfort is influenced by two factors: environmental and personal factors. The environmental factors are the air temperature, air velocity, mean radiant temperature and relative humidity, while the personal factors are the metabolic rate and clothing (Fanger, 1970). Several of models have been used and developed in order to understand and determine the thermal conditions to reach the thermal comfort level. The most recognized method of thermal comfort is the one presented by Fanger in 1970 which is based on the collection of the experimental data and the heat balance principles under the steady state condition in a controlled climate chamber. In a case of naturally ventilated buildings, the use of Fanger's model is no longer applicable. Thus another method, i.e. adaptive thermal comfort model, was introduced by De Dear's team in 1998 that can be used in a naturally ventilated buildings. The adaptive thermal comfort model is based on the hundreds of the field studies where the occupants were able to control their environment by means of clothing, sun shades, fans, operable windows and personal heaters (De Dear et al., 1998).

Typically, some inherent characteristics of historic buildings give them the ability to provide satisfactory thermal comfort levels for their occupants since their first construction. The physical parameters influencing the hygrothermal performance of historic buildings are the material, thermal mass, moisture buffering, landscape, overall form, and exterior wall openings. Even the part or building itself may constitute the system for natural ventilation and attaining thermal comfort. Besides, the indoor climate of historic buildings is controlled by occupants' behaviour such as opening and closing the windows. Hence, the building materials, orientation, space organisation and openings were properly selected to well attenuate themselves into external climatic conditions together with the users' habits for the optimum human effort.

Mosques are the religious buildings functioning as the place of worship for Muslims. By having an intermittent occupancy schedule, they differ from other type of public buildings. The worshippers require feeling calm and comfortable to perform their prayers in tranquility and reverence. Hence, thermal requirements of a mosque should be carefully examined.

Historic mosques are naturally ventilated, heated and cooled. However, limited researches have been conducted on historic mosques about their thermal comfort conditions and possible interventions for improvement of their comfort level. Since most comfort studies are likely conducted in other types of buildings such as dwellings, offices, and classrooms, there is a need to conduct more studies in mosques, especially in historic mosques. Any interventions for the improvement of thermal comfort in the historic building should be done without compromising the cultural heritage value of the building. In line with this, the thermal comfort study of historic mosques that naturally ventilated has been carried out.

1.2. Aim and Objectives of The Study

The aim of this research is to understand the indoor environment of historic mosques, and evaluate their thermal comfort requirements. Therefore, the specific objective is to analyse and enhance the thermal comfort of the historic mosque, i.e. Salepçioğlu Mosque in İzmir, Turkey, by using the adaptive thermal comfort model presented in ASHRAE Standard 55.

The thesis scrutinises the following questions:

- What is the thermal comfort requirement in the historic mosques?
- What types of construction materials are used in the historic mosque buildings? How can that information help to understand the hygrothermal performance internally?

- What is the effect of natural ventilation for enhancing the thermal indoor conditions?
- What kind of intervention scenarios that can be developed for historic mosques to improve thermal comfort without deteriorating cultural heritage value?
- What is the effect of using underfloor heating system on thermal comfort in the historic mosque?
- How much the use of passive strategies can improve the thermal comfort of mosque?

1.3. Limitations and Assumptions

The research is carried out with some limitations and assumptions in various stages. The limitations are stated as follows:

Decision for intervention scenarios: The number of scenarios for improving the thermal comfort is limited. The first reason is the very nature of historic buildings. They possess architectural heritage and aesthetic values, associate with historic people and events. In addition, these buildings are belong to the part of social history, and have connections with local building settings and other assets (Heritage, 2011).

Secondly, the case building, Salepçioğlu Mosque, is the registered building by The Turkish Ministry of Culture and Tourism, where any physical intervention and the restoration project should be proved by the İzmir No.1 Regional Council for the Conservation of Cultural and Natural Property. The use and control of first floor of building, including the main and women's prayer areas, are within the legal authority of The Prime Ministry, Directorate General of Foundations, Izmir Branch, with which variety of intervention scenarios were first introduced and discussed. The scenarios presented in this thesis are only a few of them, proved and permitted by The Prime Ministry Directorate General of Foundations, Izmir Branch, whose valuable recommendations and experience are based on the previous restoration projects conducted in the historic mosques under its authority. As a result, replacement of single glazed window glass with double clear glass, replacement of single glazed window glass with double low emissivity glasses, addition of natural insulation layer into the dome, and operation of natural ventilation by opening windows at night are the possible basic interventions determined for the thesis. Even if unapproved by the The Prime Ministry Directorate General of Foundations, Izmir Branch, the effect of using heating system for cold months were also examined to see and control the indoor environment into required comfort level. Underfloor heating system, therefore, were used for scientific purpose.

Definition of thermal characteristics of building materials: the materials used in the construction of modern buildings are known and documented. In contrast, the ones of historic buildings are little known, or inaccessible. In this study, the layer, composition and type of materials used in the walls, floors and roof of Salepçioğlu Mosque are indefinite. Yet, in order to attain the most accurate digital model, imitating the heat transfer through the envelope of mosque, the determination of thermal quality, i.e. thermal conductivity, is required. The literature survey indicated that the insitu test experiments can be conducted by using thermohygrometer devices. Hence, TESTO 635-2 temperature and moisture meter is chosen to measure the thermal conductivity values of the walls (Testo SE and Co. KGaA, 2015). The experiment has to be done in the condition when 15ºC temperature difference between inside and outside occurs. The comparison between measured inner and outer temperatures for one year indicates that 15ºC difference never occurs. Therefore, the site experiments couldn't be held. Another method to determine the overall heat transfer coefficient were investigated. Finally, the use of X-ray fluorescence (XRF) and X-ray powder diffraction (XRD) analyses were chosen in order to define the characteristics of main construction material, i.e. stone, on the walls of the mosque. The samples needed for the experiments were collected from different walls due to the differences in the material composition of the building (see Chapter 3).

Missing data: throughout the monitoring process, the measured temperature and relative humidity data were missing because of irretrievable technical problems occurred in data loggers (HOBO) such as the logger damage due to rain penetration, and power loss due to insufficient battery. Consequently, the missed measurement periods per each zone can be summarized as follows:

- Main prayer area: from 21st of March to 8th of May, 2015,
- Sub-main prayer: from 21th of June to 26 of August, 2015,
- Women prayer: from 6th to 20th of March 2015, 29th of June to 6th of July 2015, and 6th to 28th of August, 2015,
- Corridor first floor: from 17th to 26th of August, 2015,

- Corridor basement: from 30th of June to 10th of July, 2015,
- Outdoor HOBO: March 2015 and July 2015.

Several assumptions are also as follows:

Some of the walls of Salepçioğlu Mosque have non-uniform shapes, which require to do some assumptions for digital modelling. To simply the geometry, the boundary of external and internal surface of the walls were determined by drawing the straight line, constituting a tangent line to the wall surface in many points.

To overcome the absent measured data for outdoor weather, the measurements of local meteorological station by Adnan Menderes Airport were used to fill the gaps in March 2015 and July 2015.

The airtightness value, calculated via Blower Door Machine tests held in the main prayer area, is accepted as valid for all zones such as sub-main prayer area, corridor of downstairs, corridor of the first floor and women's prayer area.

For both thermal comfort analysis and modelling phase of the building, the mosque is assumed to be only occupied during the prayer times, while the rest in between is set as empty. For the Friday prayer, the mosque is modelled as fully occupied with capacity of 225, 225, 78, 70, 70 people for the main prayer area, sub-main prayer area, women prayer area, corridor of the first floor and corridor of basement, respectively (see chapter 3).

1.4. Content of The Study

The thesis is composed of six chapters. The first chapter introduces the problem, aims, objectives, assumptions and limitations of the study. The literature survey is presented in the second chapter to express a brief summary of previous studies about thermal performance and comfort analyses of recent buildings, mosques and historic ones, and adaptive thermal comfort and its application. The historic building, selected as the case study of this thesis, is presented in the third chapter. The materials of the building envelope, types of windows, doors and the site location in addition to some information about the building use and activities are introduced. In the next chapter, the methodology is described step by step. Firstly, the dynamic simulation modelling software 'DesignBuilder' and the calibration procedure are explained. The adaptive thermal comfort model defined by The ANSI/ASHRAE Standard 55, 2010 is then introduced.

The last part of the fourth chapter includes the retrofit scenarios for the betterment of thermal comfort conditions. The fifth chapter presents the results of monitoring campaign, simulations and calibration procedure. The statistical and graphical results of adaptive thermal comfort analysis for the indoor environment of main worship area was explained monthly and yearly. In addition, the results of retrofit scenarios are scrutinised. In the last chapter, the derived conclusions from this research and recommendations for the further study are discussed.

CHAPTER 2

LITERATURE REVIEW

In this chapter, the survey of literature related to the research area is presented. The first section includes the definition of thermal comfort and its theory with selected researches. Adaptive thermal comfort, then, is introduced and explained. This chapter concludes with the evaluation of selected case studies on thermal comfort in historic buildings.

2.1. Thermal Comfort

Thermal comfort is defined as the condition of mind that expresses satisfaction with thermal environment. When determining thermal comfort, two variables are necessary to be addressed: environmental variables such as air velocity, air temperature, radiant temperature, and relative humidity, and subjective variables such as activity level and clothing insulation (Fanger, 1970; Heating, Refrigerating A.S, 2004).

Many researches have been done on how people thermally, physiologically and psychologically response towards their environment. Several models were developed in order to statistically predict their sensations. The mathematical model, presented by Fanger in 1967, was the first model used to predict comfort level of people. According to Fanger model, people are thermally assumed at the steady state within their environment.

PMV (Predictive Mean Vote) and PPD (Predicted Percentage of Dissatisfied) index of thermal comfort developed by Fanger have become the most popular index in the thermal comfort study area. PMV is defined as "an index that predicts the mean value of the votes of a large group of person on the seven-point thermal sensation scale", while PPD is defined as "an index that establishes a quantitative prediction of the percentage of thermally dissatisfied people determined from PMV (ASHRAE, 2010: 3). The ideal range of PMV for the thermal environment is between -0.5 to 0.5 with 10% of PPD for occupants' dissatisfaction, while the acceptable range is from -0.85 to 0.85 PMV with 20% of PPD.

The consideration of thermal comfort are essential for user satisfaction in buildings where the occupancy is involved (Ibrahim et al., 2014). Saeed (1993, 1996) conducted two surveys on thermal comfort requirements in hot dry regions of Riyadh, Saudi Arabia, based on Fanger's comfort model. The first study was done for university students, while the second one was in the mosque for Friday prayer to decide thermal comfort needs. By measuring the main environmental variables, e.g. air temperature, radiant temperature, air speed and relative humidity, Fanger's seven-point voting system was used to rate thermal comfort sensations.

The study for university showed that students prefer a temperature range between 24°C to 26ºC with relative humidity value from 40% to 50%, air speed around 0.5 m/s and clo value from 0.5 to 0.7 in summer season. In winter season, they prefer a temperature range from 23ºC to 25º° with relative humidity from 40% to 50%, air speed less than 0.5 m/s, and clo value between 0.7 to 0.9. The findings of resulting survey were compared with the Fanger's comfort equations, and show the reasonable agreement (Saeed, 1993).

Saeed's other study in 1996 was for the Friday prayers to evaluate the thermal comfort on mosque (Saeed, 1996). The study was conducted through the hot season due to that the highest outdoor temperature and lowest relative humidity values occur. He found that 60% of the worshipers prefer the clo value of 0.5, from 13% to 21% of the worshipers voted for the hot range (6-7), while 3 to 7% voted for the cold range (1-2). The result obtained from survey was compared with Fanger's equation, and shows fairly good agreement.

Thermal comfort has the important factor not only for the user satisfaction, but also to determine energy consumption in buildings and ensuring its sustainability (Nicol et al., 2012).

2.2. Adaptive Thermal Comfort

Adaptive thermal comfort model is defined as the theory suggesting that human can adapt their immediate environment (and even to prefer) to a wider range of thermal condition by the connection to the outdoors. The concept of adaptive thermal comfort has emerged when ventilating buildings naturally became more concerned because of the rising interest around energy efficiency and indoor air quality (Moossavi, 2014).

The adaptive comfort standard is generated from the analysis of 21,000 datasets that conducted in 160 buildings, not only from naturally ventilated buildings but also from the conditioned ones, located on four continents in different climatic zones. The adaptive model is the alternative theory of thermal perception (Brager and De Dear, 2001).

The adaptive model explains the relationship between indoor design temperature and outdoor meteorological or environmental parameters. It emphasizes that thermal comfort can be achieved by human adaptation. The relation between the environments and people can be evaluated by the adaptive method, considering the adjustment on the thermal environment and cloth that made by people to ensure comfort. People can maintain their comfort by adjusting the body's heat balance (De Dear et al., 1998).

The adaptive method is developed over many years of thermal comfort studies by Richard de Dear, Andris Auliciems and Gail Brager (Humphreys et al., 2007). It can be applied to different areas such as building design and construction, thermal controls provision and use climatology, history and sociology of clothing and human thermal physiology. A theoretically coherent option that provided by adaptive comfort model opens up many cost-effective, low-energy design alternatives (De Dear, 2007).

The adaptive model proposes that indoor comfort temperature can be estimated from the outdoor air temperature (Nicol and Humphreys, 2002), (De Dear and Brager, 2001). By plotting them tighter with the monthly or daily outdoor maximum, minimum and mean air temperatures, this can help designing comfortable buildings. It enables to analyse the possibility of using passive cooling and/or heating design systems in the examined climate (Nicol and Humphreys, 2002).

Occupants should have the ability to adjust the indoor thermal condition of building to suit themselves. Effective, appropriate, usable controls can decrease the discomfort. Few ways can be used by people to adapt their environment (Nicol and Humphreys, 2002). In 2013, Toe and Kubota (2013) developed an equation for adaptive thermal comfort in naturally ventilated buildings in hot humid climates by using ASHRAE RP 884 database that covered different climatic zones. They found that based on the daily mean outdoor air temperature for hot humid climate, the adaptive equation has the highest coefficient of determination. In hot humid climate, the acclimatisation of previous day is not essential for the prediction of thermal responses of occupants. Natural ventilation is an accepted technique used in hot humid climate to cope with the increase in energy demand for air-conditioned buildings.

Adaptive thermal comfort standard can be used as a powerful tool to provide full picture of occupants' thermal comfort conditions. It has an advantage over the conventional thermal comfort standard: a wider range of thermal comfort can be achieved by providing occupants in the building with the ability of control and use of the building by operable windows, adjusting clothes and control indoor thermal comfort (Corgnati et al., 2007) (De Dear et al., 1998). The studies conducted by De Dear (1998) and Nicol and Humphreys (2002) assert the unrealability of typical thermal comfort method, i.e. Fanger method, in case of the natural ventilated buildings.

As a summary, the adaptive thermal comfort method is perceived as the guide to examine thermal performance of naturally ventilated buildings. It is based on the assumption that the person has the ability to adjust his/her environment according to the relation between the outside and inside conditions. The comfort indicators of PMV and PPD do not applicable to naturally ventilated buildings, because it only regards for thermal adaptation processes to indoor climate (De Dear et al., 1998).

2.3. Review on Selected Studies about Thermal Comfort of Historic Buildings and Mosques

The selective literature survey was conducted for the studies about thermal comfort, which have been documented since the 1970s. The main purpose of this section is to highlight the associated studies in literature and make them the source of inspiration for the framework of the thesis. The literature survey was conducted under two main group of buildings categories: historic buildings with natural ventilation and mosques with intermittent occupancy. It included various information sources such as three books and one thesis, as well as 19 articles related to the research area. Table 2.2. Indicates the general view of the literature survey. indicates the several characteristics of selected literature.

The state of topic on thermal comfort in the recent literature reveals that there are plenty of studies mainly scrutinizing assessment of naturally ventilated buildings. The adaptive thermal comfort method is one of the focused topics related to thermal comfort assessment of historic buildings.

Historic buildings may be different from the ones constructed in modern times by having complexity in geometry such as vaulted ceilings, rounded towers, sloping floors, or walls with different thicknesses. Moreover, historic buildings may experience lack of insulation and sufficient moisture barrier. They usually show different strategy of ventilation depending on natural one (Widström, 2012).

The selection of retrofitting strategies and investigation for the materials used in historic buildings are more complicated to perform due to their cultural value that is initial to be preserved. They should be done without compromising the heritage value.

Building type, orientation, position and dimension of openings are the factors affecting on the indoor thermal comfort in historic buildings. Yet, changing facade configuration or replacement of building materials do not the considerable option for historic buildings. In this case, the only factor related to building façade in historic areas is the wind speed (Chu et al., 2015).

The limited information on their construction techniques caused the thermal performance of historic buildings hard to analyze, and predict. Gagliano et al. (2014) studied the thermal performance of massive historic buildings located in Catania, Italy. They found that the prevention from overheating, ensuring a good level of comfort, and minimising demands of cooling systems in summer can be achieved by high thermal mass corroborated with natural ventilation.

The recent studies mostly concern on permanently or periodically occupied/operated buildings such as houses, schools and offices. Few studies were noted on intermittently occupied/operated buildings such as mosques and churches. Ibrahim et al. (2014) examine thermal comfort conditions in the mosque located at Kota Samarahan, Malaysia. They found that the thermal comfort is not achieved. The simulation study is conducted by using Energy Plus dynamic simulations software. The new materials applied into digital model enhance the thermal comfort.

In 2009, Al-Homoud et al. published the study on evaluation of thermal comfort and energy use in several mosques as intermittently occupied buildings in hot humid climate. They conclude that in most of the studied mosques, specifically the one without insulated, the thermal comfort is not accomplished. The addition of thermal insulation material to the mosques leads to improve in thermal comfort to the acceptable level. Beside to insulation material, the air conditioning system with intermittent operation can improve the level of thermal comfort with use of less energy

Table 2.1. Main characteristics of the recent studies identified by the selected literature

PUBLICATION DATE	AUTHORS	TYPE	COUNTRY	BUILDING TYPE	HISTORIC BUILDING	NATURAL VENTILATED BUILDING	THERMAL COMFORT ANALYSIS	ADAPTIVE MODEL	FANGER MODEL	HOT-HUMID CLIMATES	INTERMITTENTLY OPERATED BUILDINGS
1970	Fanger, Poul O	Book	_				✓		✓		
1993	Saeed, S.	Article	Saudi Arabia	Mosque			✓		✓		✓
1997	De Dear, and Brager	Technical Report	Australia					✓			
1998	De Dear and Brager	Article	Australia					✓			
1998	Saeed, S.	Article	Saudi Arabia	School			✓		✓		
2001	De Dear and Brager	Article	The USA			✓	✓	✓			
2001	Noh pat et al.,	Article	_				✓				
2002	Nicol and Humphreys	Article	The UK				✓	✓			
2002	Nicol and Humphreys	Article	The UK					✓			
2004	Sateri, J	Book	_				✓				
2005	Darby, S and White, R	Article	The UK				✓				
2007	De Dear	Article	Australia	University/ Business			✓	✓			
2007	Humphreys et al.	Article	Australia				✓	✓			
2007	Corgnati, et al	Article	Italy	School/ University			✓		✓		
2009	Al Homoud. et al.	Article	Saudi Arabia	Mosque		✓	✓			✓	✓
2012	Humphreys et al.	Book	_				✓	✓			
2012	Widström	Thesis	The UK	Church	✓						
2013	Toe and Kubota	Article	Malaysia			✓		✓		✓	
2014	Ibrahim, S. et al.	Article	Malaysia	Mosque			✓		✓	✓	✓
2014	Moossavi and Seyed Morteza	Article	India	Residences and Offices				✓			
2014	Gagliano A, et al	Article	Italy		✓		✓				
2015	Chu et al.	Article	Taiwan	Historical Areas	✓	✓	✓		✓		

CHAPTER 3

DESCRIPTION OF THE BUILDING

The city of İzmir consists of several metropolitan districts such as Balçova, Bayraklı, Bornova, Buca, Çiğli, Gaziemir, Güzelbahçe, Karabağlar, Karşıyaka, and Konak. Konak, Izmir, the area rich in historic buildings and cultural heritage, it is important that to be committed to preserving for its heritage value. By seeing historic buildings it is shows us the city culture and complexity. Tourist attractors which means an important economic factor, tourists can provide residents with jobs and extra income. One of the most important types of historic buildings in Izmir is mosques. In this part variety of mosques located in Izmir, Konak are presented in comprising to the case study of this research.

Many historic mosques are located in Konak square, Izmir. Figure 3.1 shows some of the mosques located in the same area with Salepçioğlu Mosque. Here some of the most important mosques are presented due to their architectural character and historic context.

Figure 3.1. Konak Square Mosques (Source: Google Maps)

Kestane Pazarı Mosque

The mosque was built by Ahmet Aga in 1663. The mosque consist of two floors where the ground floor used for shops and stories and the first floor were the main prayer area of the mosque is located. Hewn and un-hewn were used together for building the mosque. The main prayer area has a square shape. The mosque has three domes that fitted with glass panes recently (Figure 3.2).

Figure 3.2. Kestane Pazarı Mosque (Source: Izmir Kent Rehberi 2015)

Konak (Yalı) Mosque

The mosque was built by Mehmet Pasa's doughter Ayse in 1754. The mosque is one floor with one main prayer area with an octagon shape covered with one dome. It has been damaged by the earthquakes and restored in 1920 and 1964. It is built in ottoman architecture style. Stone and brick were used to build the mosque, inside the mosque it is decorated with tiles and outside it is covered with ceramic tiles (Figure 3.3).

Figure 3.3. Konak (Yalı) Mosque (Source: Izmir Kent Rehberi 2015)

Kemeraltı Mosque (Center)

Kemeraltı Mosque, it is a one floor mosque with square main prayer area covered with a central dome. The mosque was built in 1671 by Yusuf Çamazade Ahmet Ağa. (Figure 3.4)

Figure 3.4. Kemeraltı Mosque (Source: Izmir Kent Rehberi 2015)

Hisar Mosque

The mosque was built during 1597- 1598 by Aydınoğlu, Özdemiroğlu. It is the biggest and the oldest mosque in Kamaralti according to its essence and construction techniques. The inscription in the garden gate that details the mosque was restored in

1881 after it has been demolished by the earthquakes 1881. The mosque is one floor with one square main prayer area covered with one dome supported with eight columns. The mosque was built of hew and unhewn stone. The minaret was damaged in 1927 and repaired in the same year (Figure 3.5).

Figure 3.5. Hisar Mosque (Source: Izmir Kent Rehberi 2015)

Table 3.1 illustrate the mosques with its area, year of construction and the commissioner.

Table 3.1 Konak Mosques area and year of established.

Name	Area in (m²)	Commissioner	Years
Hisar Mosque	500	Aydınoğlu Yakup Bey	1598
Kestanepazarı Mosque	400	Ahmet Ağa	1668
Kemeraltı Mosque		Yusuf Çamazade Ahmet Ağa	1671
Yalı (konak) Mosque	100	Ayşe Hanım	1755
Salepçioğlu Mosque	300	Salepçizade Hacı Ahmet Efendi	1905

3.1. Description of the Case Study

Salepçioğlu Mosque is a historic mosque located on the Aegean Sea coast at Izmir Konak square with coordinate (38°N, 27°E) and see level of 12.7 m. The Figure 3.6 (a) shows İzmir map and (b) illustrates the approximate position of Salepçioğlu Mosque.

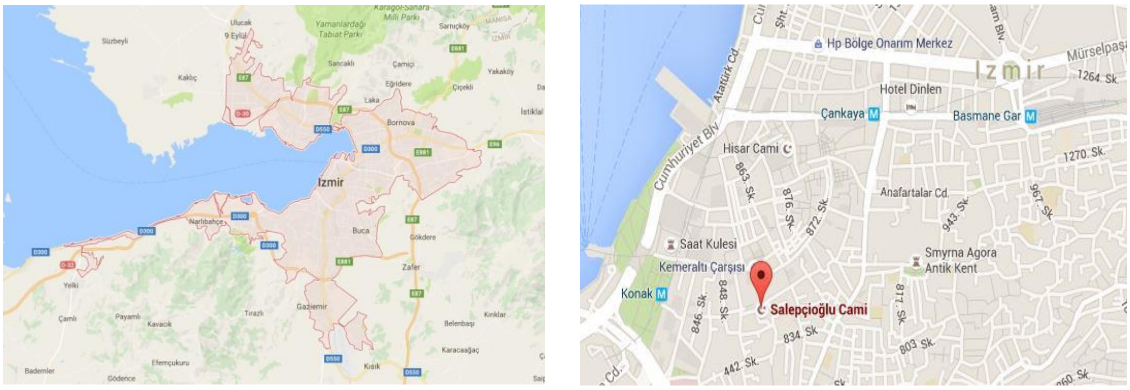

(a) (b)

Figure 3.6. (a) İzmir map. (b) Salepçioğlu Mosque
(Source: Google Maps)

The mosque was built by Haci Ahmet Efendi in 1906 in the area of 300 m². The outside walls are decorated with marble and green stone. Figure 3.7 illustrate the front view of the mosque. The minaret is built separately from the structure of the mosque, and located in the northeast of the building. In 1927 and 1974 the minaret was under the restoration process by *İzmir Ticaret Odası* . The main prayer area covered with a big dome that decorated with engraving. The *Mihrab* is a niche with white and grey round marble. The pulpit is a marble, adorned with geometric pattern above. In Figure 3.8 (a) illustrate the main prayer area with its unique and important carvings on the walls and domes while that of (b) shows pulpit and Mihrab are shown as well.

Figure 3.7. Front View of Salepçioğlu Mosque.

Figure 3.8. (a) Dome engraving, (b) pulpit and Mihrab

The mosque is two stories building, the basement is divided to two sections separated by corridor. The first section has four class rooms with sub-main prayer area used for preforming the pray by the students. On Friday the sub-main prayer area is used by worshipers to perform Friday pray. In the second section which the imam room and other classroom are located. Figure 3.9, shows the plan of the basement with its zones.

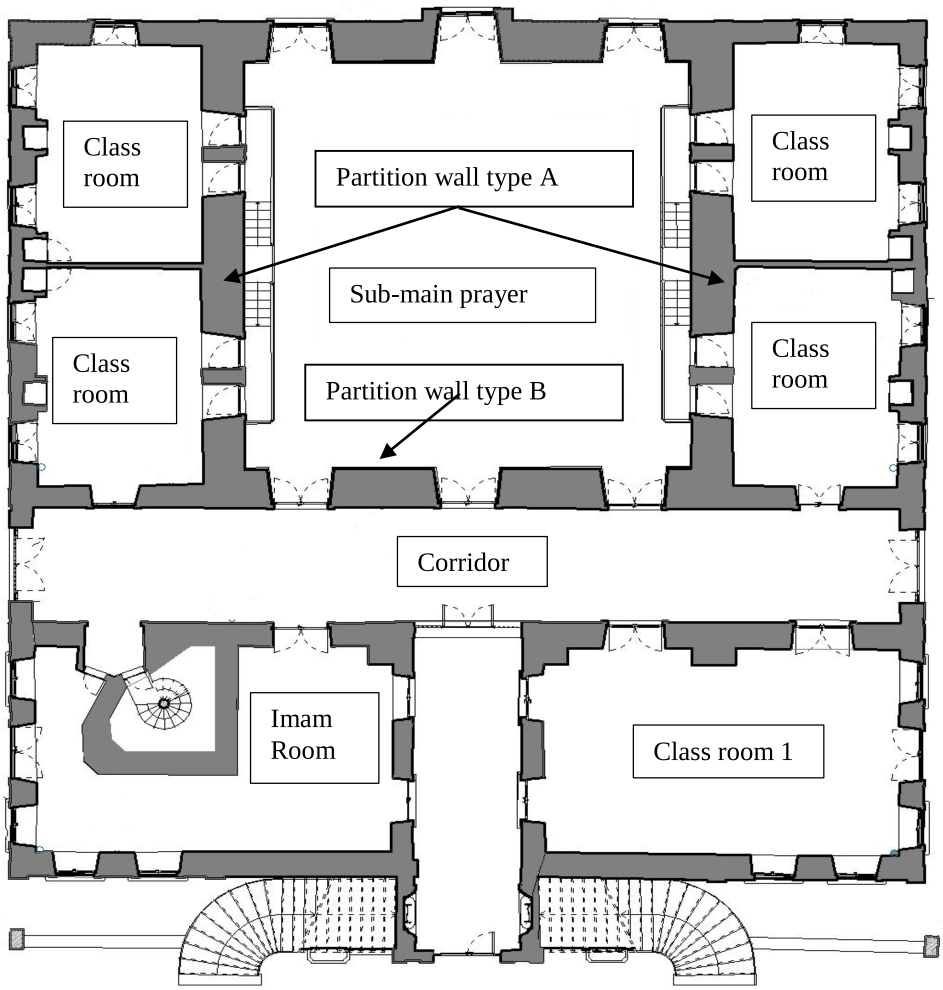

Figure 3.9. Basement floor plan
(Modified from the drawings provided by Dept. of Architectural - IZTECH)

The main worship is located on the first floor with square shape plan and covered with big dome, before the main prayer worship area there is a small area “corridor first floor” which used as a sub-main prayer when the mosque fully occupied. Beside the main prayer worship area and the sup main prayer area there is another area which used by women most of the time to perform their prayer, except on Friday prayer time which used by men, Figure 3.10 shows the first floor area plan with its zones. This area is located up the sub-main prayer area, and it is covered with three small domes.

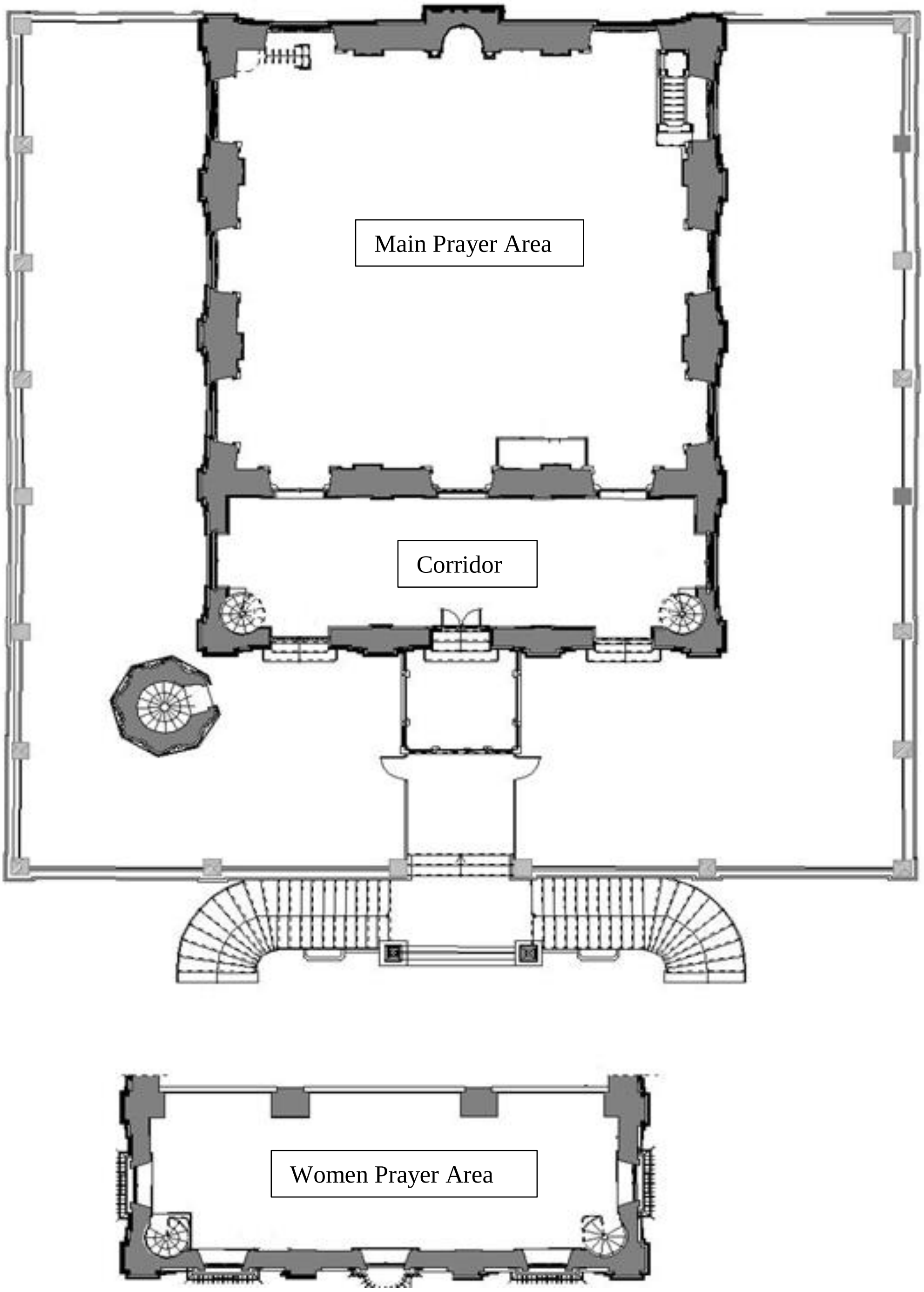

Figure 3.10. First floor plan
(Modified from the drawings provided by Dept. of Architectural – IZTECH)

3.2. Structure of the Building

The structure of the building should be specified well for the better result that well obtain from the software. On the other hand, in thermal comfort analysis the material construction of the building one of the important parameters that influence the indoor environment. The present situation of the mosque materials construction For example walls, roof, floors, doors and windows well be presented in this chapter.

Generally, structure of buildings have composite system which consist of wood construction technique, concrete and stone/brick masonry. In this study, construction material of the mosque were defined by filed investigation and experimental tests.

For the sake of overall heat transfer coefficient determination two experimental test were done. X-ray fluorescence (XRF) and X-ray powder diffraction (XRD) were carried out in order to define the material construction of the mosque. Samples were collected from different walls due to the differences in the material composition of the building, Figure 3.11 illustrates samples that used in these experiments. Figure 3.12 shows the samples location on the building, the once that not shown in the Figure were collected from the garden. X-ray fluorescence is an analytical technique used to define the materials composition of an elemental. X-ray powder diffraction is an analytical technique generally used to identify phase of a crystalline material and provide information about cell dimensions. Five samples were collected from Salepçioglu Mosque that present walls, roofs and floor materials. According to the analysis result the building material, construction was specified, by interpretation of the chemical component of each element. Once the chemical components were identified, the building material then determined. U value of the materials chosen from the DB software library due to the material's name or generated by the user. These two experimental analyses were chosen after the use of Testo device measured failed, due to the usage condition of the device where the temperature difference between inside and outside does not fulfil the requirement of the device.

(a)

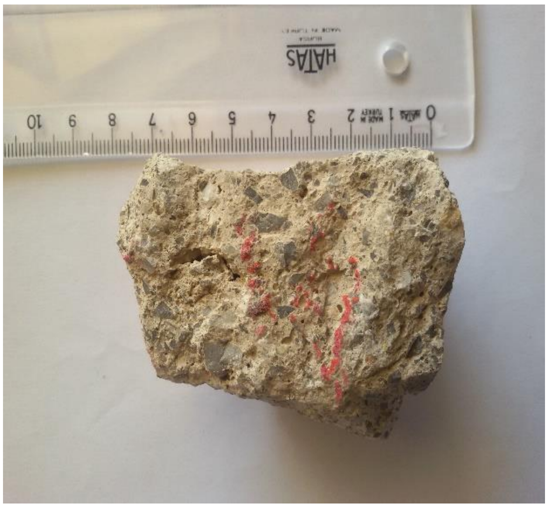

(b)

(c)

(d)

(e)

Figure 3.11. (a) Stone sample 1 (b) Stone sample 2 (c) Stone sample 3 (d) Stone sample 4 (e) Stone sample 5

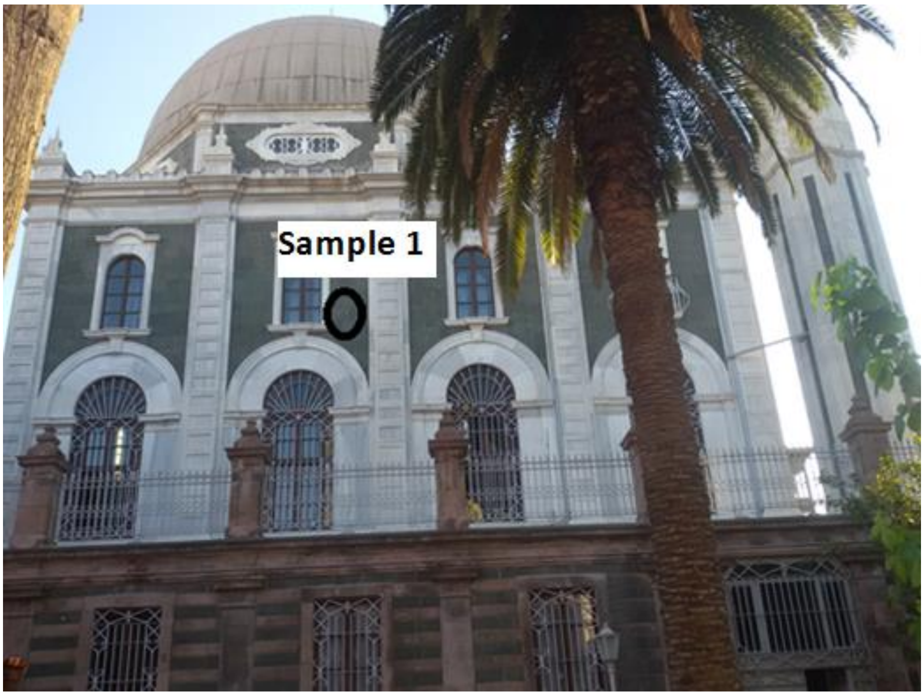

(a)

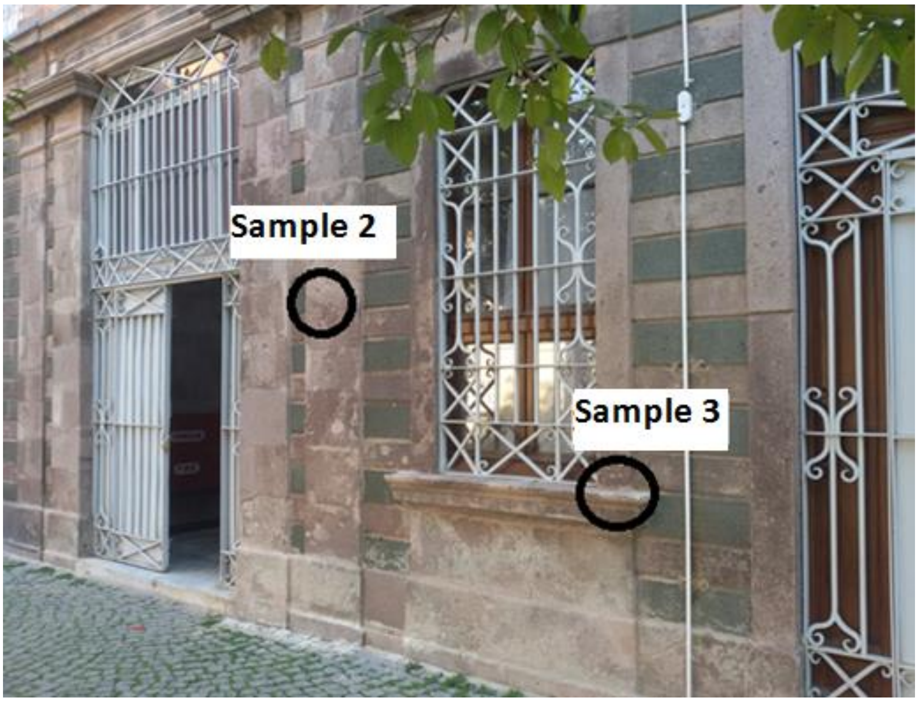

(b)

Figure 3.12. (a) position of samples 1, (b) position of sample 2 and sample 3

3.2.1. Walls, Roofs, Floors

Walls are the main construction of any buildings that used to separate zones. Walls can be external and internal according to their location.
Salepçioğlu Mosque has different types of walls materials and constructions with nonhomogeneous distribution. Wall, roof and floor in each zone has different material and thickness which generate different overall heat transfer coefficient. In this study the building divided to two levels first floor level and basement level and each level divided to zones in the first floor level the zones are main prayer area, women prayer area and corridor 1 and the basement zones are sup-main pray area and corridor. In the Tables below the walls presented according to their zones.

3.2.1.1. First Floor Zones

The first floor are contained three zones as explained before, in this section the material construction of each zone will be described.

3.2.1.1.1. Main Prayer Area

Main prayer area has four types of walls according to their material component, thickness and the overall heat transfer coefficient. The walls presented due to their location in the main prayer area as an external walls, internal walls. Beside the material construction of the roof and floor of the main prayer area is described from the outside to the inside.

3.2.1.1.1.1. External Walls from Outside to Inside

The physical properties of the external walls in the main prayer area and the cross section Figures are stated in the Table 3.2.The walls construction consist of two layer, Lime plaster as an inside layer and Granite as an outside layer, with overall heat transfer coefficient 2.144 W/m².K.

Table 3.2. Physical characteristics of main prayer area external walls.

Material Component	Thick (cm)	U Value (W/m².K)	Cross-Section
Granite	76	2.144	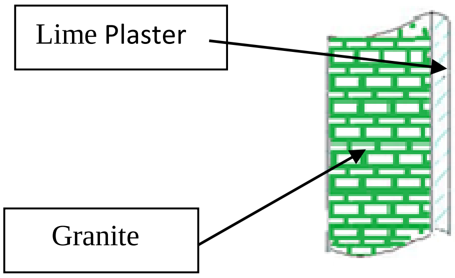
Lime Plaster	2		

3.2.1.1.2. Internal Partition Wall from Outside to Inside

Internal partition wall in the first floor is the wall separate between the main prayer area and the corridor first floor. The inner surface of the wall in the main prayer area and the outer surface in the corridor first floor. The materials construction of the partition are Gypsum Plaster, Marble and Lime stone from inside to the outside respectively. The overall heat transfer coefficient for the partition wall calculated as 1.309 W/m².K, the material component, thickness and the cross section of the partition wall component are presented in the Table 3.3.

Table 3.3. Physical characteristics of main prayer area internal partition wall.

Material component	Thick (cm)	U Value (W/m².K)	Cross-Section
Marble	3	1.309	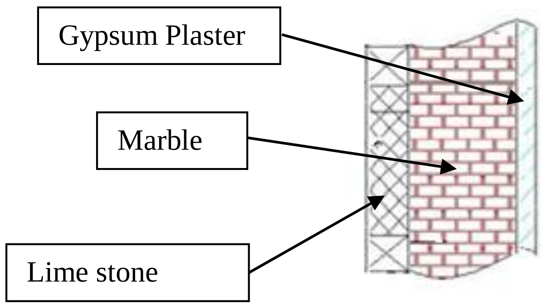
Lime Stone	80		
Gypsum Plaster	2		

3.2.1.1.3. Roof from Outside to Inside

The first floor level, main prayer area and women prayer area are not a flat roof but it is covered with domes as common feature in mosques. Domes took different shapes. In Salepçioğlu Mosque, domes have a hemisphere shape. In the Table 3.4 physical characteristics, material component, thickness, overall heat transfer coefficient and the cross section of the roof are explained. The dome contain three materials from outer to the inner layer are cupper, brick and gypsum plaster. The overall heat transfer coefficient for all component to gather is 1.096 W/m².K.

Table 3.4. Physical characteristics of main prayer area Roof.

Material component	Thick (cm)	U Value (W/m².K)	Cross-Section
Copper	2	1.096	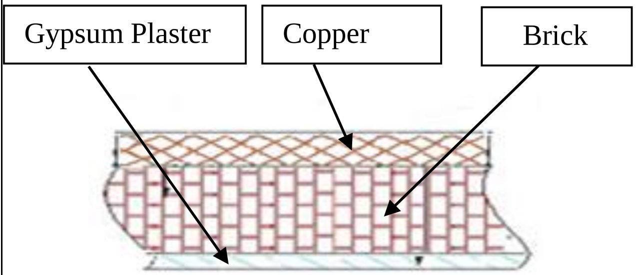
Brick	50		
Gypsum Plaster	2		

3.2.1.1.4. Floor from Outside to Inside

The first floor area zones have same material component for floor. The material component, thickness of the layers, overall heat transfer coefficient and the cross section of the floor are described in the Table 3.5. From the all walls, roofs and floors the floors in first floor they are the only one have an insulation system in their component. The floors material construction from the outside to the inside are concrete, air gap, timber flooring and wool felt underlay. The overall heat transfer coefficient calculated to be 1.203 W/m².K.

Table 3.5. Physical characteristics of main prayer area Floor.

Material Component	Thick (cm)	U Value (W/m².K)	Cross-Section
Concrete	25	1.203	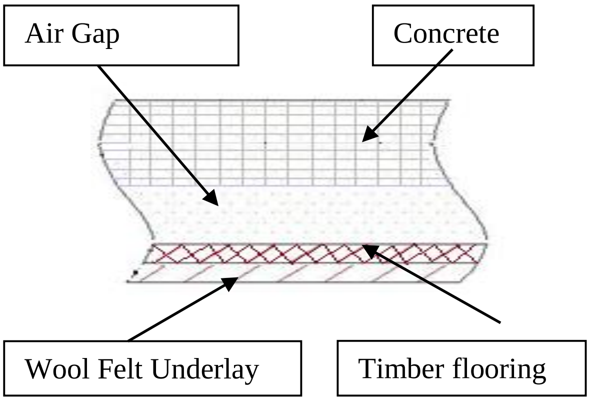
Air Gap	10		
Timber flooring	3		
Wool Felt Underlay	0.5		

3.2.1.1.2. Corridor First Floor Area

The corridor first floor area has the same material construction with the walls in the main prayer area. Despite of the minor differences in the walls thickness which mean that the overall heat transfer coefficient is different than that was calculated for the main prayer area walls. The overall heat transfer coefficient for the external walls calculated to be 2.79 W/m².K. Roofs and floors in the corridor have the same material construction that used in the main prayer area with same overall heat transfer coefficient 1.096 W/m².K and 1.203 W/m².K respectively.

3.2.1.1.3. Women Prayer Area

The external walls in the women prayer area have same material component with that used in the main prayer area. The layer are granite as an outer layer and lime plaster as an inner surface layer. The only difference is the thickness that generate different U value. It is calculated as 2.62 W/m².K. The women prayer area roofs and floors have same material component with the main prayer. The overall heat transfer coefficient for roofs and floors calculated as 1.096 and 1.203 W/m².K respectively.

3.2.1.2. Basement level Zones

Two main zones are presented in this section for the basement level to be explained in terms of the materials construction. The two zones are Sub-main prayer area and Corridor basement. Walls and the ground floor material constructors are described in this section.

3.2.1.2.1. Sub-Main Prayer Area

Two types of walls will be explained in the Sub-main prayer area, according to their material construction, thickness and overall heat transfer coefficient. The two types of walls are external walls and internal partitions.

3.2.1.2.1.1. External Walls

External walls in the basement composed of two layers plaster as an inner surface and lime stone as an outer layer. The overall heat transfer coefficient for all component is calculated as 1.251 W/m².K. In Table 3.6. The material component, thickness, overall heat transfer coefficient and the cross section of the walls are presented.

Table 3.6. Physical characteristics of main prayer area external walls.

Material	Thick (cm)	U Value (W/m².K)	Cross-Section
Lime Stone	78	1.251	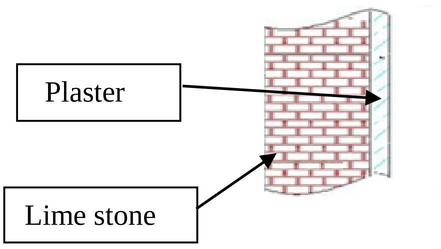
Plaster	5		

3.2.1.2.1.2. Internal Partition

The internal partitions in the sub-main prayer area are divided to two types, according to their material components. The two types are internal partition walls type A and internal partition walls type B as shown in Figure 3.3.

a) Internal Partition Walls type A

Internal partition type A have two materials component which are plaster and lime stone. The wall thickness, material component, overall heat transfer coefficient and cross section of the walls are presented in Table 3.7. The overall heat transfer coefficient of the partition type A are calculated to be 0.944 W/m².K.

Table 3.7. Physical characteristics of sup_main prayer area internal partition walls A.

Material	Thick (cm)	U Value (W/m².K)	Cross-Section
Lime Stone	1.176	0.944	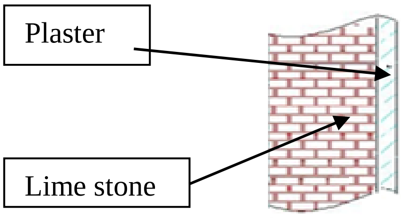
Plaster	5		

b) Internal Partition Wall B

Internal Partition Wall B is the wall separate between the sub-main prayer area and the corridor basement. Lime stone is the only material in this wall with overall heat transfer coefficient 0.944 W/m².K. In Table 3.8. The layer component, thickness, overall heat transfer coefficient and cross section of the wall are explained.

Table 3.8. Physical characteristics of the internal partition walls type B.

Material component	Thick (cm)	U Value (W/m².K)	Cross-Section
Lime Stone	1.176	0.944	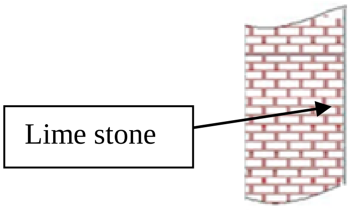

3.2.1.2.1.3. Floor

The marble is used as a material component in the floor, with overall heat transfer coefficient 3.196 W/m².K. Table 3.9 is present the material component, thickness, overall heat transfer coefficient and the cross section of the floor.

Table 3.9 Physical characteristics of sub-main prayer area Floor.

Material Component	Thick (cm)	U Value (W/m².K)	Cross-Section
Marble	25	3.196	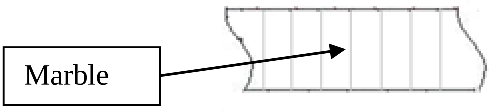

3.2.2. Doors, Windows Material Construction

Doors and windows are important factors that effect on the thermal comfort analysis. For this reason, it is essentially to define their component and heat transfer coefficient carefully. In Salepçioğlu Mosque there are different types of doors and windows. In this study the classification of the doors and windows are beside on their materials construction and the overall heat transfer coefficient for their important effect on the inside environment.

Three types of door founded in Salepçioğlu Mosque, there are iron doors, pine wood and glass door with iron frame with different heat transfer coefficient. While for widows there are two types of windows in Salepçioğlu Mosque, single glasses and double glasses with pine wood frame. All the windows have rectangular shape and open in vertical direction which allow more air to transfer from outside to the building.

The pictures below were taken during the study that shows the doors and the windows types of Salepçioğlu Mosque. In Figure 3.13. Shows the pine wood doors. On the left side picture for the main prayer area door and on the right side the external door for the first floor corridor.

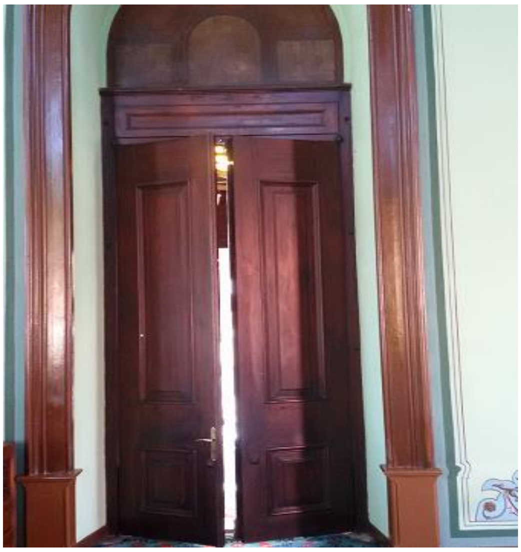

Figure 3.13. Doors types in Salepçioğlu Mosque main prayer area and corridor

Figure 3.14. Illustrated the external doors for the basement and the first floor respectively. The basement door are shown on the left side while on the right side we can see the first floor external door.

Figure 3.14. External doors in Salepçioğlu Mosque basement and first floor entrance

Widows for first floor and basement floor are shown in the Figure 3.15. On the lift side picture it is illustrate the first floor windows while the right side for the basement floor windows.

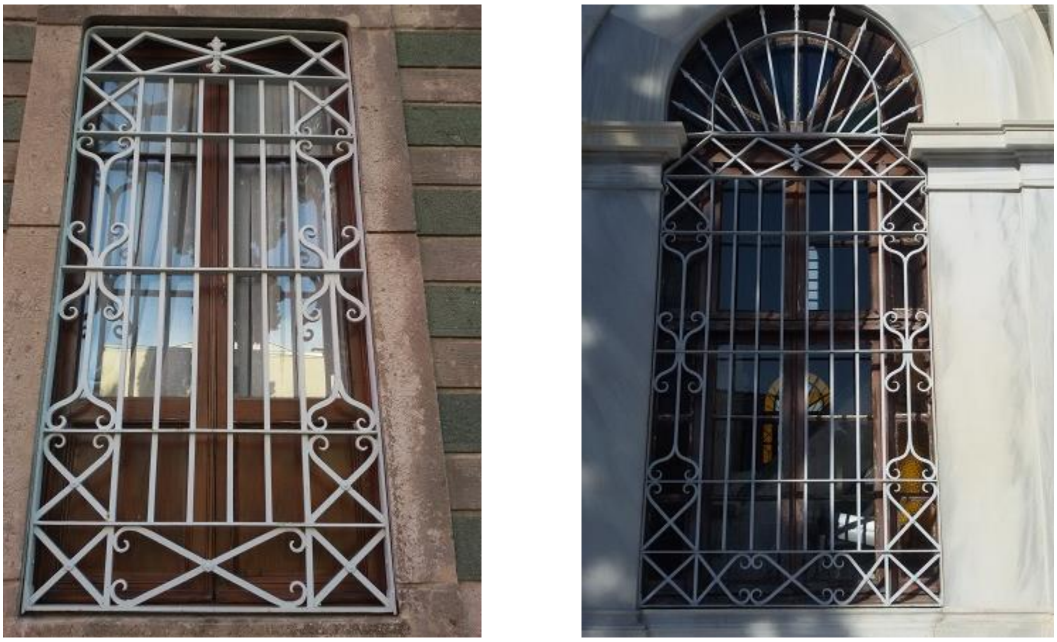

Figure 3.15. Windows types first floor and basement

DesignBuilder software provide wide range of the construction materials for the doors and windows. In this study all the material for the doors and the windows are selected from the library of the software. The construction material and the overall heat transfer coefficient of the doors are presented in the Table 3.10.

Table 3.10. Material construction of doors and overall heat transfer coefficient.

Door Type	Material	U-value (W/m^2K)
First floor External	Pine	1.685
Entrance doors	Iron	3.84
Basement doors	Iron	3.84
Internal doors	Pine	1.685

Two types of windows used in Salepçioğlu Mosque single glasses and double glasses. Table 3.11. Contain the material construction and overall heat transfer coefficient of the windows with windows types.

Table 3.11. Windows components, types and their overall heat transfer coefficient.

Window Component	Window type	U-value (W/m^2K)
Pine wood Frame Glass (6mm) Glazing	Single	5.77
	Double	2.71

3.2.3. Lighting Type

The building has the lighting system which is manually operated by the occupants depending on the luminance level in the space. An incandescent light bulb with 230 Volt - 40 Watt are used for lighting. (Figure 3.16)

Figure 3.16. lighting type in Salepçioğlu Mosque

3.3. Schedules

One of The pros of DesignBuilder software is that, it’s enable the users to specify verity of schedules that related to energy simulation calculation. The software consist of different types of schedules for instance 7/24 schedule, compact schedule and day schedule. In this study compact schedule was used for designing the occupancy, lighting and opining operation schedules, in spite of the fact that, it maximizes the operational time needed for energy simulation calculations. It used Based on the fact that, the mosques have an intermittent operation schedule and also the different in the time prayer from month to month which suspend the use of 7/24 schedule and day schedule.

3.3.1. Occupancy Schedule

Mosques are distinguished by have an intermittent occupancy schedule, which is varied from month to month according to the change in prayer time. Due to that fact mosques are occupied according to the prayer time that makes designing of the operation occupancy schedule difficult.

For having a better result in this study the occupancy schedules are designing monthly for each pray time, since there are five time prayer a day which are: Fajr, Dhuhr, Asr, Maghrib, Isha. In addition to a one specific prayer that preform a day in the week on Friday. Table 3.12 summarized the terminologies meanings and prescribed time period used in this study.

Table 3.12. Religious Terminologies and Prescribed Time Period

Name	English	Prescribed time period	
		Start	End
Fajr	Dawn-Prayer	When the morning light appears	Just before the sunrise
Dhuhr	Mid-Day Prayer	Sun appears the highest in the sky	Beginning of the Afternoon-prayer
Asr	Afternoon-Prayer	Shadow of an object reaches certain length-ratio in the afternoon	Prior to local sunset
Maghrib	After-sunset Prayer	When the sun is fully set	Beginning of the Night-Prayer
Isha	Night-Prayer	When the western sky begins to darken	Beginning of first Dawn-prayer

The study is done for one year period as mentioned before, so that it is important to indicate the month of Ramadan with unique operation schedule and number of people performing pray compering with the rest of the months. The occupied of the zones are different from zone to another, while the submain prayer area, women prayer area, corridor first floor and basement corridor have same occupancy schedule the main prayer area has different occupancy schedule (Table 3.13).

The occupancy operation schedule for the sub-main prayer area, women prayer area corridor first floor and basement corridor are simple where these area just weekly occupied during Friday pray time "*Cuma Namaz*" from 12:00pm to 14:00pm with full occupancy density 225, 78, 70, 70 people respectively.

The main prayer area daily occupancy operation schedule over a year is shown in the table below including the prayer time range through the month, which is the range of the varying in time per a day. Table 3.11. Shows the occupancy schedule for the main prayer area. Besides the period for the pray range is shown for each prayer time.

Table 3.13.Occupancy schedule for the main prayer area and the prayer time range.

Prayers	Fajr		Dhuhr		Asr		Maghrib		Isha		Friday prayer	
Months	Prayer time (Hrs:Mins)	Prayer time range (Mins)	Prayer time (Hrs:Mins)	Prayer time range (Mins)	Prayer time (Hrs:Mins)	Prayer time range (Mins)	Prayer time (Hrs:Mins)	Prayer time range (Mins)	Prayer time (Hrs:Mins)	Prayer time range (Mins)	Prayer time (Hrs:Mins)	Prayer time range (Mins)
January	5:30	60	12:00	60	15:30	90	18:00	30	18:30	30	11:30	120
February	5:30	60	12:00	60	15:00	60	17:30	60	18:30	30	11:30	120
March	5:30	60	12:30	60	15:30	90	18:00	120	20:00	120	12:00	120
April	4:30	90	13:00	60	16:30	60	19:30	60	21:00	60	12:30	120
May	4:00	60	13:00	60	17:00	60	20:00	60	21:30	60	12:30	120
Until 16 0f June	4:00	90	13:00	60	17:00	60	20:30	30	22:00	60	12:30	120
from 16 0f June to 30 of June (Ramadan)	4:00	90	13:00	60	17:00	60	20:30	30	22:00	60	12:30	120
from 18 0f July to 30 of July (Ramadan)	4:00	60	13:00	60	17:00	60	20:00	60	22:00	60	12:30	120
August	4:30	60	13:00	60	17:00	60	20:00	60	21:30	60	12:30	120
September	5:00	60	13:00	60	16:00	60	19:00	60	20:30	60	12:30	120
Until 25 October	5:30	60	13:00	30	16:00	60	18:30	60	20:00	60	12:30	120
25 of October until 31 of October	5:00	30	12:00	30	14:30	60	17:00	60	18:30	60	23:30	120
November	5:00	60	12:00	30	14:30	60	16:30	60	18:30	30	23:30	90
December	5:30	60	12:00	30	14:30	60	17:00	30	18:30	30	23:30	120

3.3.2 Lighting Schedule

Lighting is controlled by people manually, all the zones have same operation schedule for lighting it on from 17:00 to 23:30 since the mosque is not occupied after the last prayer time, so the lightings are turned off the rest of the day time. The variety of the zones area lead to the different in the number of lamps used in each zone to cover the need of the lighting in the zones. Table 3.14 shows the number of fixtures, area and the lighting energy for each zone.

Table 3.14. Number of lamps and lighting energy for each zone.

The zone	Floor Area (m^2)	Number of lamps	Lighting Energy (w/m^2_100lux)
Ground Floor			
Sub-main Prayer area	166.46	18	4.33
Corridor	85.04	4	3.76
First Floor			
Main Prayer Area	164	36	8.78
Women Prayer Area	53.84	6	4.46
Corridor 1	55.02	14	10.18

3.3.3 Opening Operation Schedule

3.3.3.1 Door Schedule

Operation schedule for internal doors and external doors should be carefully designed for the reason that there effect on the internal environment condition. DesignBuilder gives the designer ability to generate their own operation schedule for the time when the door open or close not just that, but also the door openable area from the total door area.

The door operation schedule are designed for each door separately, due the fact that some door are openable and some kept close all the time of the study. Table 3.15 below present the number of the openable doors in each zone, open time and the area of the door open.

Table 3.15. Door schedule.

The Zone	Location of the door	Number of the Door open	Time the Door Open and Close	Door Area Open (%)
Ground Floor				
Sub-main Prayer area	Internal	4	From 08:00 to 18:00	100
Corridor	External	2	From 08:00 to 18:00	50
First Floor				
Main Prayer Area	Internal	1	From 08:00 to 23:30	80
Corridor 1	External	1	From 07:00 to 22:30	90
		2	On Friday from 11:30 to 14:00	80
Entrance	External	1	From 07:00 to 22:30	90

3.3.3.2 Window Schedule

Same as the door operation schedule the windows schedule are modelled separately due to the different in patterns. For the ground level the windows always kept close. While for the first level some windows are openable and some cannot be open due to their location.

In this study window operation schedule for the first level are scheduled for summer season as open and winter season are closed, windows are opened from April to September between 10:00 to 22:00.

CHAPTER 4

METHODOLOGY

In this chapter, the research methodology used for this study is presented, in contemplation of analysis the thermal comfort of historic building and evaluate the effect of different scenarios that used for enhancing the thermal comfort of the building. The Flowchart 4.1 below shows the methodology process with its parameters and steps.

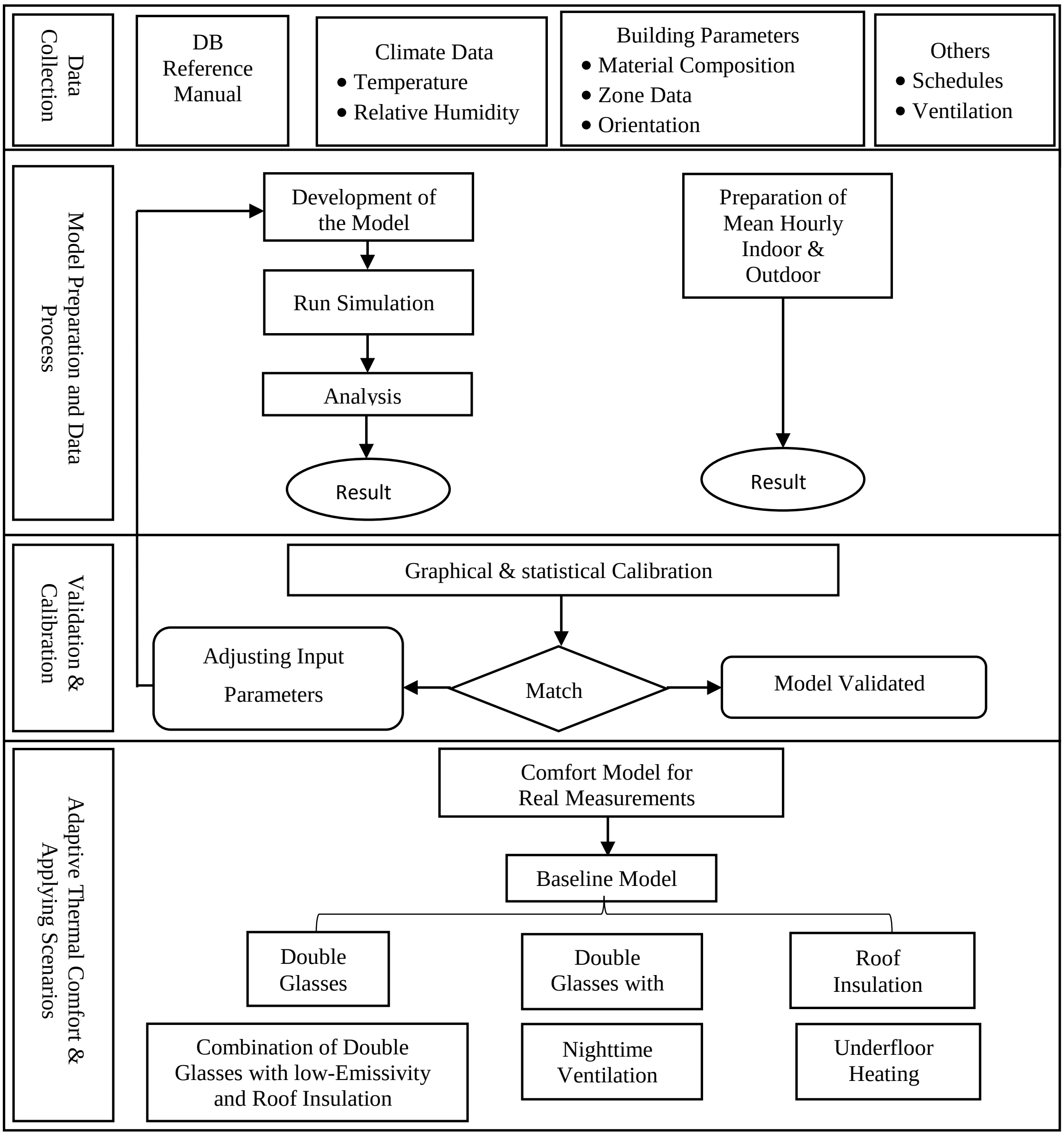

Figure 4.1. Workflow for the methodology process

First of all, the source of data and data collection are explained and the assumption done in the data is pointed out to be used later for calibration the software. The second step is that characteristics of DesignBuilder and how it is work are explained, the reasons behind using it as an energy simulation tool in this study as mentioned.

Third, the calibration ways of the simulation result are explained according to ASHRAE Guideline 14 _2002. Then, the adaptive thermal comfort in ANSI/ASHRAE 55, 2010 with the acceptable ranges is applied for examining the thermal comfort of the baseline model and the scenarios as well. The methodology process ending by introducing some strategical design scenarios for enhancing the comfort level inside the mosque with the conservation of historic values of the mosque.

4.1 Tools for Data Collection

A variety of different tools was used for collecting the necessary data to cover every aspect of this study such as Data logger, Thermal Camera and Blower Door Machine.

4.1.1. Data logger

U12 type of HOBO Data logger is used for determining the environmental parameters (Figure 4.2). Two parameters are important to be monitored in order to evaluate the indoor thermal comfort which are the air temperature and relative humidity, both of the parameters were monitored in this study. The accuracy of the data logger (HOBO U12) used in this study shown in Table 4.1.

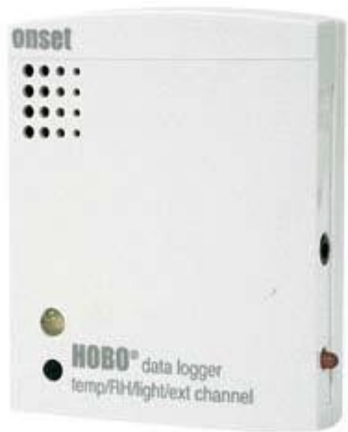

Figure 4.2. HOBO Data Logger

Table 4.1. Accuracy information of the Data logger (HOBO 2014)

Elements	Accuracy
Air Temperature	±0.35 °C at 25°C (± 0.7°F at 77°F)
Relative Humidity	± 2.5% from 10% to 90%
Measurement Capacity	43 K
External Input	± 2 mV ± 2.5% of absolute reading

For monitoring indoor and outdoor environmental conditions, in this study, eight data loggers (HOBO U12) were installed in the building. The temperature and relative humidity parameters were collected automatically every ten minutes from October 1st, 2014 to September 30th, 2015, so that all season will be covered in the study for comprehension understanding of the thermal behaviour of the mosque. Then, the hourly average was calculated using excel program. The conducted data were required later for calibrating the model.

Data loggers were mounted on the walls with different heights due to security reasons and understand stratification temperature and relative humidity. The loggers were distributed in the zones according to their sizes.

For measuring the environmental condition in the basement floor, two of the data loggers were set up at different locations: one in the corridor on 2.3 m (BC), and the other in the sub-main prayer area on 3 m (BM). For the first floor zones, five of the data loggers were used to measure the environmental condition. Three of them were placed on the main prayer due to its size with the different location as 1 m (M1), 2.8m (M2) and 3.3m (M3), one for the first floor corridor on 2.8 m (CF) and one for the women prayer are on 2m (W).

One data logger was used for monitoring the outside environment which placed on the place that not exposed to direct sunlight or the rain (O) on the height of 15.5m. The data obtained from the outside logger was used later for generating the weather file to be used in the software. In Figure 4.3a the black triangle shapes indicate to the data logger places on the basement and the first floor level. The Figure 4.3(b) and 4.3(c) illustrate the location of data loggers on the first floor and basement respectively.

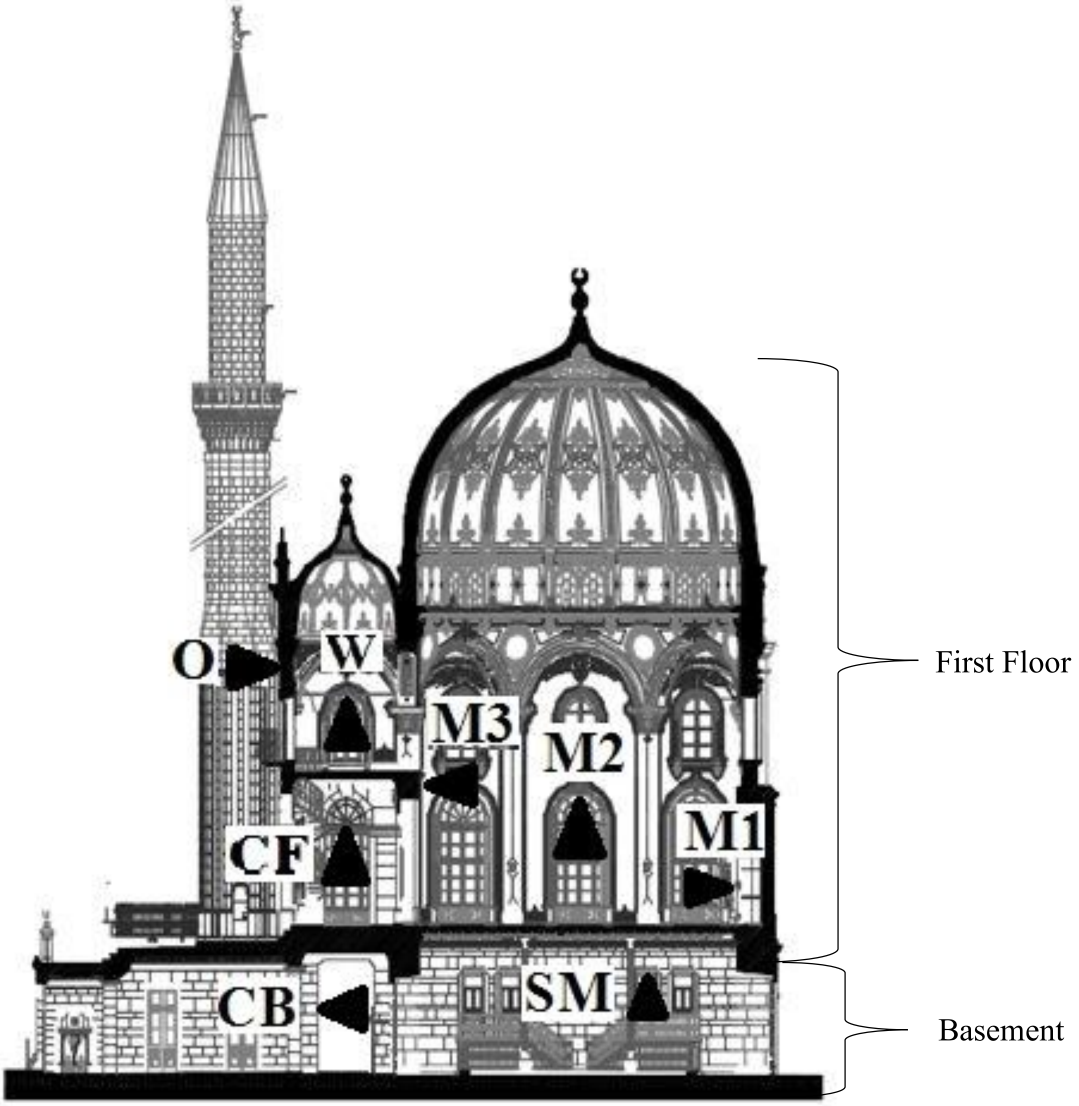

(a)

Figure 4.3. (a). Data logger location of the basement and first floor

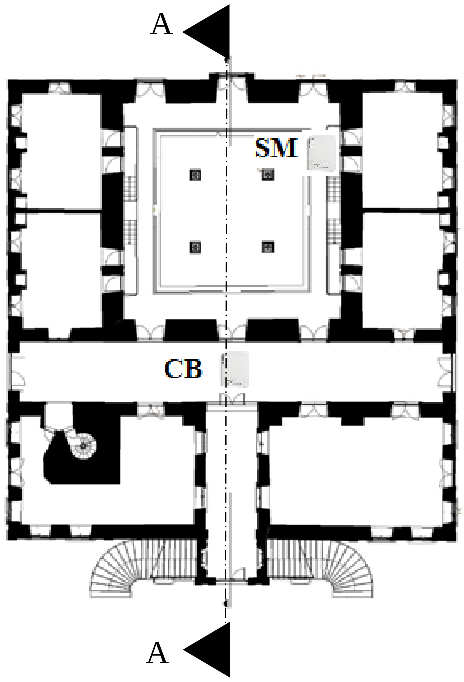

(b)

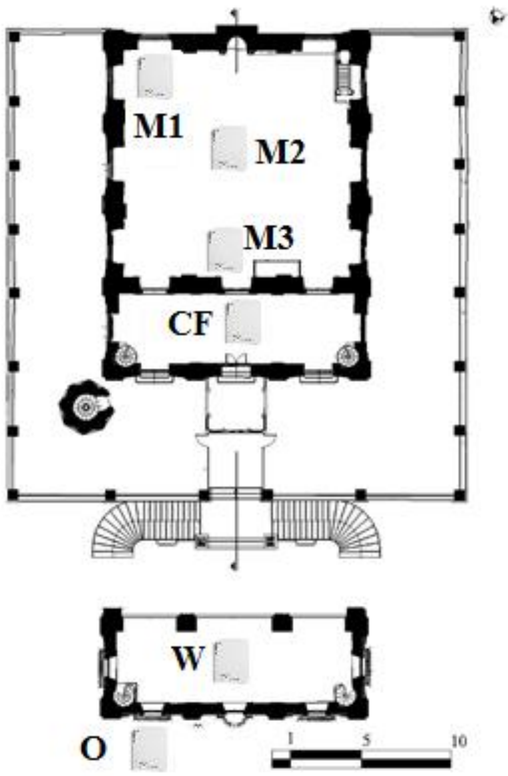

(c)

Figure 4.3 (b). Data logger location of the first floor, (c) Data logger location of the basement

4.1.2. Thermal Camera

The thermal camera is a camera that captures infra-red (IR) light instead of visible light captured by a normal camera. IR light cannot be seen by the naked eye and occurred beyond the red end of the visible light spectrum. The objects emit IR light when they are warmer than absolute zero (-273°C). More IR light is emitted when the objects more warm. The light emitted by an object translated it into a temperature. The temperature is shown in a scale bar next to the thermal image or thermogram. The thermal camera produces images with multicoloured each colour to indicate a different temperature. The thermal camera is used in a verity of applications in different disciplines. One of the areas that the thermal camera can be a useful tool is the assessment of the condition of the buildings. In the case of an investigation of the historic buildings thermal camera has especial advantages for it is a non-invasive, non-destructive method.

In this study, A Testo 875 thermal camera (Testo 2015) was used to examine the leaks, moisture damage and identify potential problems with a building's fabric. It is a useful tool to be used in historic buildings where all of that examination can be done with no contact with the buildings. The thermal camera might be used in historic buildings to specify areas of dampness and to locate thinner depths of the wall, cracking and voids. When the thermal camera is used, some parameters should be considered for their important effect on the reading such as weather conditions, orientation and the time of day when the image was taken. In addition, objects with high or low emissivity can give an inaccurate reading such as metal.

4.1.3. Blower Door Machine

In this study air tightness in the mosque is calculated by using Blower Door machine. Blower Door is a machine that used for calculating the airtightness in buildings. The blower door machine is used to reduce energy consumption and avoiding uncomfortable drafts due to air leakage, avoiding moisture problems, and determine the proper scenario to design mechanical ventilation to provide an acceptable thermal comfort range.

Blower Door machine model 4.1 (Blower Door 2015) was used in this study. It is a powerful fan, Figure 4.3 shows the preparing process of the test. The fan pushes the air out of the building to reduce the pressure inside the building, due to the pressure difference between inside and the outside the air flows through the cracks and openings, then the smoke pencil is used to detect the air leaks.

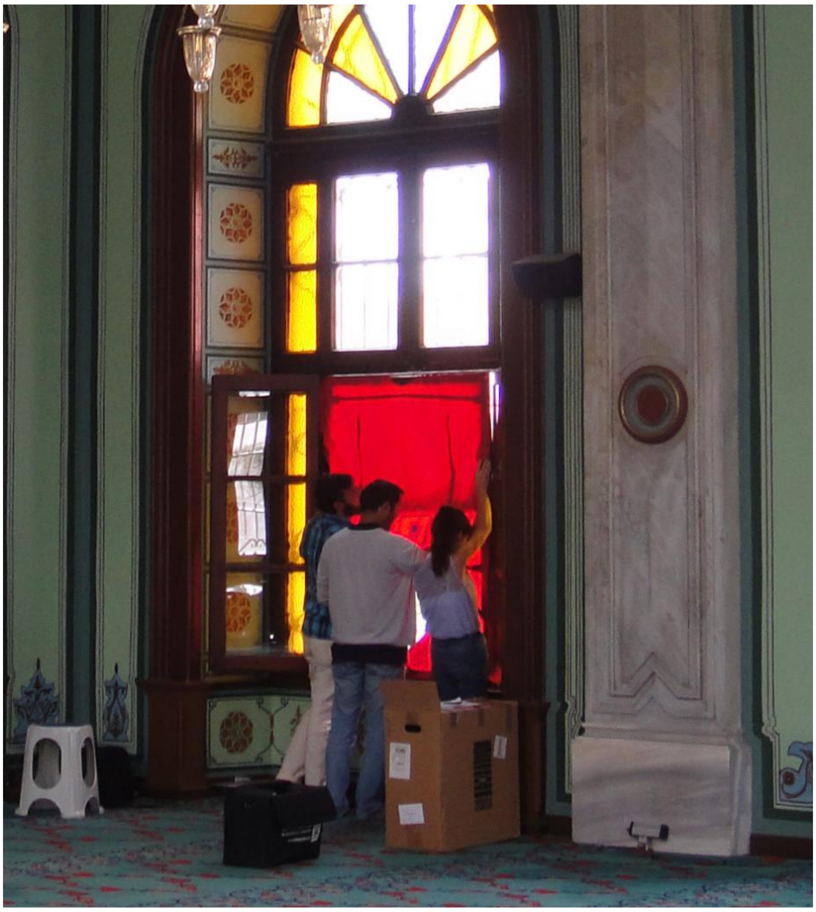

Figure 4.4. Blower Door machine

Before installation of the machine and starting the measurement some preparation should be ensured such as, closing all the windows and all the exterior doors except the door with the fan and open all the interior doors disable or shutting off the electrical power for heating equipment and non-electrical water heater. When the preparation of the building has been finished the test is ready to be started with turn the fan slowly to depressurize the building. Before cranking the fan all the way up, it is recommended that the technician can walk through the building ensure that everything is as prepared for it. The fan is speeded up until the pressure difference reaches 50 Pascals between the indoor and the outdoor. At that point, the data shown in the airflow manometer is readied and recorded by the technician.

The result is interpreted in two ways, air changes per hour at a pressure difference of 50 Pascals (ach50) or airflow at a pressure difference of 50 Pascals (cfm50).

For the airflow at a pressure difference of 50 Pascals can be read directly from the airflow manometer at the time of the test. While the air changes per hour at a pressure difference of 50 Pascals are calculated by using the volume of the building. By multiplying the cfm50 by 60 minutes per hours and divided by the building volume measured in cubic feet ach50 can be calculated.

4.2. DesignBuilder Program

DesignBuilder version 4.2 (DB 2014) has been used in this study for thermal comfort analysis of the historic building. For some vital reasons, for instance, the integration with energy plus give the ability to complete the simulation within the DesignBuilder interface. DesignBuilder offering built-in library and load profiles, flexible geometry, and the results are displayed and analysed effectively in annual, monthly, daily, hourly or sub-hourly intervals. The program has been tested under the BESTEST ASHRAE STD 140. Moreover, it is user-friendly, the 3D model can be modelled with realistic visualisation. The applications of DB are typically about comfort and overheating analysis, calculating heating and cooling loads, assessing the annual energy use and Carbon emission, Daylight analysis and Solar shading.

4.2.1 How the Software Work

As most of the computer software, DesignBuilder software needs inputs to work. As the first function the location needs to be set up, then the weather file can be loaded from the program’s library or import it as an EPW file, after setting the location and chosen the weather file, the geometry building could be generated or downloaded in DXF file format to the software as a 2D drawing. The construction materials which used for generating the geometry model is provided by the software library that consists a variety of materials and constructions with the ability for the users to create their own materials. After generating the model parameters like internal loads (occupancy schedule, activity), windows and doors openings, lighting, and HVAC system needs to be entered. After all of the required input has been entered the simulation can be done. The necessary input data needed to be entered to DesignBuilder is shown in the workflow chart in Figure 4.5.

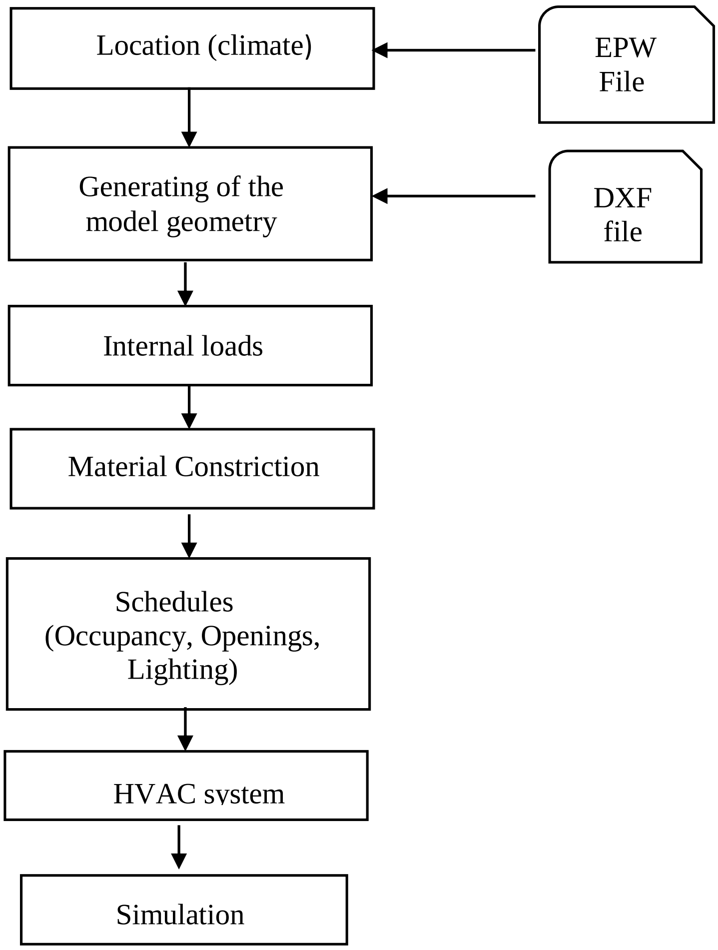

Figure 4.5. workflow for the input data needed in DesignBuilder software

4.2.2 DesignBuilder Limitations

DesignBuilder is a powerful tool, but it does have its limitations like any other computer software. These limitations are: it is not supporting all functionalities of Energy Plus, besides the software does not have detailed information about the components and topology for simple and compact HVAC system. In addition to these limitations, 3D model cannot be imported to the DesignBuilder from Energy Plus which limits the use of the program.

4.3 Calibration of DesignBuilder

It is well known using any of the computer software for the energy analysis purpose required calibration for the data that obtain from the software. The measurement will be compared with the simulation data to understand how the model will differ from the real case. In this study, calibration has been done according to ASHRAE Guideline 14 _2002. As mentioned earlier in this chapter, the outdoor and indoor environment were monitored by using data loggers (HOBO). The calibration has been done for the main zones in the first and the underground floor of the building that have been occupied most. Since the data were measured hourly, in the ASHRAE Guideline 14-2002 the calibration can be done by using two techniques, graphical comparison techniques and statistical comparison techniques.

In ASHRAE Guideline 14-2002 four types of graphical comparison techniques are presented. The first technique is that weather day types 24-hour profile plots, the second technique is binned interquartile analysis using box-whisker mean plots, the third technique is three-dimensional surfaces, and fourth technique is three-dimensional colour plots.

In this research, the first technique which is weather day type 24 hours profile plots was used for data comparative. The computer program EXCEL 2013 was used to generate hourly datasets, and then a graphical image is created from the simulated data with the measured data for trend analysis purpose.

The second technique used for data analysis and calibration is statistical comparison techniques. ASHRAE Guideline 14 2002 introduce two ways of statistical techniques, hourly Mean Bias Error (MBE) and Root Mean Square Error (RMSE).

In this study both of the techniques were used to estimate the acceptable error range between the simulated data and the measured data. Mean Bias Error is used for measured the variability in other words how the data spread from each other (AHRAE 14 2002). According to ASHRAE Standard 14 2002, the acceptable range of MBE for models to be calibrated when hourly data used is ±10%. Root Mean Square Error used to estimate how much the simulation data fits the measured data, the better calibration will be will obtain with lower RMSE. The models are calibrated if they produce RMSE within ±30% when hourly data is used.

MBE and RMSE were calculated respectively by using equation 1 and 2 respectively (ASHREA 14 2002).

$$RMSE (\%) = (100/T_{ma})*[1/N*(S (T_s-T_m)^2)]^{1/2} \quad (4.1)$$

$$MBE (\%) = (100/T_{ma})*[S (T_s-T_m)] /N \quad (4.2)$$

Where:

N: is the number of observations

T_{ma}: is the average measured temperatures for N observations

T_s: is the simulated hourly temperatures

T_m: is the measured hourly temperatures

4.4. Adaptive Thermal Comfort in ANSI/ASHRAE Standard 55, 2010

ASHRAE Standard 55 for thermal environment conditions for human occupancy provided a method for naturally conditioned spaces to calculate the thermal comfort condition. In the standard is stated that the thermal response is depending on the outdoor environment in the naturally conditioned spaces in contrast the buildings with centralised HVAC system the thermal response due to the different experiences, change in clothing, availability of control and shifts in occupancy expectations.

The adaptive thermal comfort method can be applied under certain conditions as follow:

1. No mechanical cooling system in the space.
2. The space in the equation with operable windows.
3. No heating system in operation.
4. Sedentary physical activities with the metabolic rate from 1 to 1.3 met.
5. According to the indoor and /or outdoor occupants can adapt their clothing.

For spaces that meet these criteria, Figure 4.5 can be used to determine the allowable indoor operative temperature.

In this study, the adaptive thermal comfort graph was drawn by using excel program 2013. The relation between the mean monthly outdoor air temperature, which is the arithmetic average of the mean daily minimum and mean daily maximum outdoor temperature, with the indoor operative temperature which defined according to ASHRAE standard as a measure of human thermal comfort derived from air temperature and mean radiant temperature. ASHRAE STANDARD 55 provides equations for the 80% and 90% upper and lower limit for the acceptable range of thermal comfort as shown in Figure 4.6. The 80% acceptable limits are used for the typical application. When a higher thermal comfort is required the 90% acceptable limits are used (ASHRAE 55).

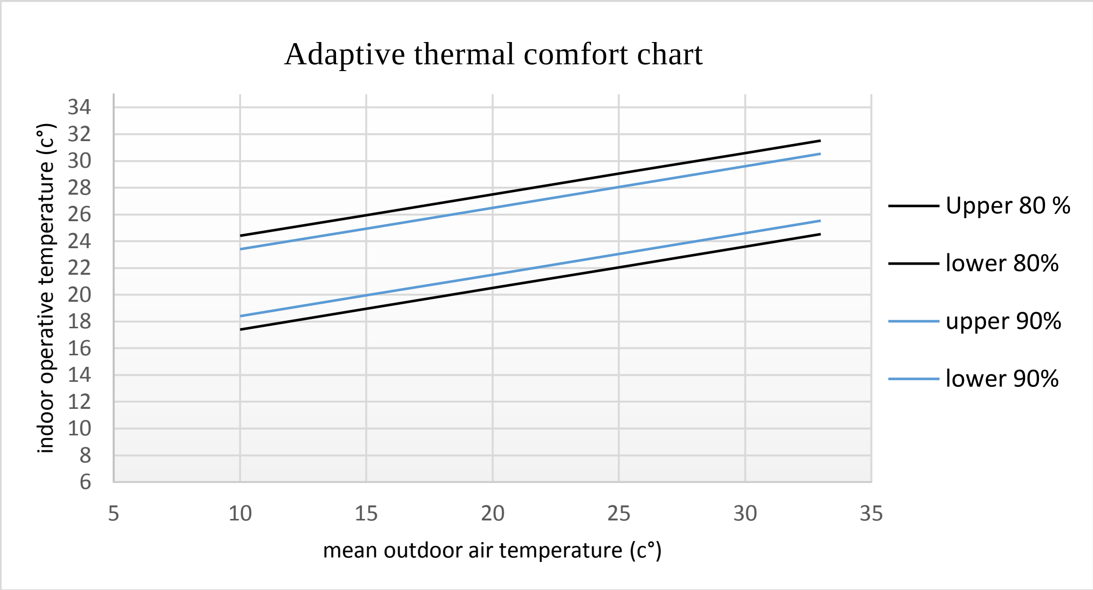

Figure 4.6. Acceptable operative temperature ranges for naturally conditioned

The 80% and 90% acceptable ranges are calculated by using the following equation:

For the 80% upper and lower limit acceptable ranges:

The upper limit (ºC) = $0.31\ T_{out} + 21.3$ (4.3)

The upper limit (ºF) = $0.31\ T_{out} + 60.5$ (4.4)

The lower limit (ºC) = $0.31\ T_{out} + 14.3$ (4.5)

The lower limit (ºF) = $0.31\ T_{out} + 47.9$ (4.6)

For the 90% upper and lower limit acceptable ranges:

The upper limit (ºC) = 0.31 Tout + 20.3 (4.7)

The upper limit (ºF) = 0.31 Tout + 58.7 (4.8)

The upper limit (ºC) = 0.31 Tout + 15.3 (4.9)

The upper limit (ºF) = 0.31 Tout + 49.7 (4.10)

Where, T_{out} is the mean monthly outdoor air temperature in (ºC) or (ºF).
When the adaptive thermal comfort is used, it is not necessary to calculate the clothing values for the spaces because in Figure 4.4 it accounts for people's adaptation in free running spaces by relating the acceptable range of indoor temperature to the outdoor climate. Also, the humidity and air speed are not required when the adaptive thermal comfort is used (ASHRAE 55).

4.5. Design Strategies for the Scenarios

Different scenarios are applied for enhancing thermal comfort level in Salepçioğlu Mosque. In the case of historic buildings, it is important that to consider the heritage value of the building when any adjustment of the materials is presented. The possible scenarios that can be done for achieving internal thermal comfort are introduced in this part. The zone selected to be analysed in terms of the thermal comfort is the main prayer area for the reason that, it is the most occupied zone in the building during the daytime by the worshipers and it is important to be in an acceptable level of thermal comfort.

Different scenarios are discussed with the Prime Ministry Directorate General of Foundations in order to enhance the thermal comfort level in Salepçioğlu Mosque. All the scenarios that have been chosen in this study according to Prime Ministry Directorate General of Foundations recommended except the underfloor heating system that was chosen by the to see the effect of underfloor heating in the thermal comfort. Since the mosque is historic, the scenarios were chosen to not compromise the heritage value of the building, for example, the painting on the walls are very sensitive to the temperature and humidity level for this reason no mechanical systems were recommended by the Prime Ministry Directorate General of Foundations. The scenarios used in this study are divided to two strategies, passive design strategy and active strategy.

4.5.1. Passive Design Strategy

German Passive House Institute provides definition for passive house as follows:
"A passive house is a building, for which thermal comfort (ISO 7730) can be achieved solely by post-heating or post-cooling of fresh air mass, which is required to

fulfil sufficient indoor air quality conditions (DIN 1946) – without a need for re-circulated air.”

In passive design strategy, the source of energy comes from the ambient instead of using purchased energy like electricity or natural gas. In this study, three strategies of the passive design are used such as windows with double glazing, windows with double green glazing thermal insulation and nighttime ventilation.

4.5.1.1. Windows with Double Glasses

Recent studies state that to achieve thermal comfort in a building and reducing energy used, can be achieved by considered some parameters such as humidity, noise, lighting and temperature (Noh-Pat et al., 2001).

According to Energy Saving Trust in an uninsulated building, a 20% of heat lost through the windows. Double glazing window reduces heat loss by 50% in comparison to a single glazed window. In addition, it also reduces the heat transmission in the summer (Energy Saving Trust 2015).

With its benefits of reducing heat loss, eliminating draughts and cold spots. Besides, it also insulates the houses from the unwanted outside noise the double glazing windows were used. The gap between to panels determine the insulation of the windows, this gap can be filled by gas or vacuumed. In this design, to reduce the transmission of heat, the gap is filled with air. To this end, single glazing windows in the main prayer area, in Salepçioğlu Mosque were replaced by double glazing windows with 3mm thickness and air gap 13 mm, in order to enhance the thermal comfort level of the main prayer area.

4.5.1.2. Double Glasses with Low-Emissivity

The improvement obtained in terms of thermal comfort by using double glazing can be improved further by using double glazing with low emissivity material (Energy Saving Trust).

The emissivity is defined as the ability of the glass surface to reflect heat. Windows with low emissivity glazing are able to reduce the heat loss through the windows. Besides it also reduces the transfer of heat from the warm pane to the cold pane.

Windows with double glasses with low-emissivity are presented as a solution in order to enhance the indoor environment to achieve the thermal comfort acceptable ranges. In Table 4.2 below shows the difference between the baseline model and the scenario model in terms of the physical properties of the windows.

Table 4.2. The physical properties of the baseline windows and the double glasses with low-emissivity

Physical proprieties	Baseline Model	Scenario
Glazing Type	Clear single	Isıcam Konfor (Ecosol+Clear glass)
Thickness (mm)	6	6
SHGC	0.819	0.43
U Value (W/m² K)	5.778	1.6
Gap	No	12 mm air

4.5.1.3. Roof Insulation

In this scenario, the insulation material for the dome in the main prayer area is applied to increase the indoor air temperature for enhancing the thermal comfort. The material used as an insulation material is Khorasan mortar with a thickness of 2.5 cm and overall heat transfer coefficient for all materials component is 1.042 W/m².K.

4.5.1.4. Combination of Double Glasses with low-Emissivity and Roof Insulation (Double LE Glass and R. Ins.)

The combination between windows with double Low Emissivity glazing and roof insulation scenario are done as one scenario in order to understand how the indoor environment will improve in terms of thermal comfort.

4.5.1.5. Nighttime Ventilation

The nighttime strategy is applying to cool the inside of the building. Opening the windows at night time to cool it in the hot daytime. This technique helps to remove the heat gains that accumulated during the day. According to this strategy, in order to prevent the hotter outdoor to heat the interior of the building, during the day time the building should not be ventilated. The nighttime ventilation influenced by some parameters such as the ambient minimum air temperature, building parameters for example building type, building openings and building materials. Besides to the building operation period and its ventilation system (Thermal Mass, Night Cooling and Hollow Core Ventilation System as Energy Saving Strategies in Buildings).

In this study, the nighttime ventilation used to lower the inside temperature of the mosque to improve the thermal comfort during the day. Nighttime ventilation is presented for the summer season “over heating time”, by open some windows that were always closed due to their height and location. This strategy supposed to decrease the indoor air temperature to the acceptable level in thermal comfort range on ASHRAE Standard. In this scenario the windows will be open according to schedule from night to early morning from 20:00 to 06:00 to provide the acceptable comfort level for the indoor environment

4.5.2. Active Design Strategy

4.5.2.1. Underfloor Heating System

Under floor heating system was based on the fact that the mosques in its characteristic have a huge height comparing with residential buildings. For achieving better thermal comfort with low energy use the mosques intended to be heated with an underfloor heating system for heating just the occupancy level with an intermittent operation schedule. In this study from the investigations that have been done on the mosque in terms of thermal comfort, it shows that the mosque experienced over cooling in January, February, March, April, November and December.

DB software provides none electrical systems for the underfloor heating system, for this reason, Energy Plus software V8.1 (EP 2015) was used to model the system. The software provides a variety of the underfloor heating system in this study the system with low-temperature radiant (electric) was used on the floor of the main prayer area in order to overcome the overcooling issue and enhance the thermal comfort of the occupancy.

Under the low-temperature radiant (electric) any types of radiant systems can be designed. The energy supplied by the electric resistance heating to the building floor. Radiant panel system or wires embedded can be modelled with this system. The system is controlled by altering the power supplied to the unit.

Some parameters need to be entered into the system. These parameters are stated below.

1. Name, the user can create a unique name for the system in this study it has been assigned as underfloor electric heating for main prayer area.
2. Availability schedule name, in this field the operation schedule of the system is identifying. The operation schedule of the electrical low-temperature radiant was operated from 10:00 to 22:00 and is assigned as off rest of the day.
3. Zone name, here the zone intended to be heated is specified and the electric low-temperature radiant is assigned up for this purpose.
4. Surface name, this input is from the surface where the underfloor heating system will be installed. In this study, the underfloor heating system is installed in the floor of main prayer area.
5. Heating design capacity method, energy plus provides four input methods that allowed to determine the maximum electrical power. The available methods are heating design capacity, capacity per floor area, the friction of authorised heating capacity and auto sizing if this field selected as zero. In this study, heating design capacity unit in watts was selected for determining the maximum electrical power. The electrical power supplied to the surface floor that converted into heat in the low-temperature radiant system is assigned as 35000 W.
6. Temperature control type, energy plus provides three zone temperature to control the low-temperature electrical radiant system which is zone mean air temperature, zone mean radiant temperature and operative temperature. In the system used in this study, the mean air temperature was selected to control the system.
7. Heating Setpoint Temperature, in this study, is set as 22°C from 10:00 to 22:00.

   Heating setpoint temperature used in conjunction with the throttling temperature range where it is selected as 2°C to determine whether the system is working or not. The throttling temperature ranges used with the controlling temperature to define the system response towards various zone condition that means when the controlling temperature at or above 23°C the power supply to the system is zero. The maximum power will be when the controlling temperature below or at 21°C. In between 23°C and 21°C the power varied linearly.

The physical properties of the materials that used for the floor presented in the Table below in Table 4.3. Where the overall heat transfer coefficient calculated from the software as 0.445 W/m².K.

Table 4.3. The material component of the floor with its physical properties.

Material component	Thickness (cm)	U Value (W/m².K)
Stone basalt	0.25	0.445
Lime sand render	0.05	
EPS Expanded Polystyrene heavy weight	0.05	
Polystyrene	0.003	
Mortar	0.01	
Ceramic Glazed	0.005	
Carpet/under lay _ synthetic	0.02	

CHAPTER 5

RESULTS AND DISCUSSION

In this chapter, the results of yearly temperature and relative humidity data are presented according to introduced literature and objectives of the study. Moreover, simulation results about present comfort condition of Salepçioğlu Mosque due to the real measurements and calibrated model, i.e. baseline, are presented in terms of adaptive thermal comfort analysis. Finally, the thermal comfort analysis of the different model scenarios is explained and compared.

5.1. Data Analysis

5.1.1. Outdoor Environment Analysis

Thermal behaviour of the buildings is influenced by the environmental weather conditions of its location. Therefore, the outdoor dry bulb temperature and relative humidity were collected near to the mosque's area, to get the real environmental condition. Besides, they are needed for generating the weather file that will be used in the software. Since there is no meteorological station located close to this area, the data is collected by data logger. The obtained datasets, dry bulb temperature and relative humidity were formulated in excel graph as illustrated in Figure 5.1.

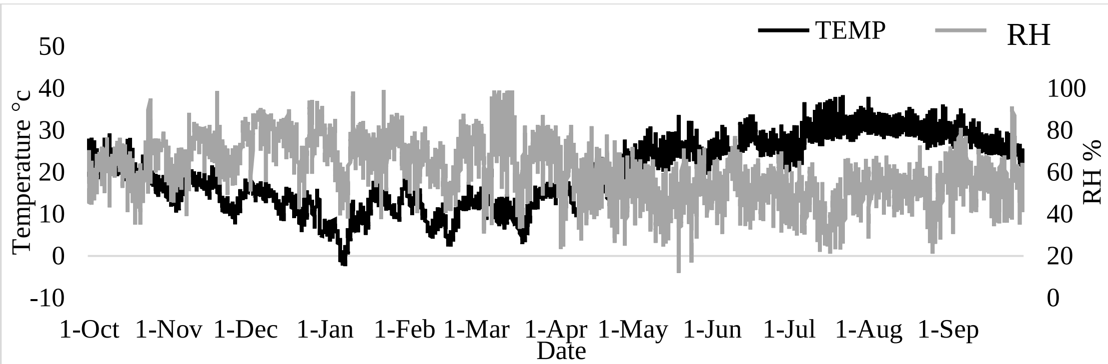

Figure 5.1. Outdoor dry bulb temperature and relative humidity for Salepçioğlu Mosque

Outdoor Dry Bulb Temperature: Figure 5.1. shows the outdoor dry bulb temeprature of Salepçioğlu Mosque. Through the studied year, the outdoor temperature ranges from -2.4 °C to 38.3 °C with 19.7 °C for the outdoor average temperature. The minimum hourly outdoor temperature was monitored on 9th of January at 07:00 while the maximum recorded on 22nd of July at 16:00.

Outdoor Relative Humidity: during the year of study, the outdoor relative humidity ranges changed from 12% to 99.2%, while the average relative humidity was 60.5% for the studied period (Figure 5.1). The minimum relative humidity was recorded on the 19th of May at 16:00, while the maximum was recorded on 24th of January at 10:00. In Table 5.1., the hourly minimum, maximum and average values of outdoor dry bulb temperature and outdoor relative humidity are presented for each month with the yearly result.

Table 5.1. Measured outdoor values of dry bulb temperature and relative humidity for Salepçioğlu Mosque (October 1st 2014 - September 30th 2015).

Month	Oct	Nov	Dec	Jan	Feb	Mar	Apr	May	Jun	Jul	Aug	Sep	Yearly
Min TEMP	13.9	7.5	4.4	-2.4	2.3	2.8	9.5	18.1	19.9	20.0	25.3	20.3	-2.4
Max TEMP	29.2	23.7	20.5	19.5	20.0	22.0	27.8	33.6	33.7	38.3	38.0	35.2	38.3
Ave TEMP	20.3	15.1	12.8	9.0	10.4	12.1	16.8	24.5	26.4	30.1	30.8	27.3	19.7
Min RH	34.9	39.0	42.3	37.5	40.4	30.7	23.3	12.0	30.5	21.0	21.0	30.4	12.0
Max RH	95.1	98.7	94.4	99.2	87.9	99.0	82.5	71.9	77.2	66.6	72.7	91.3	99.2
Ave RH	63.4	68.7	77.6	70.4	65.0	69.3	54.3	49.7	53.7	45.2	51.8	56.9	60.5

5.1.2. Indoor Environment Analysis

Indoor Temperature: in the main prayer area (HOBO M2), values vary between the minimum of 4.89ºC and the maximum of 35.94ºC, which was measured on 22 July at 19:00, and on 9 January at 08:00 respectively. Monthly average indoor temperatures for the main prayer area were between 11.29ºC and 31.61ºC and mean average temperature has found 21.547ºC through measuring period. (See Appendix B, Table B.1)

In the corridor of the first floor (HOBO CF), the temperature varies from the maximum value of 36.53ºC on 22 July at 18:00 to the minimum value of 3.38ºC on 9 January at 09:00 through measuring period. The monthly mean indoor temperature of the corridor first floor through one year measured period has found as 20.87ºC. The minimum monthly average temperature is 10.36ºC on January which is the coldest month of the measuring period for ambient temperature, while the maximum monthly average temperature founded as 31.32ºC in August which is the hottest month of the measuring period (see Appendix B, Table.B.1).

The indoor temperature during one year measured period varies between 4.8ºC and 35.53ºC for the women prayer area (HOBO W). The lowest temperature recorded for the indoor temperature for the measured period has found on 9 January at 09:00 was 4.8ºC. The highest temperature is recorded on 1 August, at 18:00 as 35.53ºC. Monthly average temperatures of women prayer area differ between 10.91ºC and 31.9ºC through the measurement period. The mean monthly temperature is detected as 10.91ºC on January which is the coldest day of the measuring period for ambient temperature. On the other hand, the highest monthly average temperature reaches to 31.9ºC in July. (see Appendix B, Table.B.1).

The mean average indoor temperature of the sub-main prayer area (HOBO SM), is found as 21.36ºC. The monthly average temperature was 12ºC in January, which is recorded as the coldest day for sub-main prayer area. In addition, the hottest day in this zone was in August with 30.66ºC average temperature. During one year measurement period indoor temperature varies between 8.56ºC and 32.227ºC. 1The maximum instant temperature, 32.227ºC is registered on 31 July, at 17:00 and the minimum instant temperature is registered on 10 January, at 14:00 as 8.56ºC. (see Appendix B, Table.B.1).

Through one year measuring period, the average of the monitoring temperature data has been recorded as 20.80ºC for the corridor in the basement (HOBO CB), as mean average indoor temperature. The maximum value of the monthly main average temperature was 30.14ºC on August, on the other hand, the minimum monthly average temperature was 11.8ºC in January. In addition, the highest instant temperature is recorded on 17 August at 15:00, as 32.132 ºC. Lowest instant temperature is recorded on 9 January at 11:00 as 7.607ºC for the corridor basement during measuring period. (see Appendix B, Table.B.1).

Relative Humidity Data: Relative Humidity value of one year measurements is listed and recordings. Monthly average RH values are found by listing hourly per day statistics per each month. Monthly average indoor RH for each zone are listed and expressed. Besides, the maximum and the minimum instant RH that monitored by data loggers are indicated by the time data. (see Appendix B, Table.B.2).

The relative humidity measurements of the main prayer area (HOBO M2), show that the value of relative humidity changes between 18.85% and 83.03% through one year measurement period. The maximum value for the RH was 83.03% on 27 March at 13:00 and the minimum value of 18.85% on 19 May at 19:00. Monthly average RH value varies from 43.96% to 69.37% on July and December respectively. Mean average RH value is found as 56.09% through one year of the measurement period. (Figure 5.2)

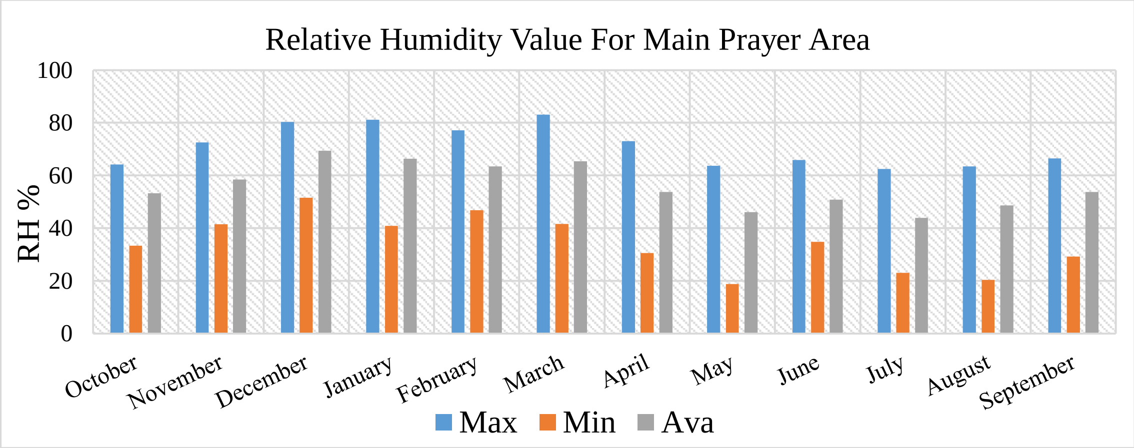

Figure 5.2. Relative humidity values in the main prayer area

One year measurements period for the corridor first floor (HOBO CF), demonstrate that RH value changes between 24.51% on 19 May at 18:00 and 87.56% on 17 January at 14:00 as seen in Figure 5.3 below.

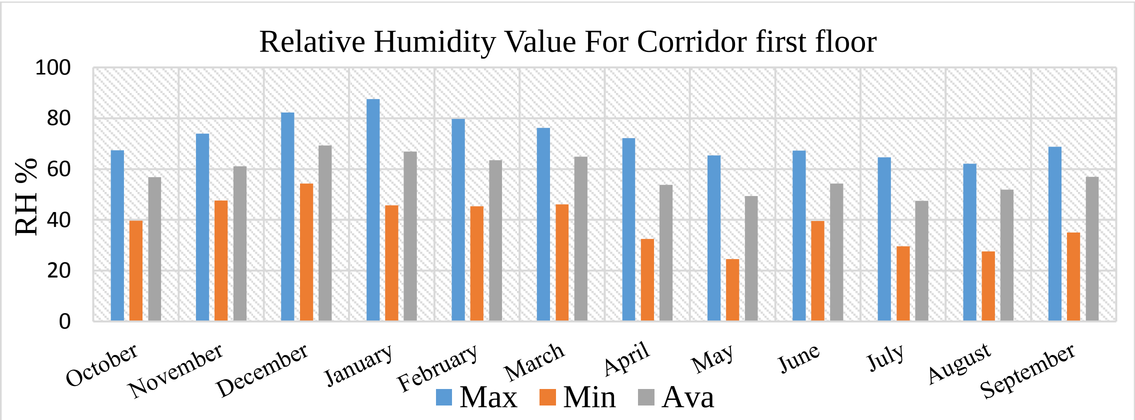

Figure 5.3. Relative humidity value for corridor first floor

The monthly average RH value decreases to 47.43% in July and achieves the maximum value of 69.29% in December. While the mean average measurements of RH found as 57.98% for a studied period.

The data recorded in the women prayer area (HOBO W), shows that the mean average RH found as 57.46% for the one year period. Monthly average RH changes from the maximum value of 71.49% in December to the minimum value of 44.36% in July. Nevertheless, instant values that are taken in every hour shows that RH value differs from 19.61% to 84.35%. The maximum value is recorded as 84.35% on 26 December at 14:00 while the minimum value recorded as 19.61% on 19 May at 17:00 through measurement period. (Figure 5.4)

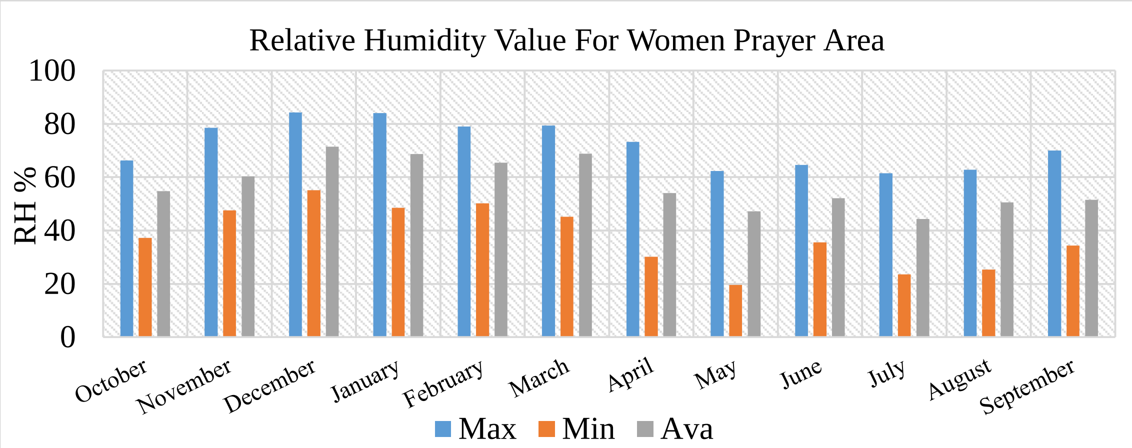

Figure 5.4. Relative humidity values for women prayer area

Figure 5.5. Illustrate that, the RH value of sub-main prayer area (HOBO SM), changes between 31.13% and 80.99% that reaches to the maximum 80.99% on 26 December at 14:00 and decrease to the minimum of 31.13% on 13 July at 16:00. Mean average RH value found as 56.99% for one year period. Where the maximum average value and the minimum average value of RH for each month was 65.40% in December and 48.13% in August respectively. (Figure 5.5)

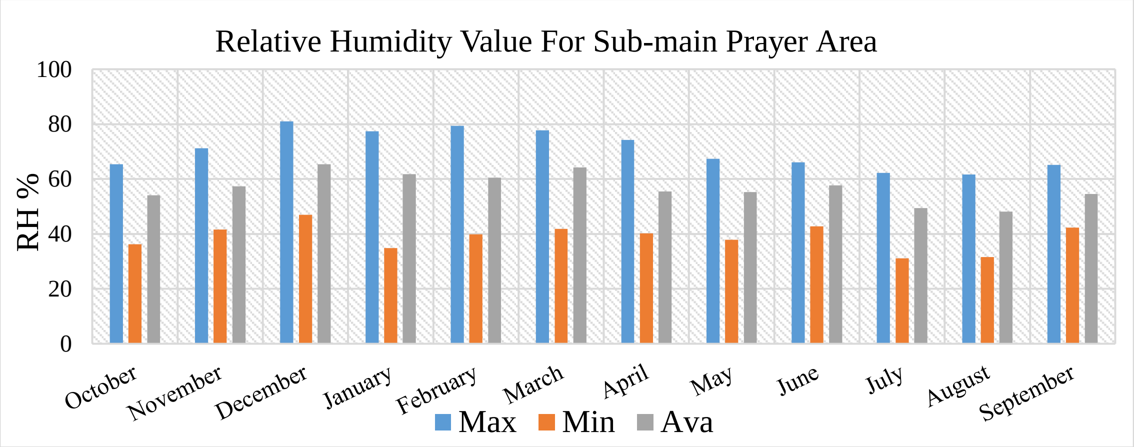

Figure 5.5. Relative humidity values in sub-main prayer area

Measurements of corridor basement (HOBO CB), illustrate that monthly average RH value changes from 51.72% in July to 68.18% in December. According to the monthly average values, the mean average value of RH has found as 60.26%. In addition to the mean average value the instant values of the corridor basement that are taken in every hour show that the maximum value of RH recorded on 12 January at 13:00 as 86.63% and the minimum value as 28.26% on 26 August at 17:00 through measurement period. (Figure 5.6)

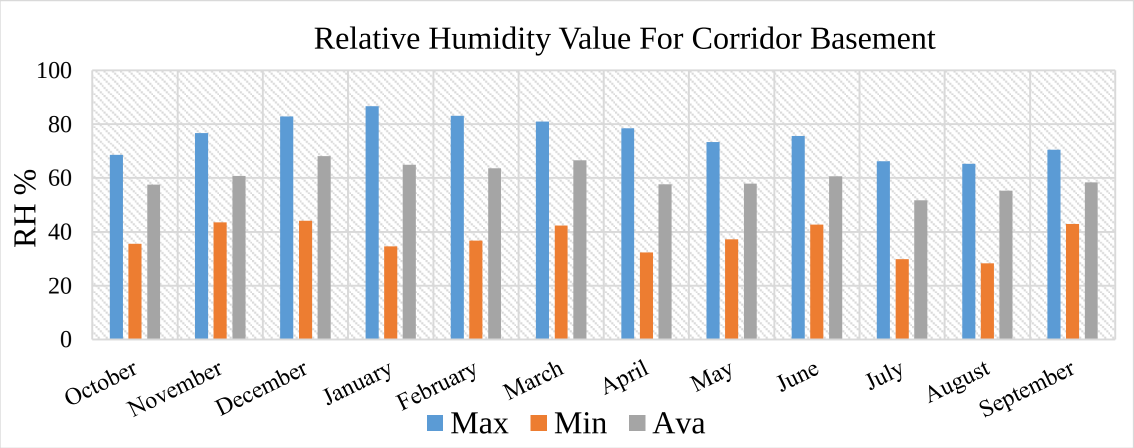

Figure 5.6. Relative humidity values for corridor basement

After the outdoor and indoor environment data has been analysed separately, the comparison has been made between the outdoor and indoor environment; the evaluation includes both of the two variables temperature and relative humidity. All zones are included in these evaluations and interpretations.

Apart from these, the important finding that noteworthy to be pointed out is that the effect of outdoor conditions of the indoor condition. As mentioned in the literature the indoor condition relay on the outdoor condition. Results of measurements which are shown in Figure 5.7 and 5.8 In this study from the comparative evaluation it has been found that outdoor temperature has a direct impact on indoor temperature, due to the absence of any mechanical system for both cooling and heating purpose and absence of insulation material to the building envelope.

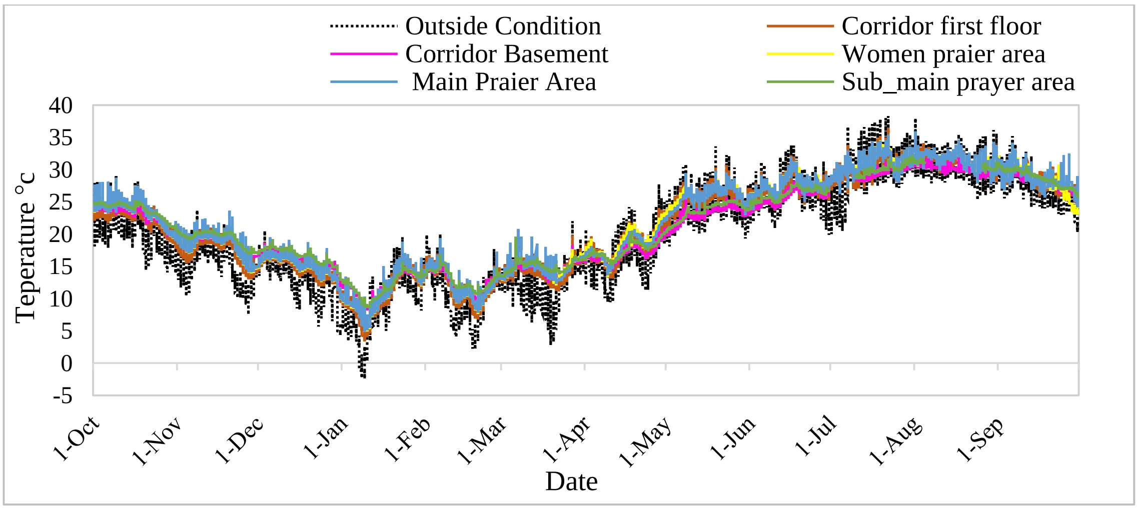

Figure 5.7. Outdoor and indoor measurements temperature for all zones

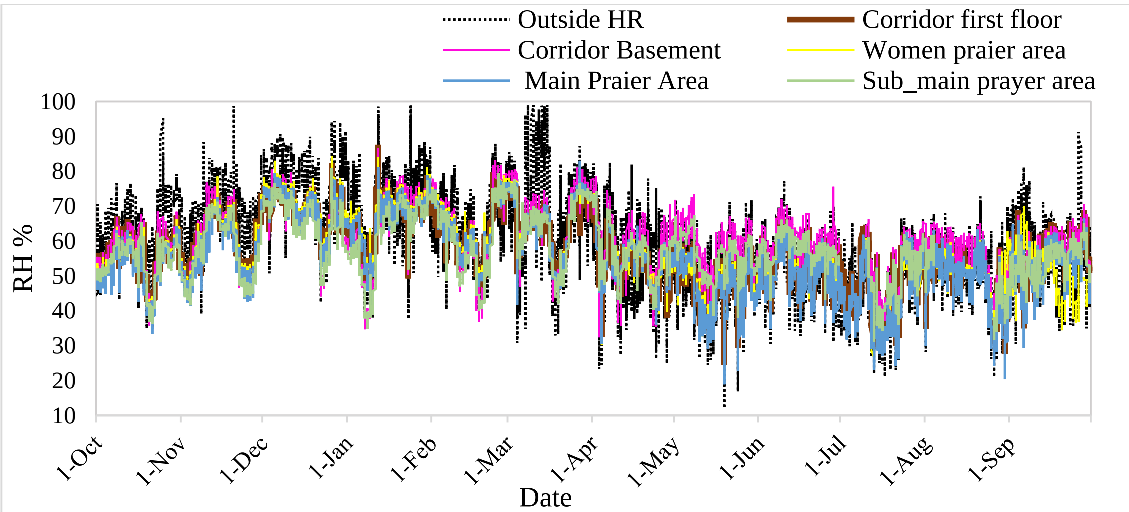

Figure 5.8. Outdoor and indoor measurements relative humidity for all zones

5.1.3. Blower Door Test Result

After the test was done the measured data were used as an input to the TECTITE software to calculate air change per hour. Table 5.2 shows the input data required for the software such as nominal building pressure, fan pressure, nominal flow and temperature adjusted flow. Moreover, inside and outside temperature, barometric pressure and zone volume and floor area were needed as well.

Table 5.2. Input data required for TECTITE.

Nominal Building Pressure (Pa)	Fan Pressure (Pa)	Nominal Flow (cfm)	Temperature Adjusted Flow (cfm)	% Error
0.0	n/a			
-20.5	349.2	7500	7411	3.9
-20.5	313.1	7113	7029	-1.4
-19.5	347.1	7478	7390	3.9
-22.0	285.6	6803	6723	-6.1
-17.5	315.4	7139	7055	-0.1
-15.0	309.9	7078	6994	-0.1
-12.5	296.1	6923	6841	-1.2
0.0	n/a			

The result obtained from the test are summarised in Table 5.3, where the air change per hour calculated as 4.55 (1/h).

Table 5.3. Test result of blower door machine.

Test Results at 50 Pascals	
Airflow (cfm)	7515 (+/- 8.1 %)
Air Changes per Hour (1/h)	4.55
Air Flow Coefficient (Cenv)	6084.4 (+/- 22.6 %)
Air Leakage Coefficient (CL)	5968.1 (+/- 22.6 %)
Exponent (n)	0.059 (+/- 0.078)
Correlation Coefficient	0.31962

5.1.4. Thermal Camera Result

Thermal camera test carried out at 20th March, 2015 at 18:30 pm in order to examine the thermal performance of the mosque, also to specify which part of the mosque has higher heat loos. During the day test the indoor air temperatures recorded (around 12.82 °C) were considerably higher than outdoor air temperatures (around 7.6 °C).

The temperature variations between the inner and outer part of the mosque is due to the non-insulating nature of the wall. This facilitates the rate of heat lost by conduction from inside to outside during the day. This rate of heat transfer varies between different parts of the building with respect to the nature of the materials of construction. The building consists of non-insulating brick walls, glass windows, and the roof is made up of copper-dome. High surface temperature was observed on the brick wall compared to other parts of the building. The dome-roof and the glass window have relatively lower surface temperatures. The heat transfer coefficient of the copper-dome is higher than that of the glass window, which in turn is greater than the walls, the high conductance of the copper-dome and the glass window seems to play a role in heat transfer between the indoor and outdoor air temperatures. Figures 5.9A to 5.9C show the front, east and back view of the mosque and the distribution of surface temperatures at different parts. The yellow color on the wall indicates an intermediate level heat loss, while the hightest amount of heat is dissipated at the walls (red color). The observations made by thermal imaging thus show that the thermal mass characteristic of walls in Salepçioğlu dominates its thermal performance in a way that heat transfer from the inside to the outside slower than the rest of the building envelope. It can be concluded that some precautions about envelope of the mosque and active heat up of inner environment are needed.

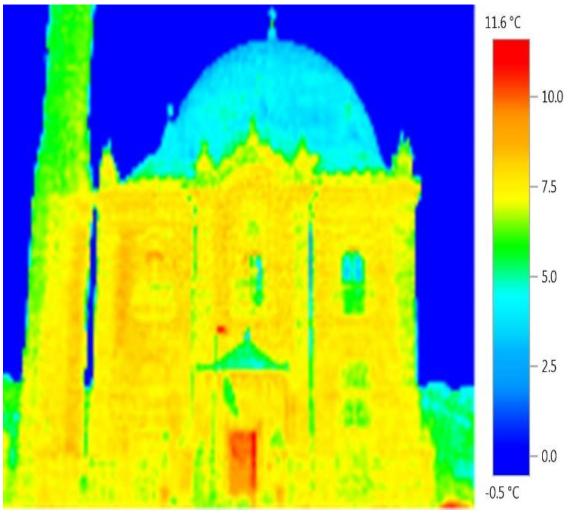

(A)

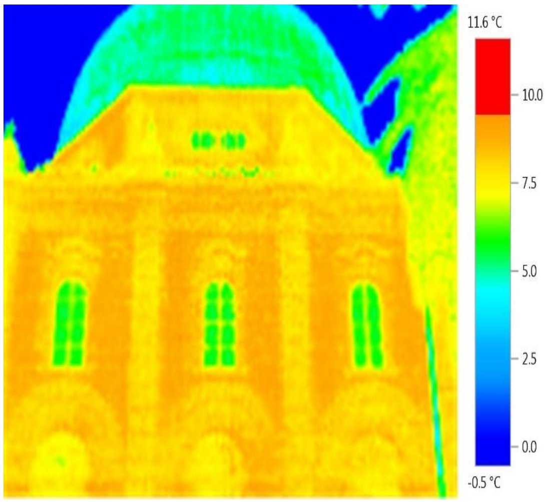

(B)

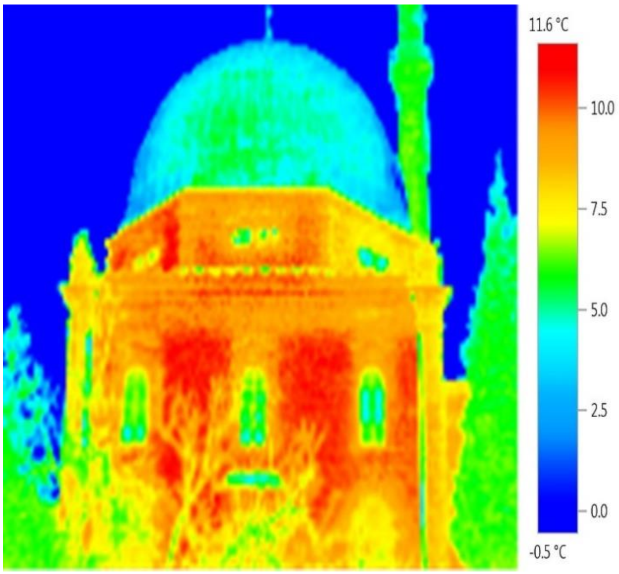

(C)

Figure 5.9. (A). Thermal image of the front view, (B) Thermal image of the east view (C) Thermal image of the back view

5.2. Building Model Creation

Three dimensional model for the case study is created using DesignBuilder software V4.2, Figure (5.3) as stated before in chapter (4), for the purpose of analysing the thermal comfort and applying several of possible scenarios in order to enhance the thermal comfort inside the main prayer area. By following the steps mentioned in (see chapter 4) (section 4.2.1) (chart 4.1), and after all the required information has been entered, the model is ready to be simulated.

The Salepçioğlu Mosque was modelled along with surrounding buildings to observe the shading effects on solar gain calculations (Figure 5.10). Architectural plans and dimensions were obtained from the Architectural Restoration Department of İzmir Institute of Technology and through field investigations.

The model consists of 26 zones as shown in the Figure 5.11. The dimensions of all the 26 zones were measured directly from the AUTOCADE file which provided by the Architectural Restoration Department of İzmir Institute of Technology. All the construction material of walls, windows, doors and domes were chosen and selected from the DB software library after the specification of the real material done as mentioned in chapter 3.

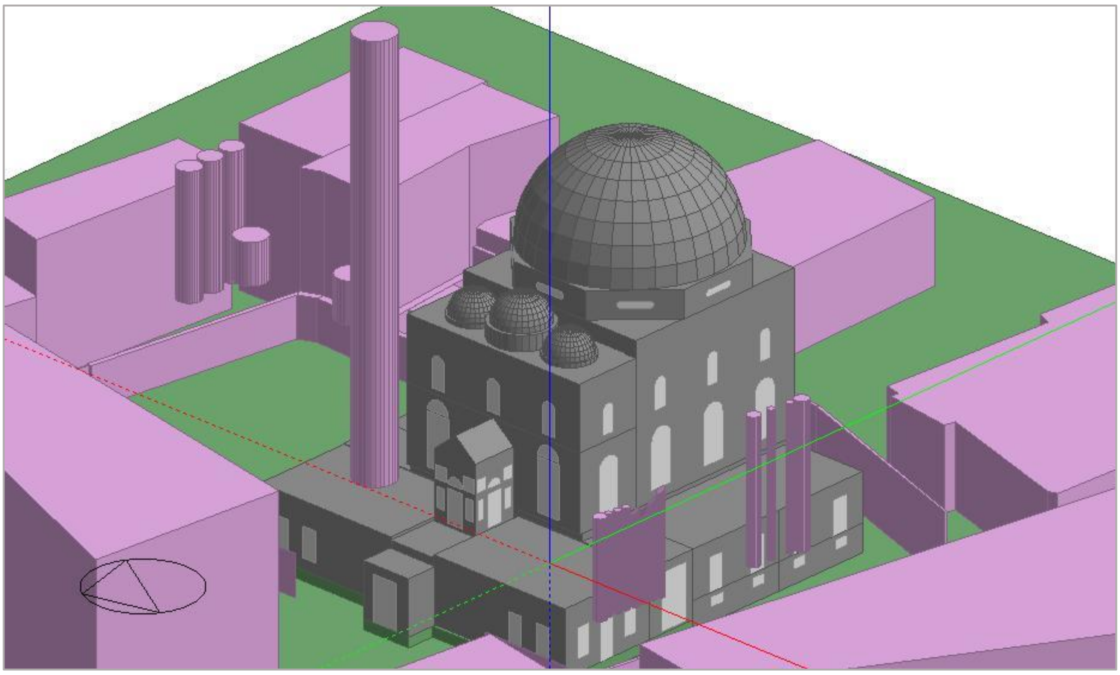

Figure 5.10. 3D model of the case study in DesignBuilder

Same as all the historic buildings, the mosques has a relatively irregular geometry comparing with the modern buildings that have regular shapes and masses. So that, during the design process some assumption were inevitable to simplify the geometry of the building. The Assumptions which made on the building geometry are stated below:

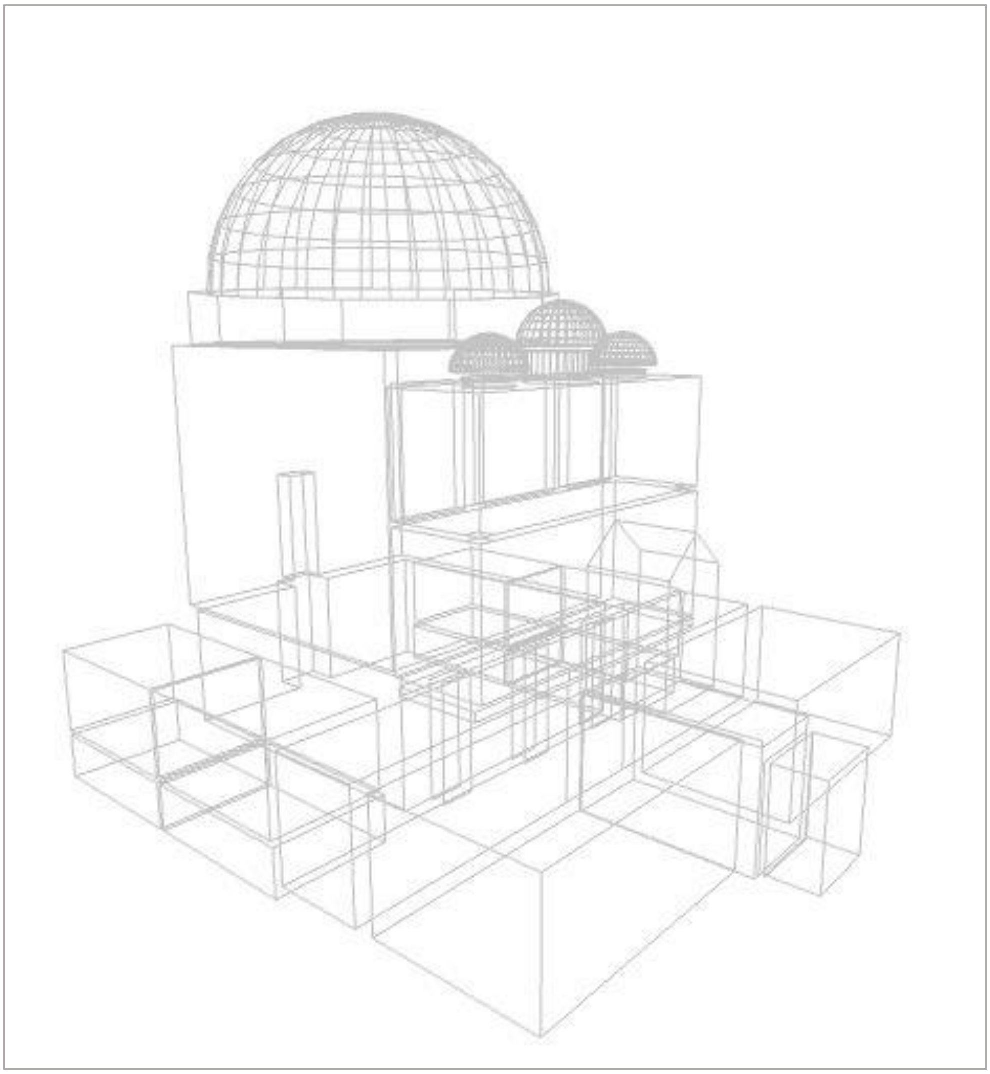

Figure 5.11. Wireframe model of the case study in DesignBuilder

1. The stairs in the building were designed as a whole with respect to its volume that occupied in total. Since DesignBuilder has no ability to model.
2. In DesignBuilder software V4.2, partitions are part of the zone, due to this halves of the partition wall drawing within the affiliated zone.
3. The height of storey is measured from the ceiling surface of a given storey and the ceiling surface of the storey below.
4. Neighbor buildings, minaret and the trees are shown in figure 5.3 in purple coloured items. They are assumed as adiabatic. In order to reduce the simulation time.
5. In DesignBuilder V4.2 has no ability to model double windows with large gaps. Thus, the maximum gap was chosen to design these types of windows.

5.3. Calibration Results

In this study, calibration of the building energy simulation will be made by comparing the measured and simulated indoor air temperature. The outdoor air temperature data were measured for one year and integrated into the simulation weather data file. The results obtained from the simulation were compared to the measured temperatures of each zone. First, the graphical result is presented and then the statistical error result for each zone.

5.3.1. Graphical Calibration for Hourly Measurement Data

In this part, the graphical calibration method is presented. The graphical calibrated were done for the main five zones sub-main prayer area, corridor basement, main prayer area, women prayer area and corridor first floor that located in the basement and the first floor. The comparative result between the measured hourly data and the simulation hourly data are explained and discussed.

5.3.1.1. Basement Floor

Basement floor contains two main zones sub-main prayer area and the corridor basement which are the most occupied zones basement floor.

5.3.1.1.1. Sub-Main Prayer Area Graphical Calibration

Figure 5.4 below shows the comparison result of the dry bulb indoor temperature. Measured data and DB simulated result for one year hourly from October 1st 2014 to September 30th 2015. As it can be seen from the Figure 5.11 some of the measured data were missing. The missing data were in the period between 30 June and 26 August the data missing due to the stop of the data logger device whether because of the battery lifetime or the storage capacity of the hobo logger. Since there was just one data logger fixed on the sub-main prayer area, this period was excluded from the comparative analysis. In Figure 5.12 the purple colour is indicated by simulation data, where the measured data is indicated by dark orange. From the graph below, it can be seen that the simulated and measured data have the same trend with negligible difference between the two datasets regarded to the time periods.

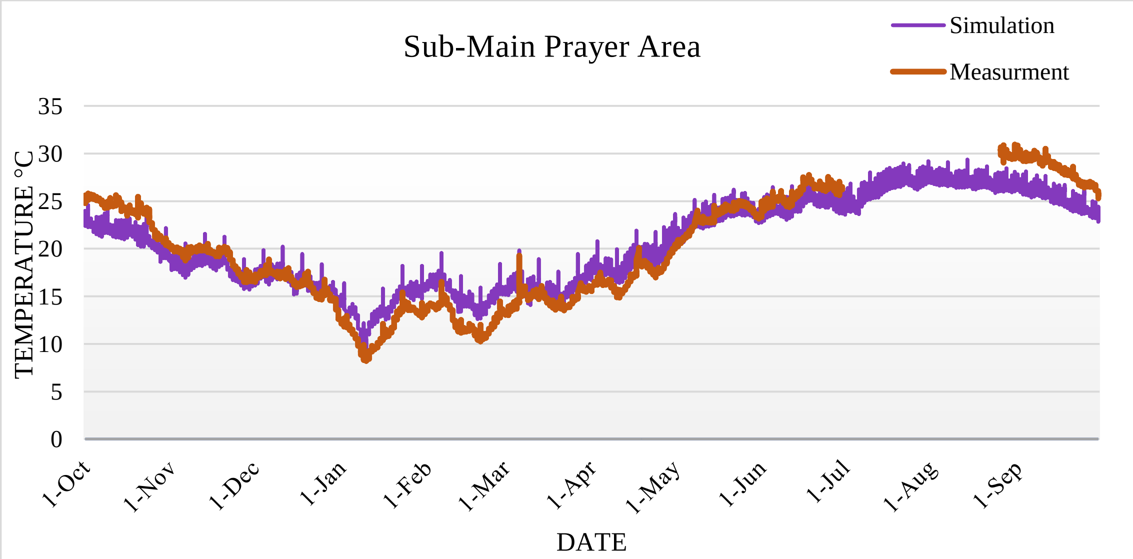

Figure 5.12. Measured vs simulated sub-main prayer area hourly temperature.

5.3.1.1.2. Corridor Basement Floor Graphical Calibration

Figure 5.13. Shows the result data obtain from the DB software for the corridor in basement floor were compared with the measured data through one year hourly from October 1st 2014 to September 30th 2015. Due to the stop of the data logger device, some of the measured data were missing. The stopping of the data logger occurred, whether, because of the battery lifetime or the storage capacity of the hobo logger. The missing data were in the period between 30 June to 10 July the data missing.

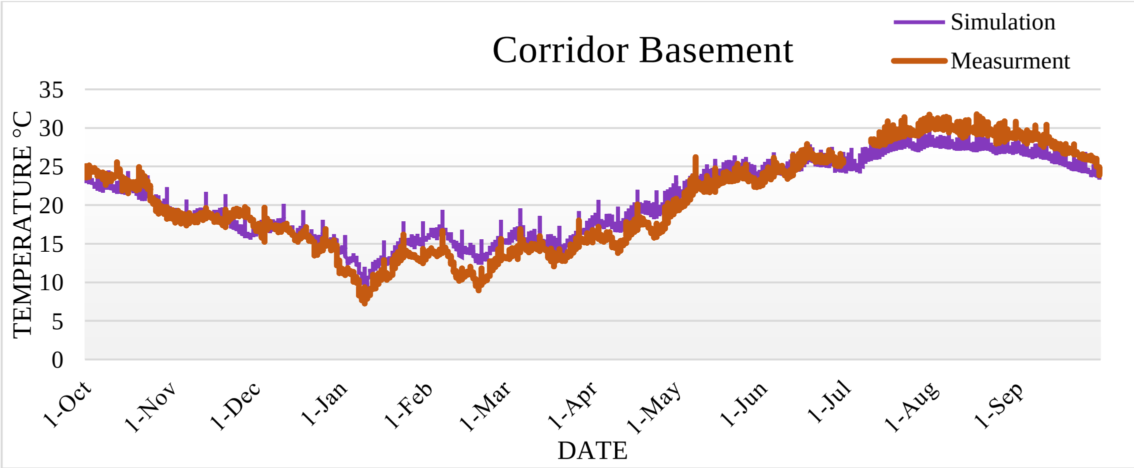

Figure 5.13. Measured vs simulated corridor basement hourly temperature

The purple line which indicates the simulation data result is slightly above the measured data from January to May and below the measured data from July to October, but the results are quite close (Figure 5.12). Furthermore, the rest of the year data are almost exactly at the simulation value from the model.

5.3.1.2. First Floor

The calibration graphical results for the first floor, main prayer area, corridor first floor and women prayer area are illustrated in the Figures below.

5.3.1.2.1. Main Prayer Area

Figure 5.14 shows the comparison between simulation result of the main prayer area and the measured data through one year hourly from October 1st 2014 to September 30th 2015. The missing data were in the period of 21 March to 8 May the data missing. The missing data were covered by another data logger which was installed in the same zone. As it can be seen from the graph the measured data and the simulation data during one-year period have the same trend with negligible temperature differences throughout the period.

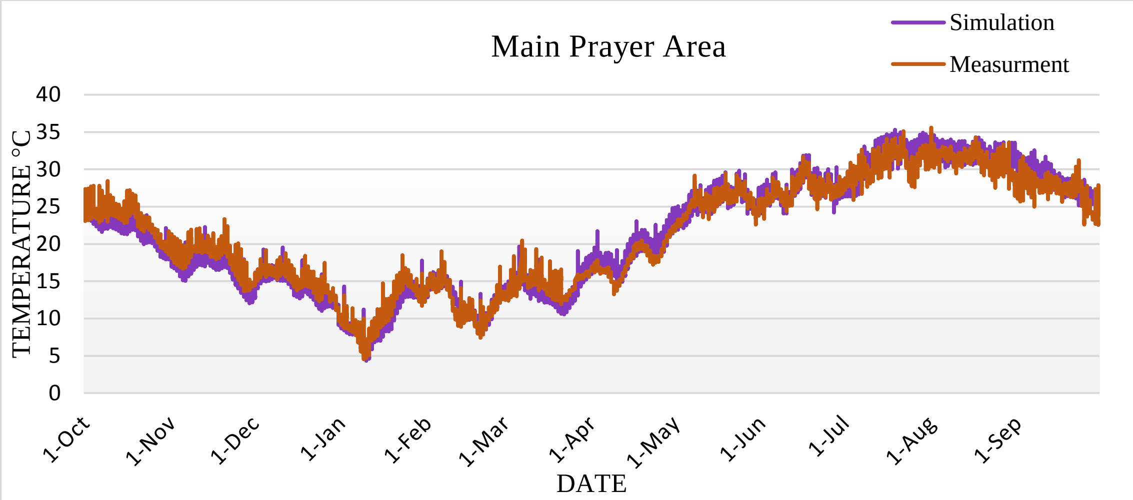

Figure 5.14. Measured vs simulated main prayer area hourly temperature

5.3.1.2.2. Corridor First Floor

Corridor first floor the comparative result illustrated in Figure 5.15. The Figure shows the result for one year hourly data calibration October 1st 2014 to September 30th 2015. Some of the measured data were missing from 17 August to 26 August we see that in Corridor first floor, measured temperatures are very nearly at the model simulation result. However, the comparative result within the uncertainty range.

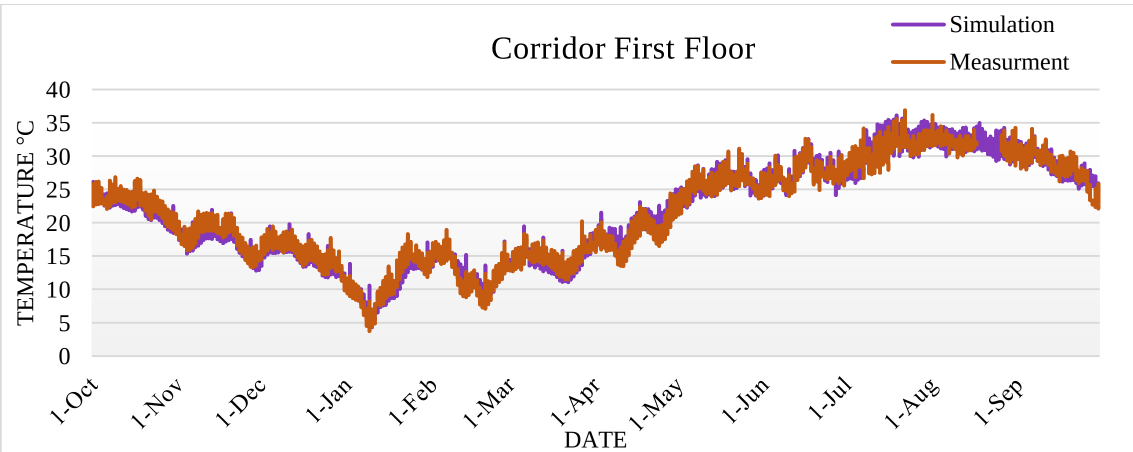

Figure 5.15. Measured vs simulated corridor first floor hourly temperature

5.3.1.2.3. Women Prayer Area

The calibration result for the women prayer area is shown in the Figure 5.16 below. The Figure illustrated that the collected indoor dry-bulb air temperature data through one year hourly from October 1st 2014 to September 30th 2015 and the DB simulation data.

Part of the measured data was missing from 6 March to 20 march, from 29 June to 6 July and from 6 August to28 August due to the technical problems of the data logger such as battery lifetime or the storage capacity of the hobo logger. However, from the graph we see that in women prayer area, model simulation result temperatures are provided results very close to measurements data.

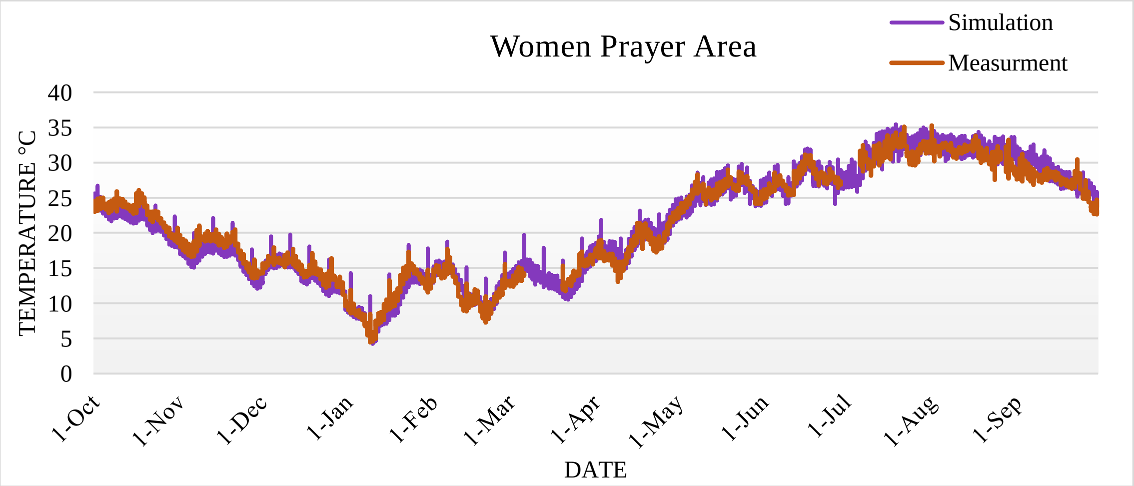

Figure 5.16. Measured vs simulated women prayer area hourly temperature

5.3.2. Statistical Calibration for Hourly Measurement Data

The statistical calibration between the simulation hourly dry-bulb temperatures and the measured hourly dry-bulb temperatures result for the each zone are summarised in Table 5.4. The mean bias error (MBE) and root mean square error (RMSE) were calculated using equation 4.1 and 4.2 respectively. The model is assumed to be calibrated since the acceptable range for the errors were achieved for all zones as explained in chapter 4.

Table 5.4. Error calculation between the simulated data and the measured data for each zone.

Zones	MBE %	RMSE %
Main prayer are	-0.80	6.93
Women prayer area	-0.617	5.91
Corridor first floor	0.14	4.97
Sub-Main prayer area	0.017	10.19
Corridor downstairs	1.54	8.95

For the main prayer area, the errors were calculated for each month, to ensure that we will obtain the high accuracy of the analysis. The main prayer area is the most occupied zone in the building during the day, and in this study, the comfort analysis was done in the main prayer area so it is more accurate that to calibrate the zone monthly by using hourly data. In Table 5.5 errors analysis between the simulated hourly data and the measured hourly data for the main prayer area are presented. The obtained results show that the acceptable tolerance which provided by ASHRAE Guideline 14 (ASHRAE 2002) were within the acceptable range of the MBE and RMSE when the hourly dry bulb temperature data were used.

Table 5.5. Monthly summary for Root Mean Square Error and Mean Bias Error for the main prayer area.

Month	MBE (%)	RMSE (%)
Jan	-8.81	14.10
Feb	1.68	7.62
Mar	-5.00	11.98
Apr	5.48	9.38
May	0.60	3.70
Jun	0.97	3.52
Jul	1.30	4.47
Aug	1.87	3.92
Sep	4.12	6.81
Oct	-5.59	6.87
Nov	-9.26	10.56
Dec	-6.69	9.48

5.4. Thermal Comfort Analysis

The results of thermal comfort analysis of the Baseline model and six scenarios that used for enhancing the thermal comfort in the historic mosque are presented and summarised. The analysis was done for one year with a total period of 8760 hours, for the main prayer area.

The ASHRAE graphical results are explained in appendix A, on monthly comparison for all scenarios and the baseline model. The compression between the scenarios and the baseline model were done monthly and for the total period. The analysis dealt with the total daytime (night and day periods). Figure (5.16-5.24) present the data analysis for the total time of the day, for the baseline model and the scenarios. It is presented monthly and for the whole year for each scenario.

5.4.1. Thermal Comfort Analysis of the Baseline Model (Measured Data)

The measured data that collected through the period of study are analysed and examined in terms of thermal comfort. From the analysis, it is found that the mosque experienced discomfort hours by 5042 hours by 57.55% out of 8760 hours in the year. The highest number of discomfort hours were found in January, February and December with 100% out of the acceptable range. The second highest discomfort hours recorded in March, April, November and August with 726 hours by 97.58%, 598 hours by 83.05%, 590 hours by 81.94%, and 536 hours by 72.04% respectively. The lowest discomfort hours found in May as 6 hours by 0.80%, June as 8 hours by 1.11%, July as 379 by 50.94%, September as 17 hours by 2.36% and October as 22 hours by 2.95%. (Figure 5.17)

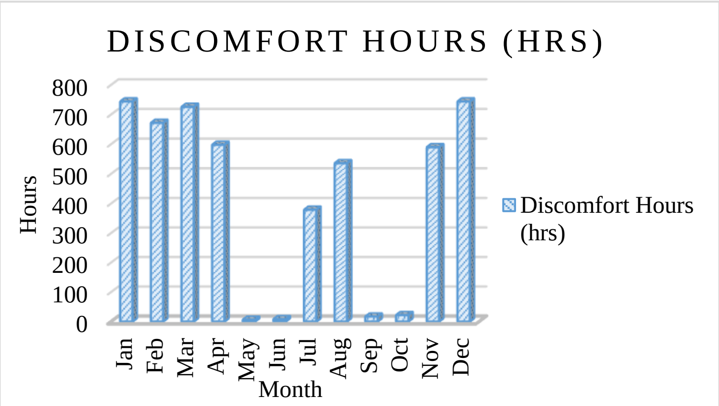

Figure 5.17. Discomfort hours (Measured Data)

5.4.2. Thermal Comfort Analysis of the Baseline Model (simulation Data)

On a monthly comparison, for the baseline model the highest number of discomfort occurs in January, February, March and December as 744, 672, 744, and 744 where they accounted for 100% out of the range, respectively. Besides these months, August, November and April experienced a high number of discomfort as 742 hours by

99.73%, 717 hours by 99.58% and 527 hours by 73.19% respectively. The lowest discomfort hours were found on May as zero hours and it is followed by June as 19 hours by 2.64%, September as 70 hours by 9.72%, October as 139 hours as 18.68% and July as 500 hours by 67.20%. Through one year simulation period occupants reported experiencing 5618 hours of discomfort hours by the percentage of 64.13%. (Figure 5.18)

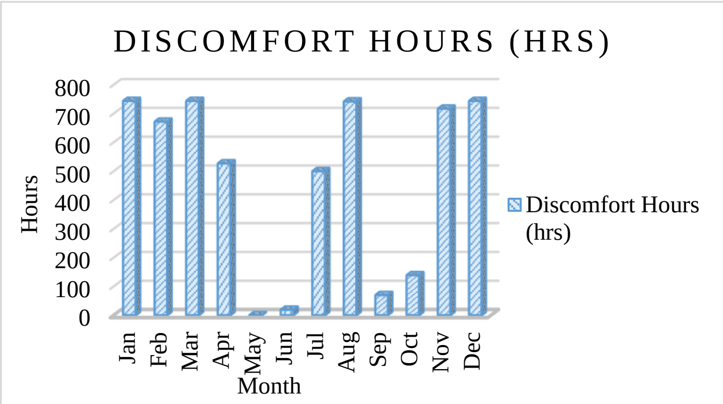

Figure 5.18. Discomfort hours (simulation Data)

Comparing the results that found from the measured data with that found from the simulation of the baseline model, it shows a remarkable similarity in terms of thermal comfort analysis. Through one year analysis, the discomfort hours was 5042 hours by 57.55% from the measured data while that found from the simulation of the baseline model was 5618 hours by 64.13% which is higher than the real case by 576 hours of discomfort. Month to month comparison it was found that the discomfort hours differ from month to month. While some experience increase in discomfort hours and some experience decrease and others stayed same. In January, February and December, the discomfort hours of the simulated baseline model were found same as the measured data recorded from the mosque. The decrease of the discomfort hours was in April as 71 hours and May as 6 hours, where the increasing in the discomfort hours found in march, June, July, august, September, October, and November as 18, 11, 121, 206, 53, 117, 127 hours. (Figure 5.19)

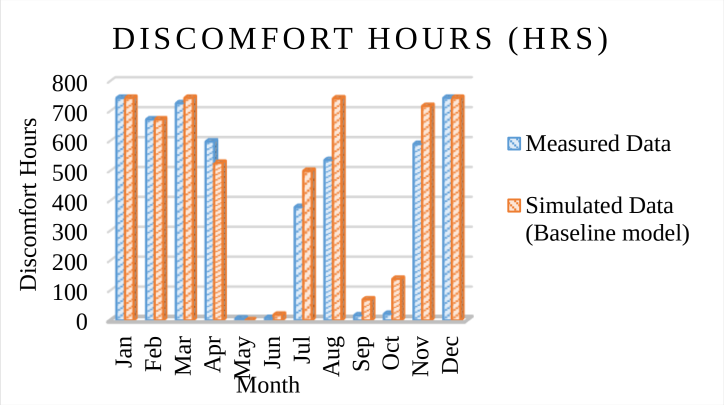

Figure 5.19. Discomfort hours.
(Compression of measured data against simulation data)

5.4.3. Thermal Comfort Analysis of the Design Strategies

The scenarios used in order to find the best way to increase the level of comfort time inside the mosque in the main prayer area.

5.4.3.1. Windows with Double Glasses

Windows with double glass are used to enhance the thermal conductivity of the windows. In order to reduce the amount of heat transfer from or to the building to increase the number of comfort hours.

The highest number of discomfort hours were found in January, February, March and December without any changes in the number of discomfort hours comparing with the baseline model. The discomfort hours calculated in April as 527 hours, May as zero hours and November as 717 hours which are the same results found for the baseline model. In compression with the baseline model, the occupants experienced decreasing in discomfort hours in June where it is dropped from 19 hours to 18 hours, in July from 500 hours to 491 hours, August from 742 hours to 740 hours and October from 139 hours to 131 hours. While increasing the discomfort hours founded in September from 70 hours to 75 hours. (Figure 5.20)

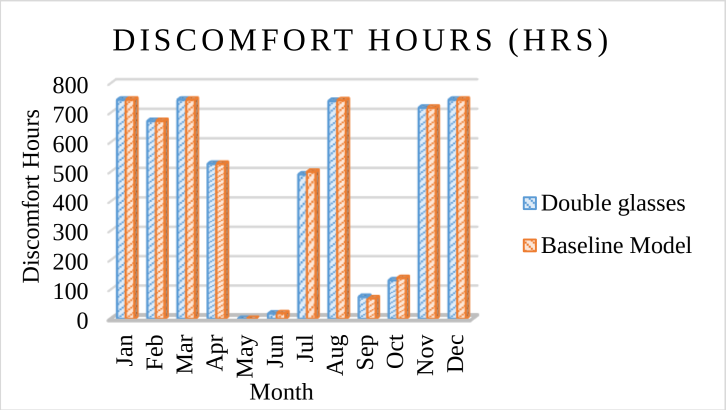

Figure 5.20. Comparison of the discomfort hours between windows with double glasses and baseline model

Through one year simulation period occupants reported experiencing 5603 hours of discomfort hours by percentage of 63.96%. While for comfort hours, it is reported as 3157 hours by 36.04%. This is a 0.17% of the reduction in the discomfort hours by 15 hours from the baseline model.

5.4.3.2 Double Glasses with low-Emissivity

The reduction in discomfort hours occurred on June as 12 July as 51 hours August as 40 hours September as 11 hours and October as 4 hours. The number of discomfort hours stayed without change comparing with the baseline model in months (January, February, May and December). In April and November recorded an increase in discomfort hours by 49 and 1 hours, respectively. (Figure 5.21)

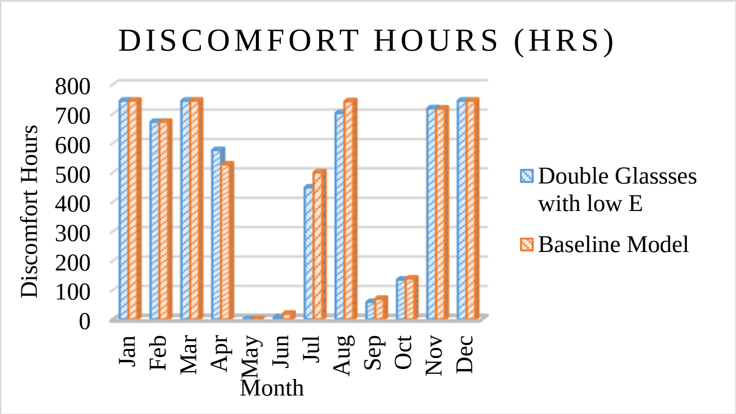

Figure 5.21. Comparison of the discomfort hours between double low-emissivity glasses and baseline model

Through one year simulation period occupants reported experiencing 5550 hours of discomfort hours by percentage of 63.36 %. While for comfort hours, it is reported as 3210 hours by 36.64%. This is a 0.77% of the reduction in the discomfort hours by 68 hours from the baseline model.

5.4.3.3. Roof Insulation

Comparing with the baseline model no change were observed on January, February, March and December where the number of discomfort hours found same as 100% out of the comfort range. The discomfort hours calculated on May as zero hours, July as 500 hours and November as 717 hours which are the same results found for the baseline model. The occupants experienced decreasing in discomfort hours on April where it is dropped from 527 hours to 524 hours, June from 19 hours to 18 hours and October from 139 hours to 127 hours. While increasing the discomfort hours founded in August from 742 hours to 743 hours and September from 70 hours to 78 hours. (Figure 5.22)

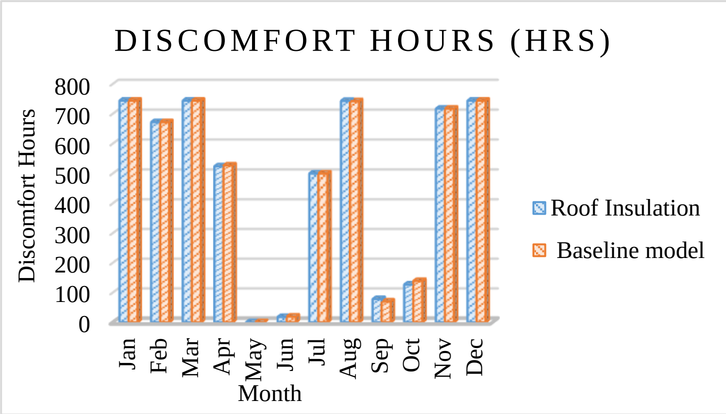

Figure 5.22. Comparison of the discomfort hours between roof insulation and baseline model

Through one year simulation period, occupants reported experiencing 5611 hours of discomfort hours by percentage of 64.06%. While for comfort hours, it is reported as 3149 hours by 35.94%. The baseline model experience a negligible reduction in discomfort hours as 7 hours by 0.08%.

5.4.3.4. Combination of Double Glasses with Low-Emissivity and Roof Insulation (Double LE Glass and R. Ins.)

Figure 5.23 shows discomfort hours of the combination between scenarios 2 and 3. Occupants experienced discomfort for 5534 hours throughout the year. This is 63.17% discomfort against 64.13% discomfort hours of the baseline model out of the total simulation period. There is 84 hours by 0.96% of t reduction in the baseline model discomfort.

The highest number of discomfort registered on January, February, March and December which is the same result obtained from the baseline model. The effect of this scenario appear on June, July, August, September and October by reduction of discomfort 17, 57, 40, 8 and 14 respectively with a total reduction of 136 hours. On May discomfort hours stayed constant with zero hours while April and November experience increase in discomfort hours by 51 and 1 hours as shown Figure 5.23 below.

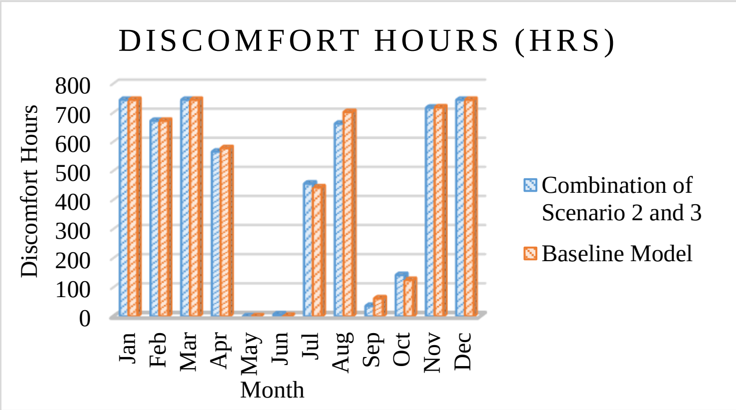

Figure 5.23. Comparison of discomfort hours between combination of double glasses with low-emissivity and roof insulation and baseline model

5.4.2.5. Nighttime Ventilation

The nighttime ventilation technique was used for overheated months. Therefore the effect of this scenario appeared on the hot months from May to October. Figure 5.24. Shows the result of nighttime ventilation with respect to baseline mode result. Comparing with the baseline model, the output shows that discomfort hours stayed constant with zero hours. However, in June, July, August and September occupants experienced a decline in discomfort hours as 12, 44, 80, 34 hours respectively. This is 170 hours of reduction in discomfort hours which is 3.78% decreasing in the baseline model discomfort hours.

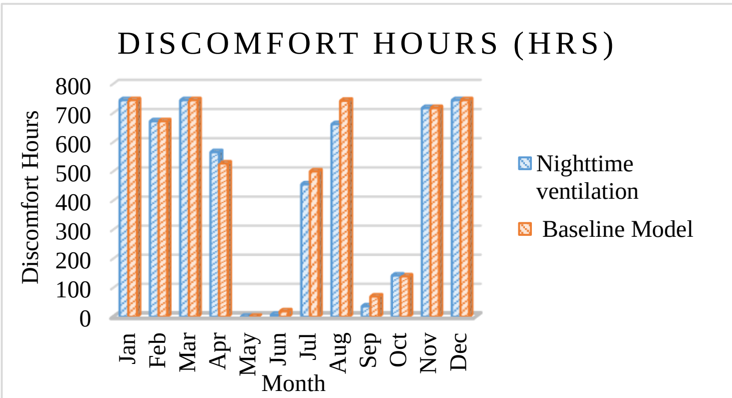

Figure 5.24. Comparison of the discomfort hours between nighttime ventilation and baseline model.

5.4.2.5. Underfloor Heating System

The underfloor heating system was designing for winter period (January, February, March, October November and December) where there are overcooling. Therefore, on summer season no change occurred on the discomfort hours that due to the system was set as off. The lowest discomfort hours were obtained on October as zero hours by decreasing 139 hours from the baseline model discomfort hours. While the highest number of discomfort registered on January as 446 hours by 60% of discomfort in the baseline model was 744 hours 100% of discomfort. In February, March, November, December discomfort hour founded as 257, 247, 157, 262 hours respectively. (Figure 5.25)

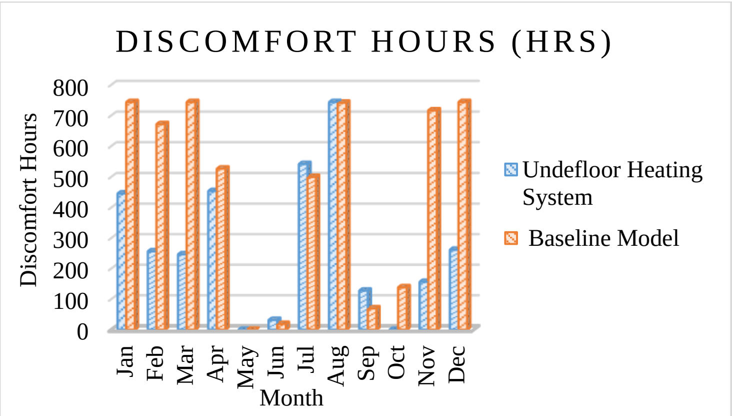

Figure 5.25. Comparison of discomfort hours between model with underfloor heating and baseline model

Through the cold season, occupants reported experiencing 1369 hours of discomfort hours by 31.34% while the comfort hours were calculated as 2999 hours out of 4368 total hours. However, baseline model it was reported as 3760 of discomfort hours by 86.08% and 608 of comfort hours. As a result of applying underfloor heating strategy, baseline model experiences a reduction in discomfort hours by 54.74% in the cold season period.

CHAPTER 6

CONCLUSIONS

One-year thermal comfort analysis of a naturally ventilated historic mosque located in Izmir, Turkey was studied to evaluate and enhance suitable thermal conditions. The analysis was simulated using DesignBuilder software modelling. Graphical and statistical calibrations were done based on ASHRAE Guideline 14 _2002. Statistical acceptance ranges were done using the mean bias error (MBE) and root mean square error (RMSE). Then thermal comfort was investigated based on adaptive thermal comfort method provided by ASHRAE standard 55-2010. Different scenarios were examined throughout the study in order to establish the most effective thermal comfort conditions in the mosque.

The result of the simulation indicated that, the model on baseline scenarios showed a higher number of hours of thermal discomfort during the cold period. The occupants experienced 5618 hours of discomfort amounting to 64.13% of the study period; and the comfort period of 3142 hours (35.87%).

Application of double glass window strategy caused a negligible (0.17%) reduction in the discomfort of the baseline model. The result obtained from double glasses with low emissivity, estimated the reduction in the baseline model discomfort hours as 0.77%. On using the roof insulation strategy, reduction of discomfort amounted to 0.08% hours from the baseline. The combination of windows with double low-E glasses and roof insulation somewhat improved thermal comfort by 0.96%; slightly better than the previous strategies.

During the hot season, nighttime opening-window method of ventilation was found to improve thermal comfort by 3.78%. The last scenario was done for cold months by using an underfloor heating system. The result showed a better enhancement of thermal comfort in the mosque, with 54.74% improvement during the study period. This strategy lowered the initial 64.13% percentage thermal discomfort to 31.34% (1369 hours).

In a seasonal analysis, for the winter season (January, February and December) the best result was found with underfloor heating system scenario with 45% of discomfort hours. The rest of the scenarios showed no significant improvement on thermal discomfort hours when compared with the baseline model. Figure 6.1 illustrates the comparison of different scenarios with the baseline thermal discomfort conditions during the winter season.

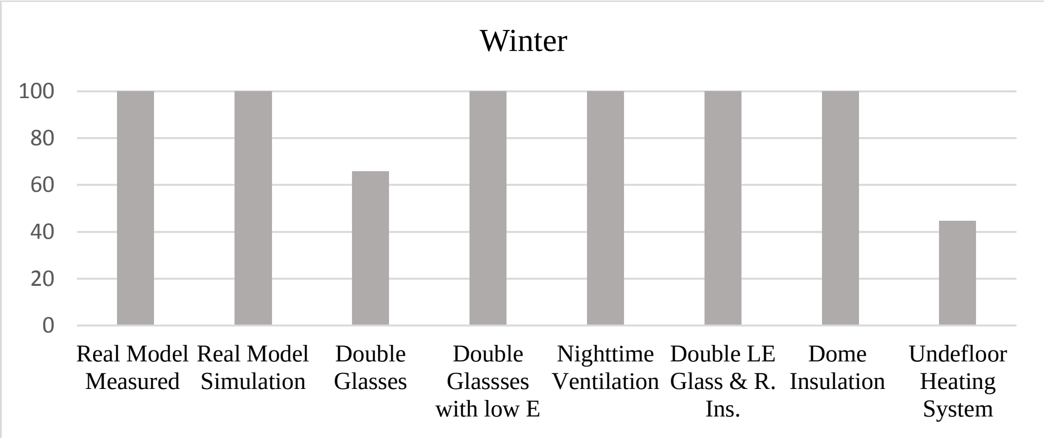

Figure 6.1.discomfort hours of winter season for scenarios and baseline models

In spring season (March, April and May) the lowest percentage discomfort (45%) was found in the application of underfloor heating system. The second best result was obtained by using roof insulation system, where the discomfort percentage amounted to 57.43%. Figure 6.2 shows the performance of different thermal comfort strategy in comparison with the baseline model during the spring season.

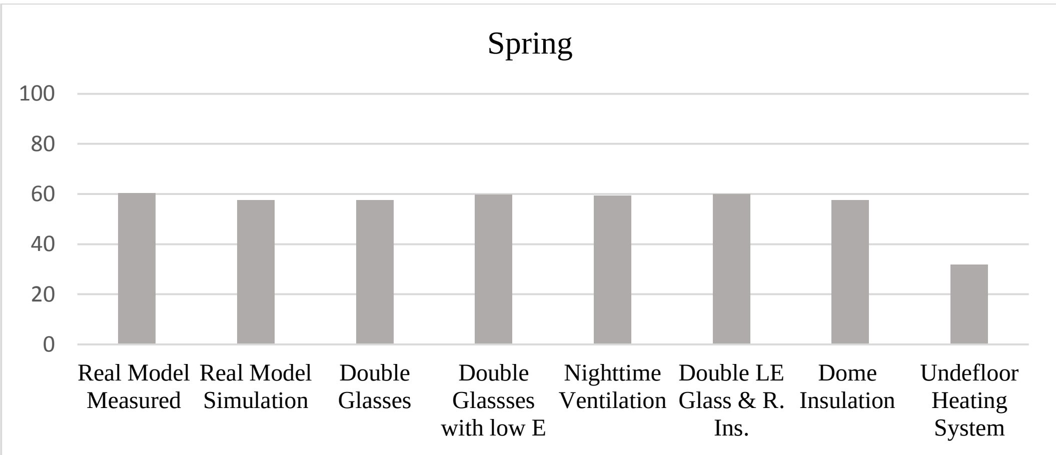

Figure 6.2. Discomfort hours of spring season for scenarios and baseline model

During the summer period (June, July and August), the baseline measured and baseline simulated analysis recorded 41.80% and 57.11% of discomfort hours respectively. From the scenarios, there was no substantial reduction in the percentage discomfort. However, the best result was obtained on the use of nighttime ventilation strategy (50.95% of discomfort hours). This is followed by the combination of double glasses with low-emissivity and roof insulation with 51.95% discomfort as shown in Figure 6.3.

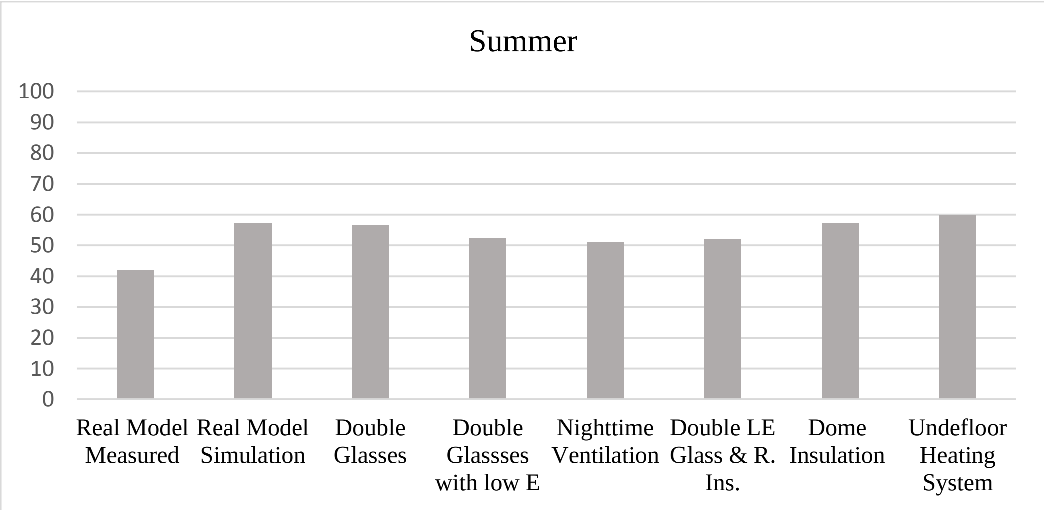

Figure 6.3. Discomfort hours of summer season for scenarios and baseline models

Figure 6.4 shows the percentage of discomfort hours for the autumn season for both scenarios and baseline model. In autumn season (September, October and November) the discomfort hours for the baseline measured and simulated data were found as 28.8% and 42.4% respectively. The lowest number of discomfort hours was found on the use of the underfloor heating system with 13.05%. The second best result was obtained for the nighttime ventilation strategy with 40.98% discomfort hours.

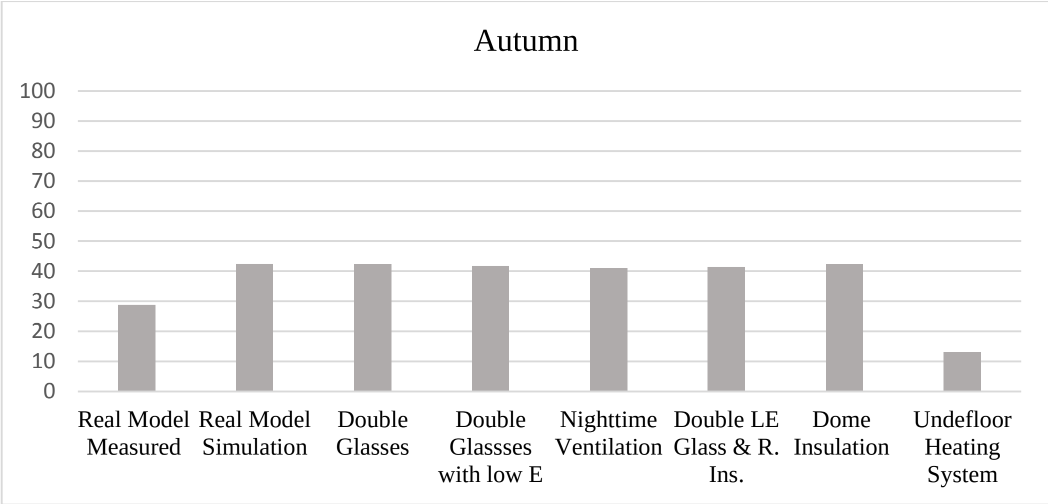

Figure 6.4. Discomfort hours of autumn season for scenarios and baseline models

In the case of historic buildings, any scenario should be carefully chosen in order not to compromise the heritage value of the building. This thereby limited the number of scenarios that could be evaluated. The mosque has a unique painting on the walls for which no mechanical system is allowed to be used. From this study we concluded that the scenarios presented have significant effects on the hot season while the cold season does not render sufficient enhancement on the number of comfort hours. Therefore, application of heating and cooling systems may be necessary depending on the season. For example, during the winter (December, January, February and March), only the underground heating technique substantially increased thermal comfortability of the building. However, a slight compromise may be required base on the sensitivity of the building materials to the proposed thermal comfort scenarios.

Most mosques, due to their high ceiling will create an upper warm zone because of the air stagnation warm periods. To ensure achieving thermal comfort at reduced energy requirements, underfloor heating and cooling system can be used to heat and cool the lower level (level of occupancy). It is however recommended that the strategy of nighttime ventilation with the Combination of Double Glasses with low-Emissivity and Roof Insulation be used together. This is expected to improve the insulation system of the building; thereby lowers the rate of heat transfer from the environment. On the other hand, underfloor heating system with intermittent operation schedule facilitates better thermal comfort; while also preserving the sensitivity of the building. This same strategy is applicable with underfloor cooling system during the hot season. In summary, application of any of these strategies must be in conformity with heritage value of the building.

One thing should be considered, is that the effect of the relative humidity on the painted wall and the mosque envelope. Since the thermal comfort is a state of mind that each person has a different response to the same environmental condition, questionnaire by using a Fanger’s model of thermal comfort recommended being done at least once a month for each season to a better understanding of thermal comfort in the mosque. The linear regression analysis can be done for the actual mean vote on operative temperature, then the neutral operative temperature for Prayers can be estimated and compered with the adaptive thermal comfort model.

REFERENCES

Al-Homoud, M. S., Abdou, A. A., and Budaiwi, I. M. (2009). Assessment of monitored energy use and thermal comfort conditions in mosques in hot-humid climates. *Energy and Buildings, 41*(6), 607-614. doi: 10.1016/j.enbuild.2008.12.005

ASHRAE, A. (2010). ASHRAE/IES standard 55-2010, thermal environmental conditions for human occupancy. *American Society of Heating, Air-Conditioning and Refrigeration Engineers, Inc, Atlanta*.

Brager, G. S., and de Dear, R. (2001). Climate, comfort, and natural ventilation: a new adaptive comfort standard for ASHRAE standard 55.

BlowerDoor.(2015)http://www.builditsolar.com/Projects/Conservation/Southface22blowdoor.pdf (Accessed, 2015)

Chu, Y.-C., Hsu, M.-F., and Hsieh, C.-M. (2015). A Field Assessment on Natural Ventilation and Thermal Comfort of Historic District—A Case of the Wugoushui Settlement in Taiwan. *Journal of Earth Science and Engineering, 5,* 463-472.

Corgnati, S. P., Filippi, M., and Viazzo, S. (2007). Perception of the thermal environment in high school and university classrooms: Subjective preferences and thermal comfort. *Building and Environment, 42*(2), 951-959.

Darby, S., and White, R. (2005). Thermal Comfort: Background Document C for the 40% House Report. *Environmental Change Institute University of Oxford*.

DB. (2014). "DesignBuilder - Building Simulation Software." Retrieved from. http://www.designbuilder.co.uk/content/view/43/64/.

De Dear, R. (2007). *Adaptive comfort applications in Australia and impacts on building energy consumption.* Paper presented at the Proceedings of the 6th International Conference On Indoor Air Quality, Ventilation and Energy Conservation in Buildings (IAQVEC 2007), Sendai, Japan.

De Dear, R., and Brager, G. S. (2001). The adaptive model of thermal comfort and energy conservation in the built environment. *International Journal of Biometeorology, 45*(2), 100-108.

De Dear, R. J., Brager, G. S., Reardon, J., and Nicol, F. (1998). Developing an adaptive model of thermal comfort and preference/Discussion. *ASHRAE transactions, 104*, 145.

Energy Saving Trust.(2015). Retrieved July 12, 2015, from the webpage http://www.energysavingtrust.org.uk/

EP. (2015). "EnergyPlus Energy Simulation Software." Retrieved from the webpage http://apps1.eere.energy.gov/buildings/energyplus/energyplus_about.cfm.

Fanger, P. O. (1970). Thermal comfort. Analysis and applications in environmental engineering. *Thermal comfort. Analysis and applications in environmental engineering.*

Gagliano, A., Patania, F., Nocera, F., and Signorello, C. (2014). Assessment of the dynamic thermal performance of massive buildings. *Energy and Buildings, 72,* 361-370.

Heating, A. S. o., Refrigerating, Engineers, A.-C., and Institute, A. N. S. (2004). *Thermal environmental conditions for human occupancy* (Vol. 55): American Society of Heating, Refrigerating and Air-Conditioning Engineers.

Heritage, E. (2011). Energy Efficiency and Historic Buildings, Application of Part L of the Building Regulations to historic and traditionally constructed buildings. *English Heritage, March*.

HOBO. (2014). "Data Loggers HOBO® Data Logger Products by Onset." Retrieved from http://www.onsetcomp.com.

Humphreys, M. A., Nicol, J. F., and Raja, I. A. (2007). Field studies of indoor thermal comfort and the progress of the adaptive approach. *Advances in Building Energy Research, 1*(1), 55-88.

Ibrahim, S., Baharun, A., Nawi, M., and Junaidi, E. (2014). Assessment of thermal comfort in the mosque in Sarawak, Malaysia. *International Journal of Energy and Environment, 5*(3), 327-334.

İzmir Kent Rehberi. (2015). Retrieved July 12, 2015, from the webpage https://www.izmir.bel.tr/IzmirKentRehberleri/131/185/tr.

Moossavi, S. M. (2014). Adaptive Thermal Comfort Model.

Nicol, F., Humphreys, M., and Roaf, S. (2012). *Adaptive thermal comfort: principles and practice*: Routledge.

Nicol, J. F., and Humphreys, M. A. (2002). Adaptive thermal comfort and sustainable thermal standards for buildings. *Energy and Buildings, 34*(6), 563-572.

F. Noh-Pat, J. Xaman, G. Alvarez, Y. Chaves, J. Arce. (2001). Thermal analysis for a double glazing unit with and without a solar control film (SnS–CuxS) for using in hot climates *Energy Build., 43 , 704–712.*

Saeed, S. (1996). Thermal comfort requirements in hot dry regions with special reference to Riyadh part 2: for Friday prayer. *International journal of ambient energy, 17*(1), 17-21.

Saeed, S. A. (1993). Thermal comfort requirements in hot dry regions with special reference to Riyadh, Part 1: For university students. *International journal of ambient energy, 14*(3), 147-154.

Sateri, J. (2004). Performance Criteria of Buildings for Health and Comfort. *CIB REPORT*.

Toe, D. H. C., and Kubota, T. (2013). Development of an adaptive thermal comfort equation for naturally ventilated buildings in hot–humid climates using ASHRAE RP-884 database. *Frontiers of Architectural Research, 2*(3), 278-291. doi: 10.1016/j.foar.2013.06.003

Testo. (2015) "thermal camera producted by testo" Retrieved April 15, 2015 from https://media.testo.com/media/64/de/166633d61c83/testo-875-Instruction-manual.pdf

Testo SE and Co. KGaA (2015). Retrieved April 15, 2015, from the webpage https://media.testo.com/media/c5/bc/d68aebc9060a/testo-635_Data-Sheet.pdf

Widström, T. (2012). Enhanced Energy Efficiency and Preservation of Historic Buildings: Methods and Tools for Modeling.

APPENDIX A

GRAPHICAL RESULT OF ADAPTIVE THERMAL COMFORT

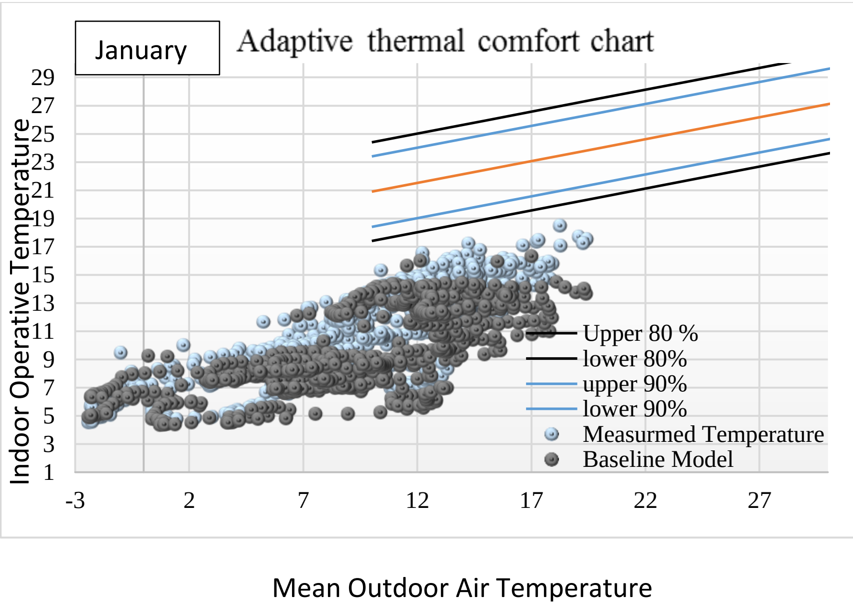

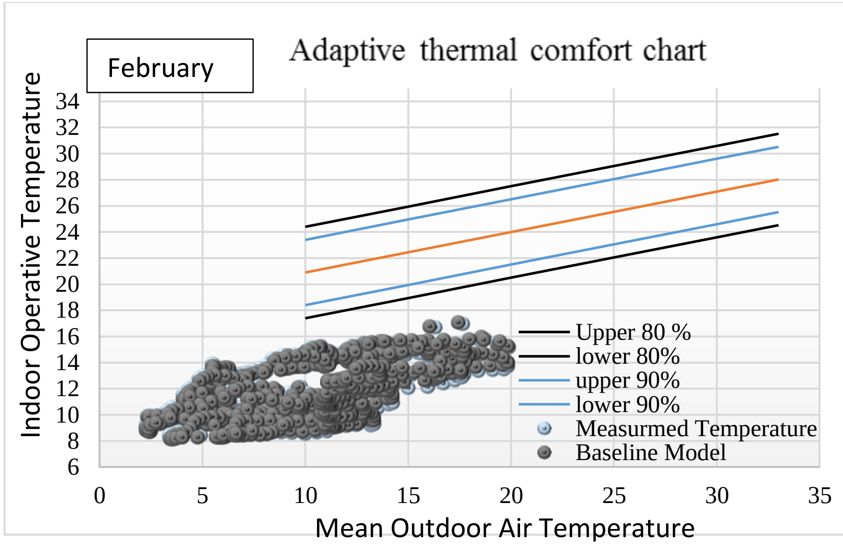

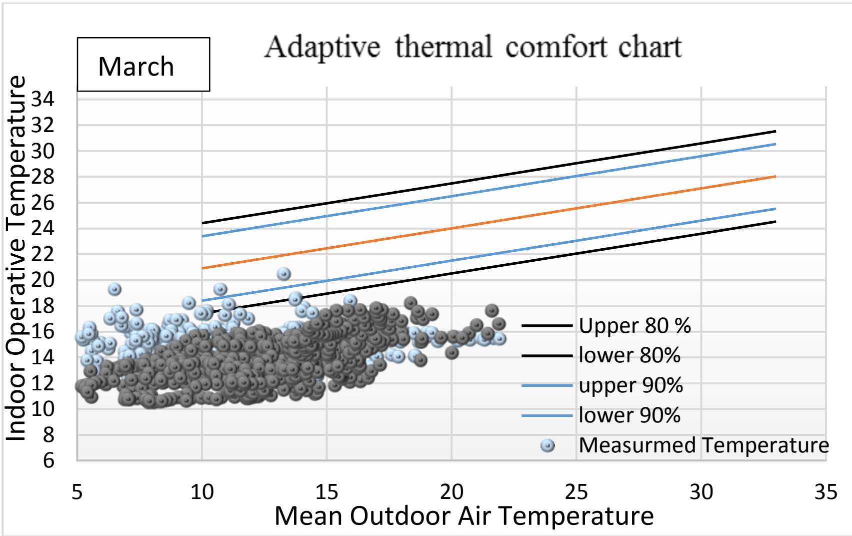

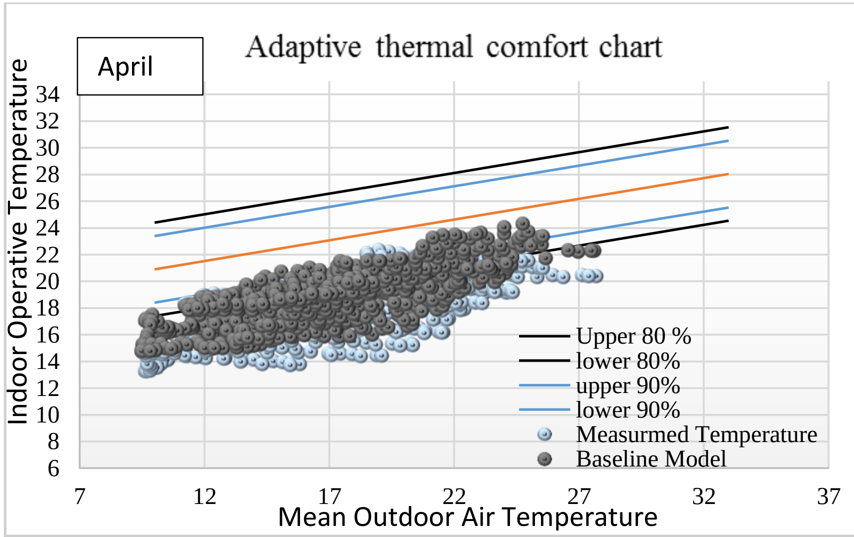

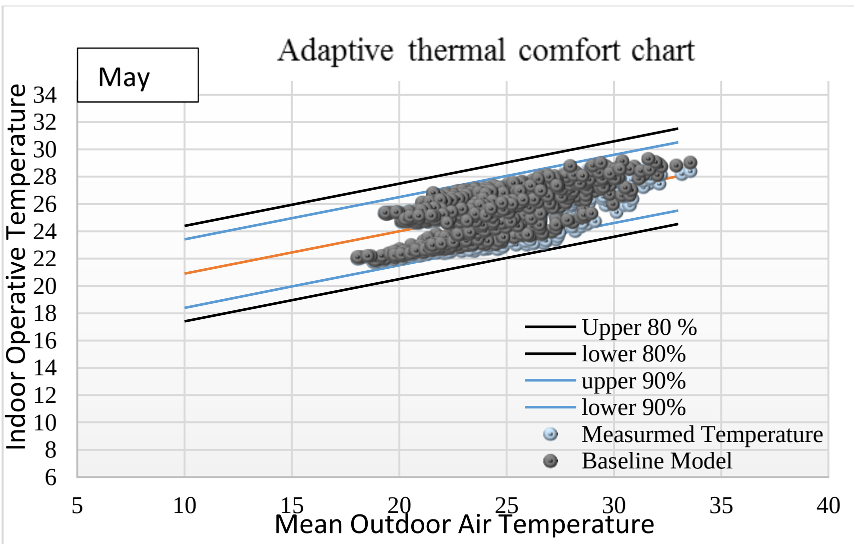

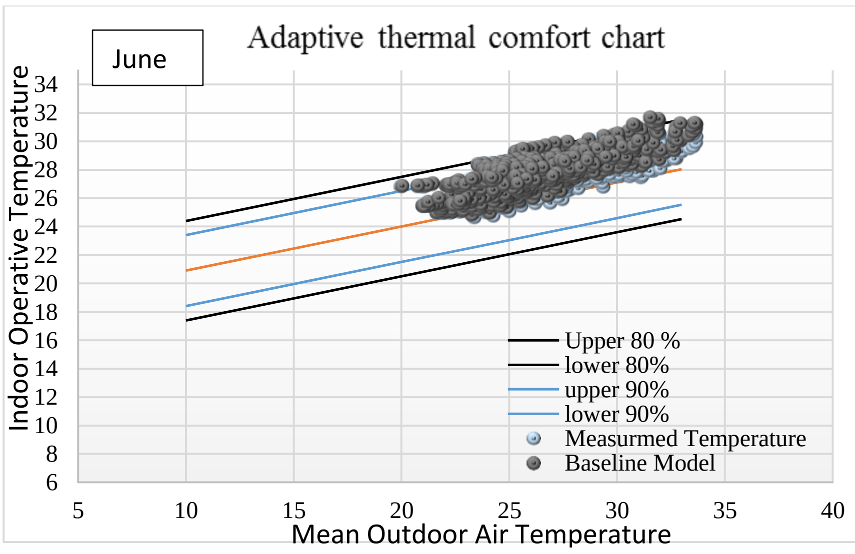

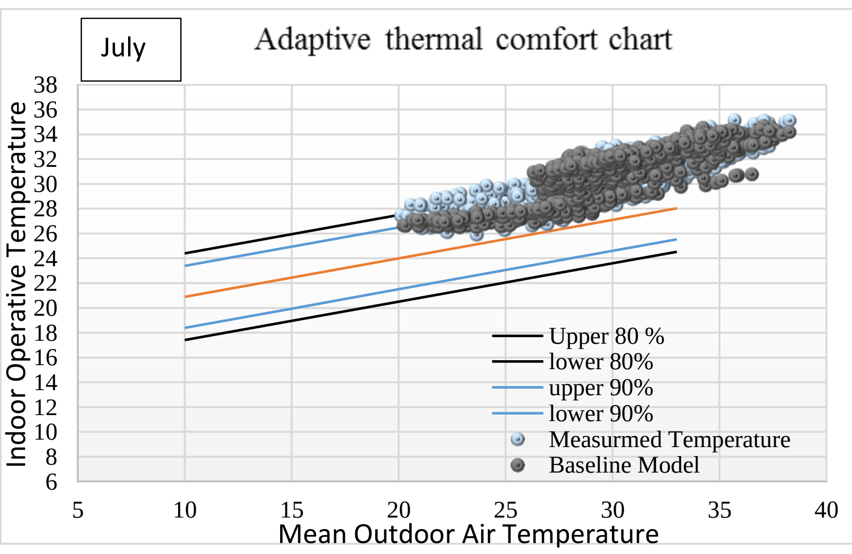

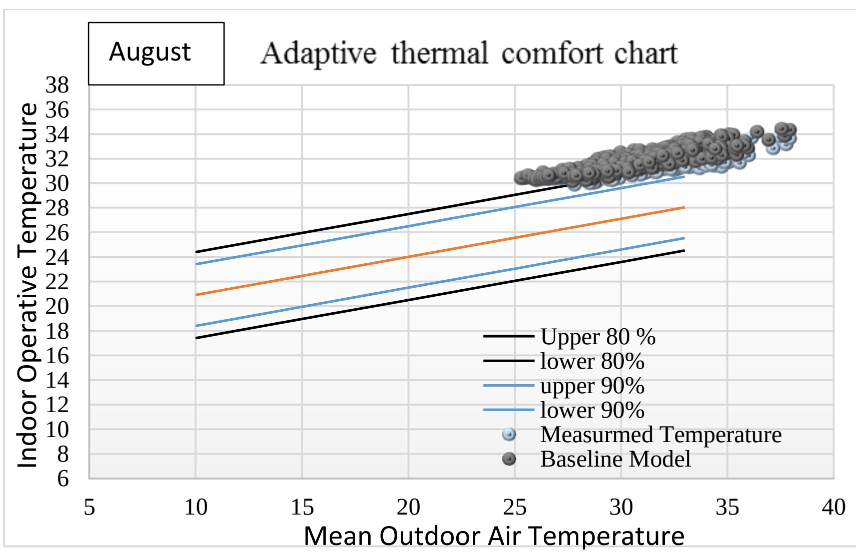

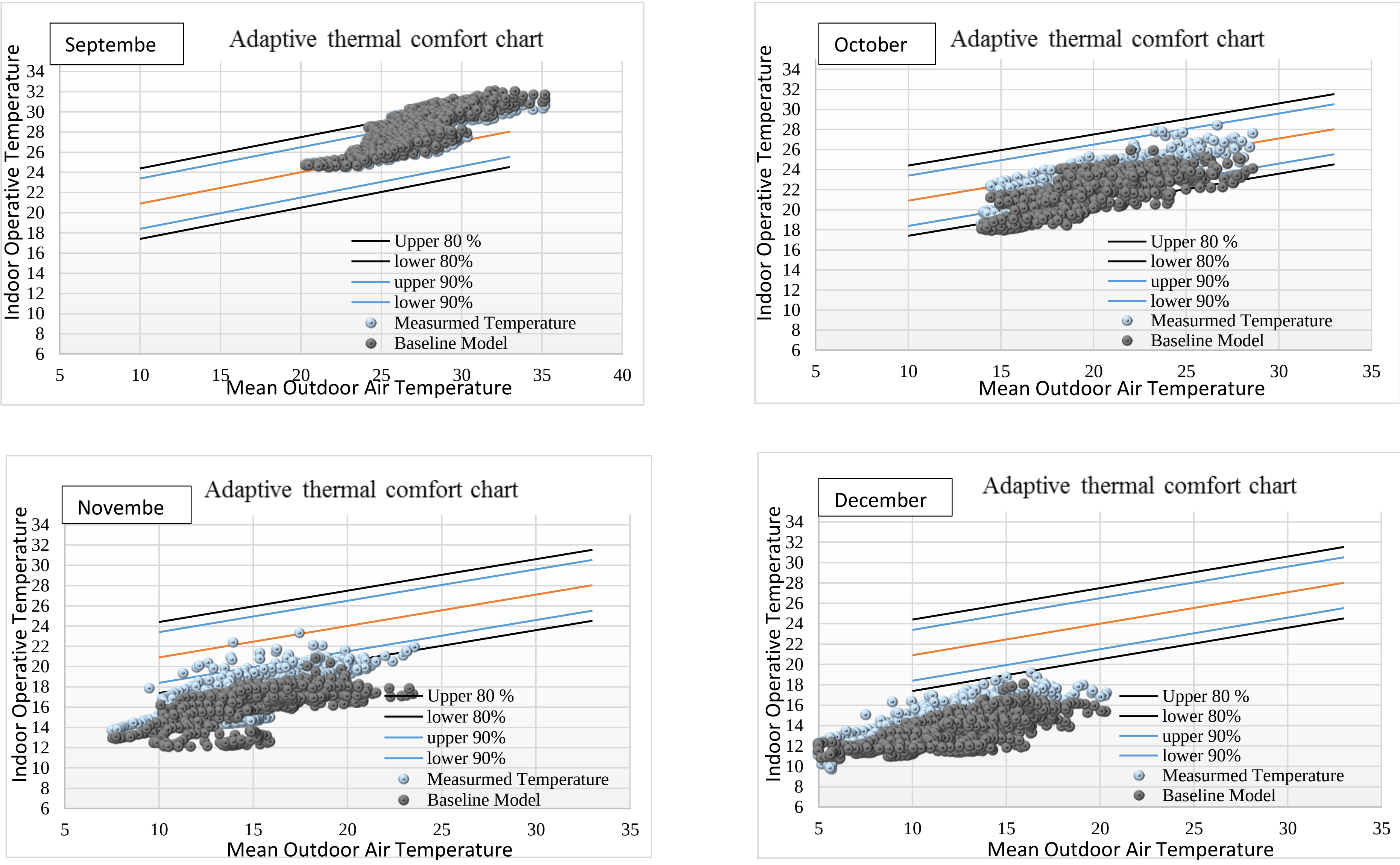

Figure A.1. Comparative between Baseline model with real model measured data.

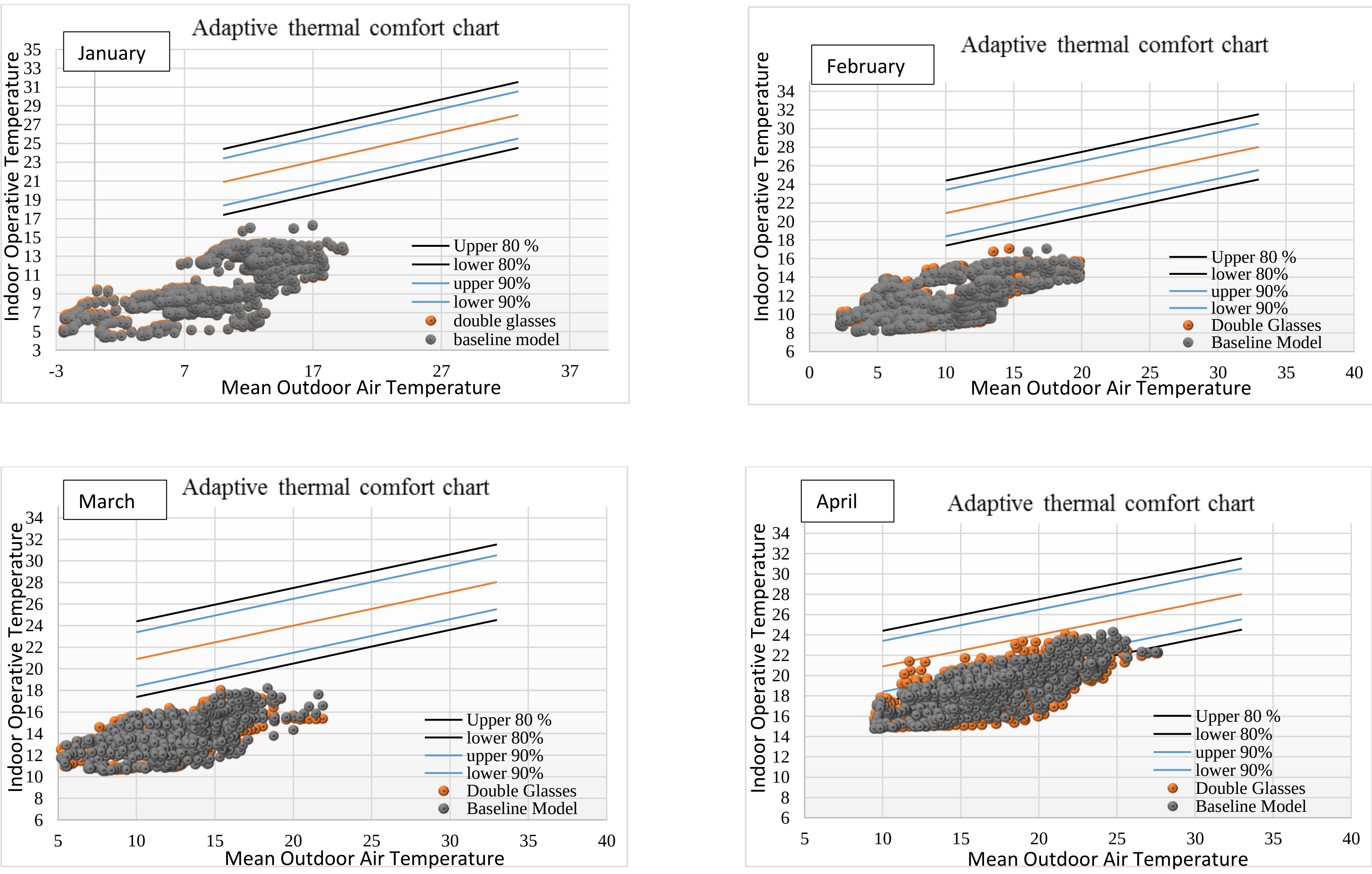

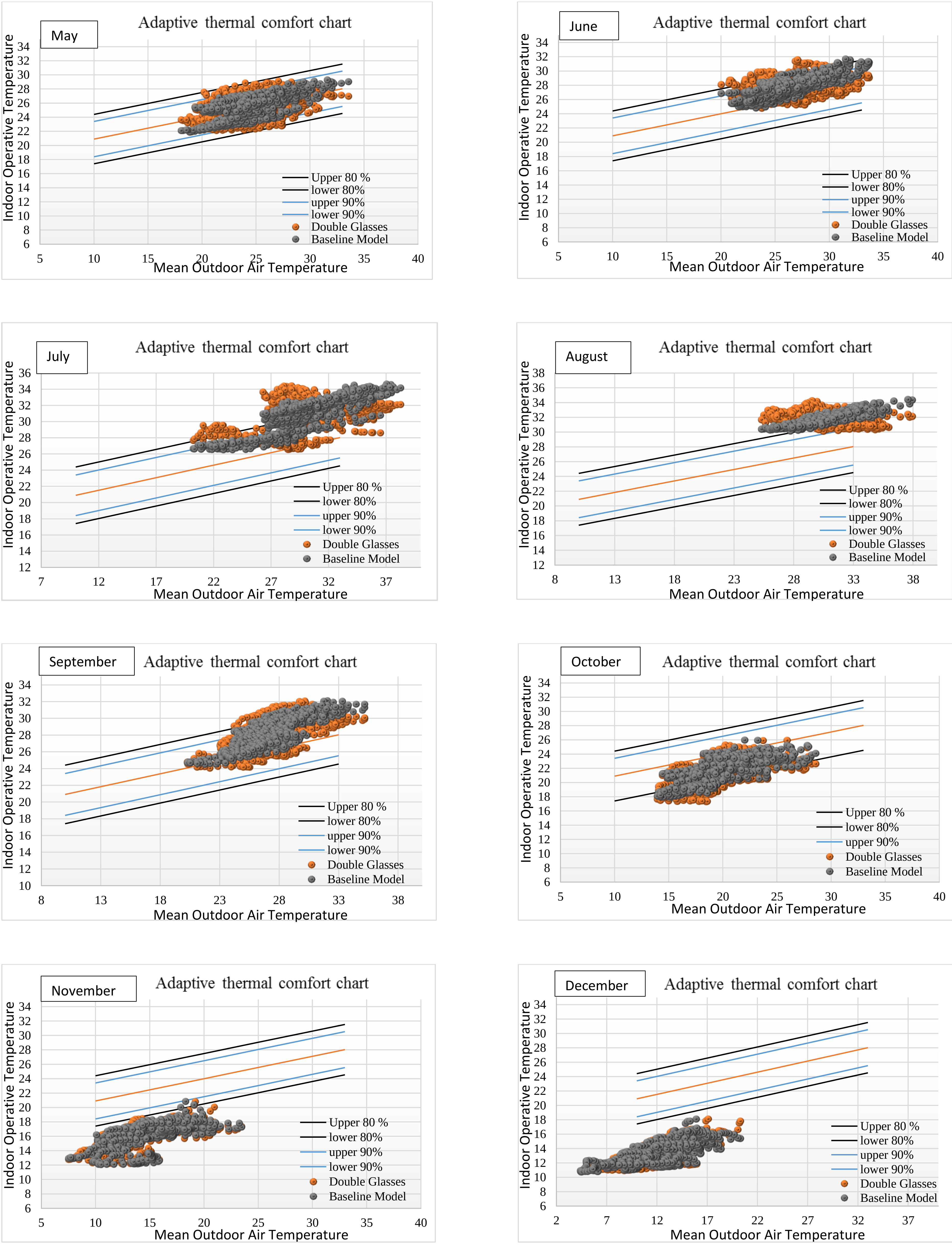

Figure A.2. Comparative between Baseline model with windows double glasses.

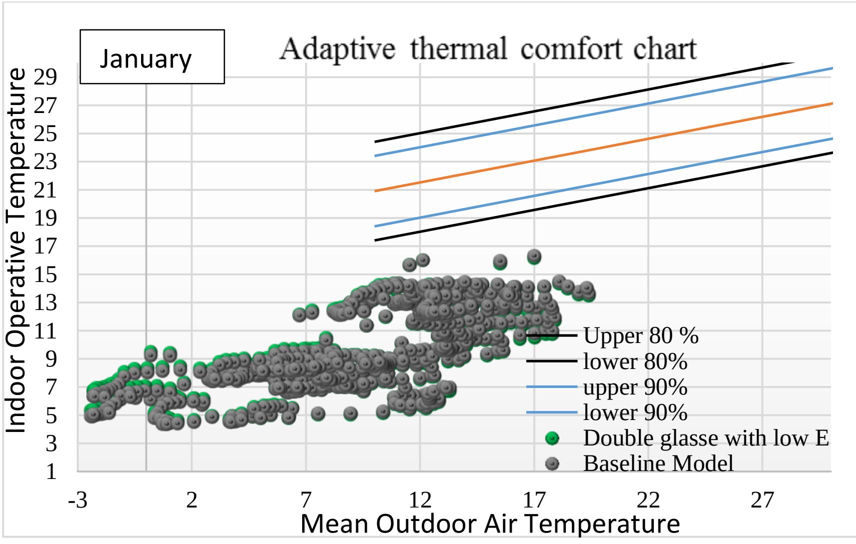
January
Adaptive thermal comfort chart
Indoor Operative Temperature
Mean Outdoor Air Temperature
Upper 80 %
lower 80%
upper 90%
lower 90%
Double glasse with low E
Baseline Model

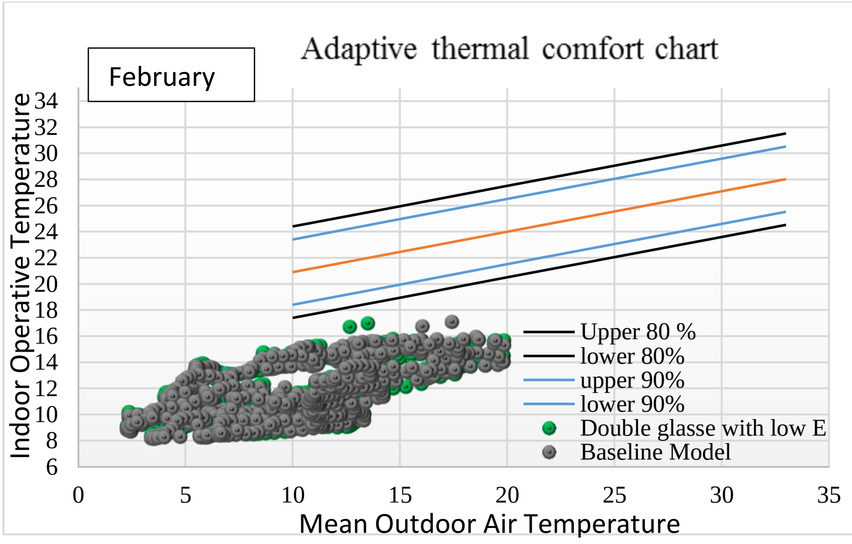
February
Adaptive thermal comfort chart
Indoor Operative Temperature
Mean Outdoor Air Temperature
Upper 80 %
lower 80%
upper 90%
lower 90%
Double glasse with low E
Baseline Model

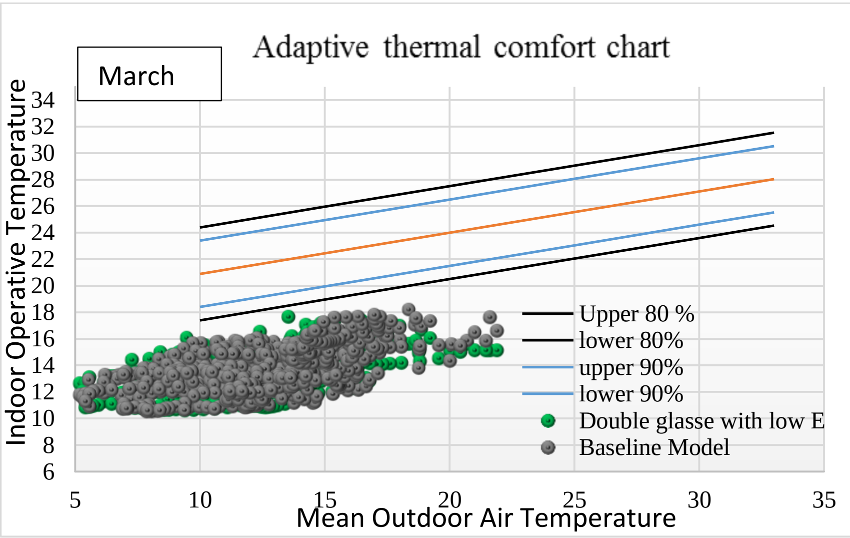
March
Adaptive thermal comfort chart
Indoor Operative Temperature
Mean Outdoor Air Temperature
Upper 80 %
lower 80%
upper 90%
lower 90%
Double glasse with low E
Baseline Model

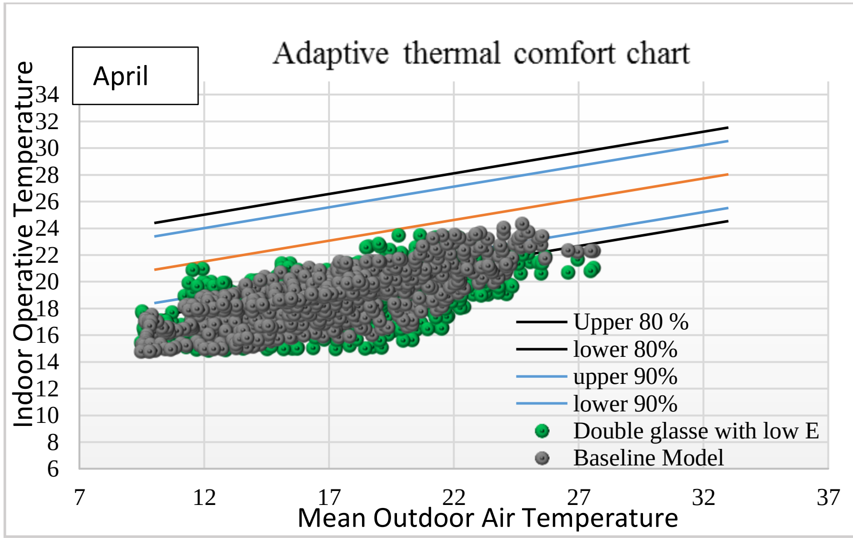
April
Adaptive thermal comfort chart
Indoor Operative Temperature
Mean Outdoor Air Temperature
Upper 80 %
lower 80%
upper 90%
lower 90%
Double glasse with low E
Baseline Model

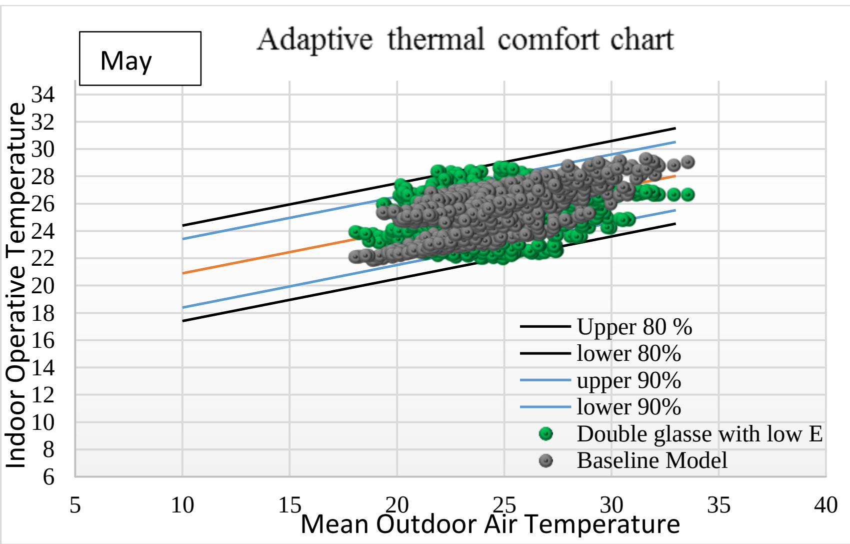
May
Adaptive thermal comfort chart
Indoor Operative Temperature
Mean Outdoor Air Temperature
Upper 80 %
lower 80%
upper 90%
lower 90%
Double glasse with low E
Baseline Model

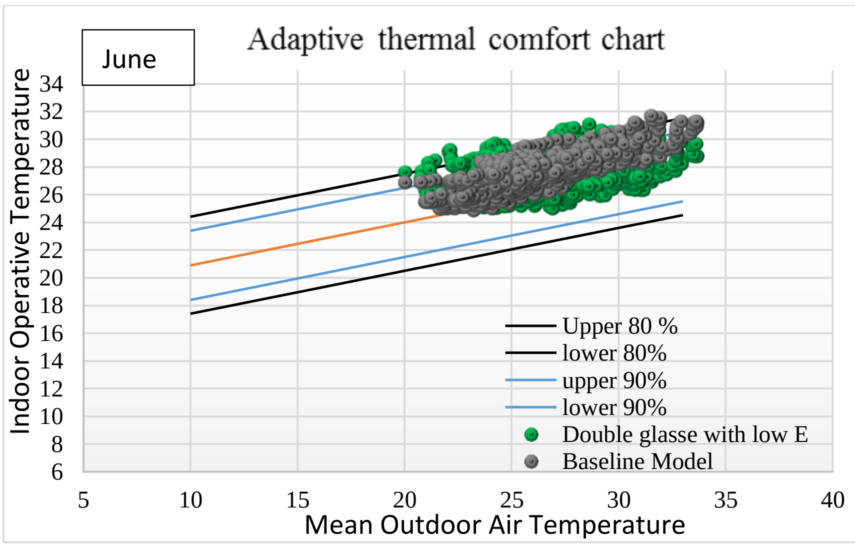
June
Adaptive thermal comfort chart
Indoor Operative Temperature
Mean Outdoor Air Temperature
Upper 80 %
lower 80%
upper 90%
lower 90%
Double glasse with low E
Baseline Model

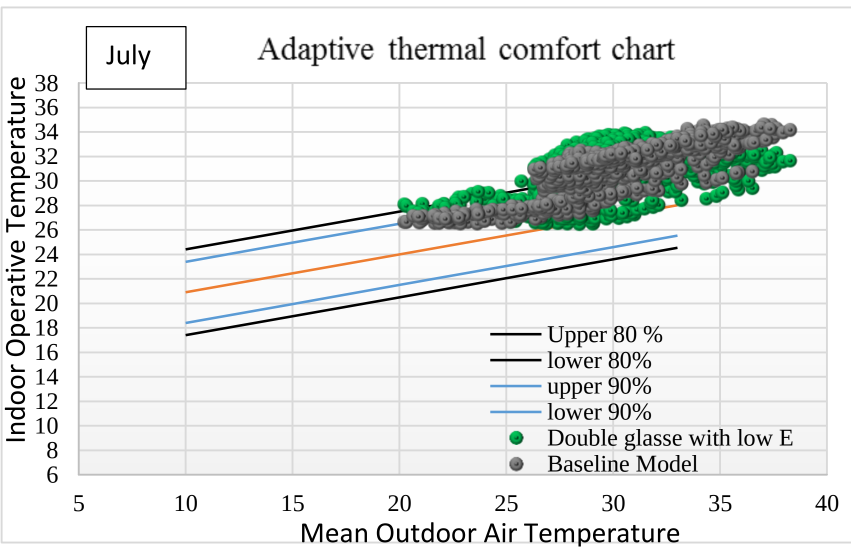
July
Adaptive thermal comfort chart
Indoor Operative Temperature
Mean Outdoor Air Temperature
Upper 80 %
lower 80%
upper 90%
lower 90%
Double glasse with low E
Baseline Model

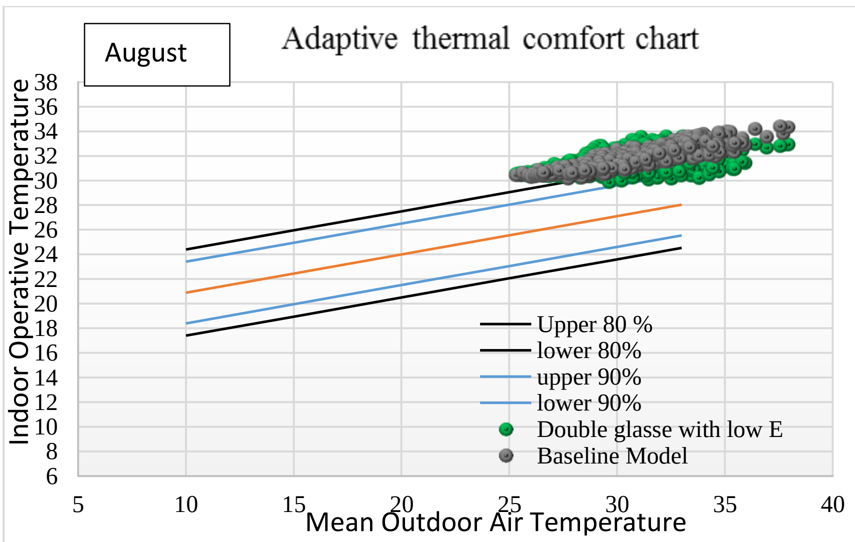
August
Adaptive thermal comfort chart
Indoor Operative Temperature
Mean Outdoor Air Temperature
Upper 80 %
lower 80%
upper 90%
lower 90%
Double glasse with low E
Baseline Model

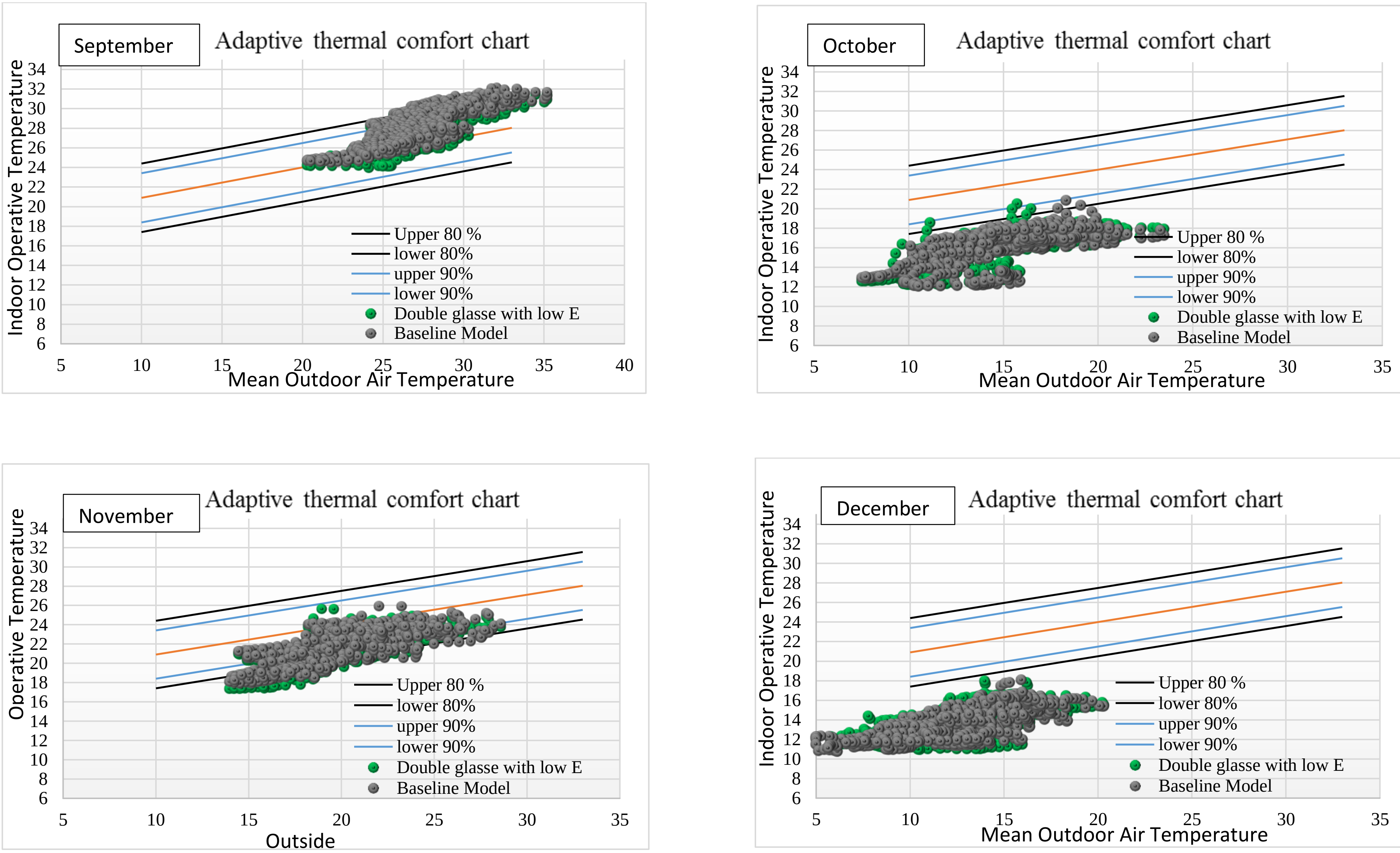

Figure A.3. Comparative between Baseline model with double low Emissivity Glasses.

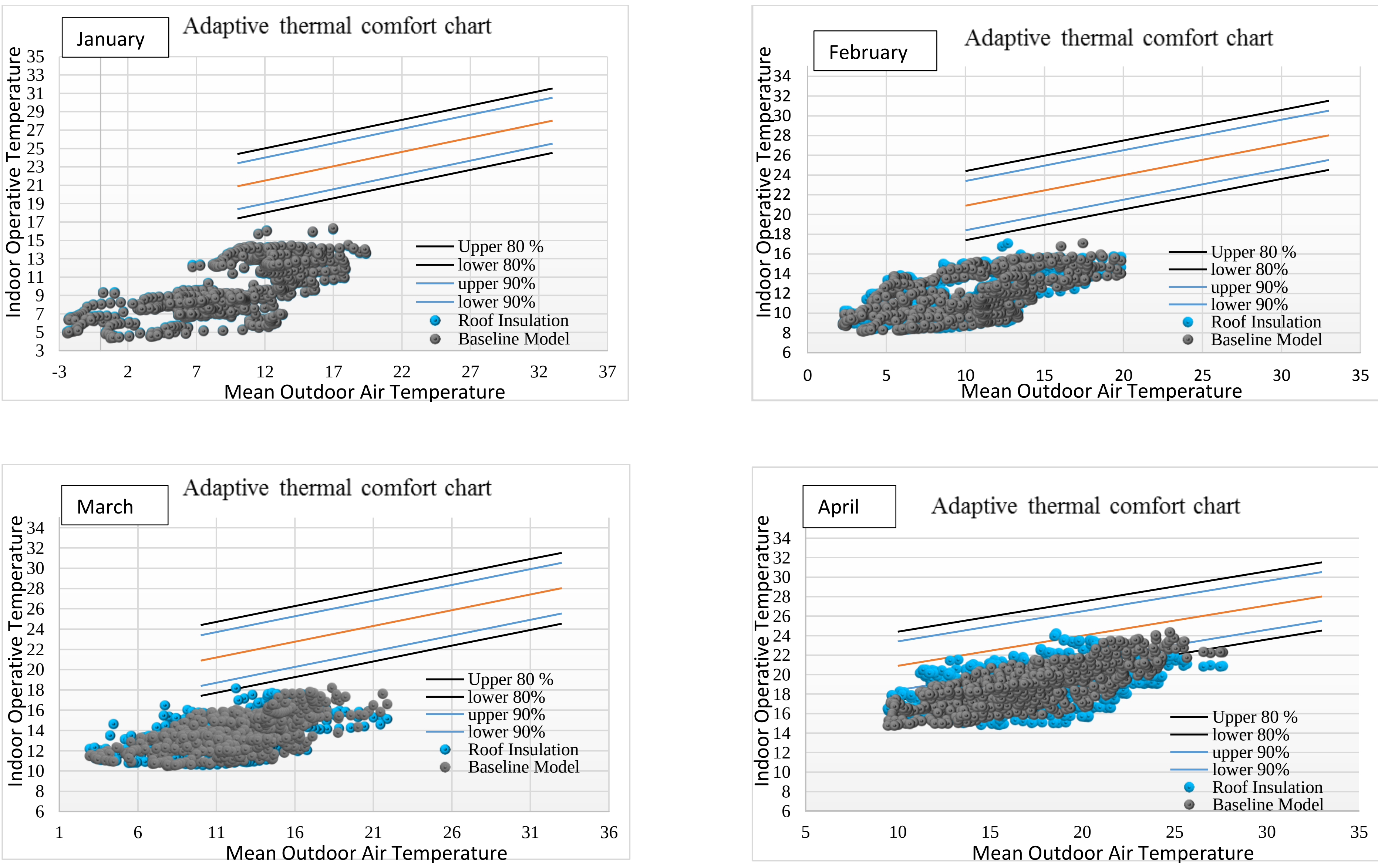

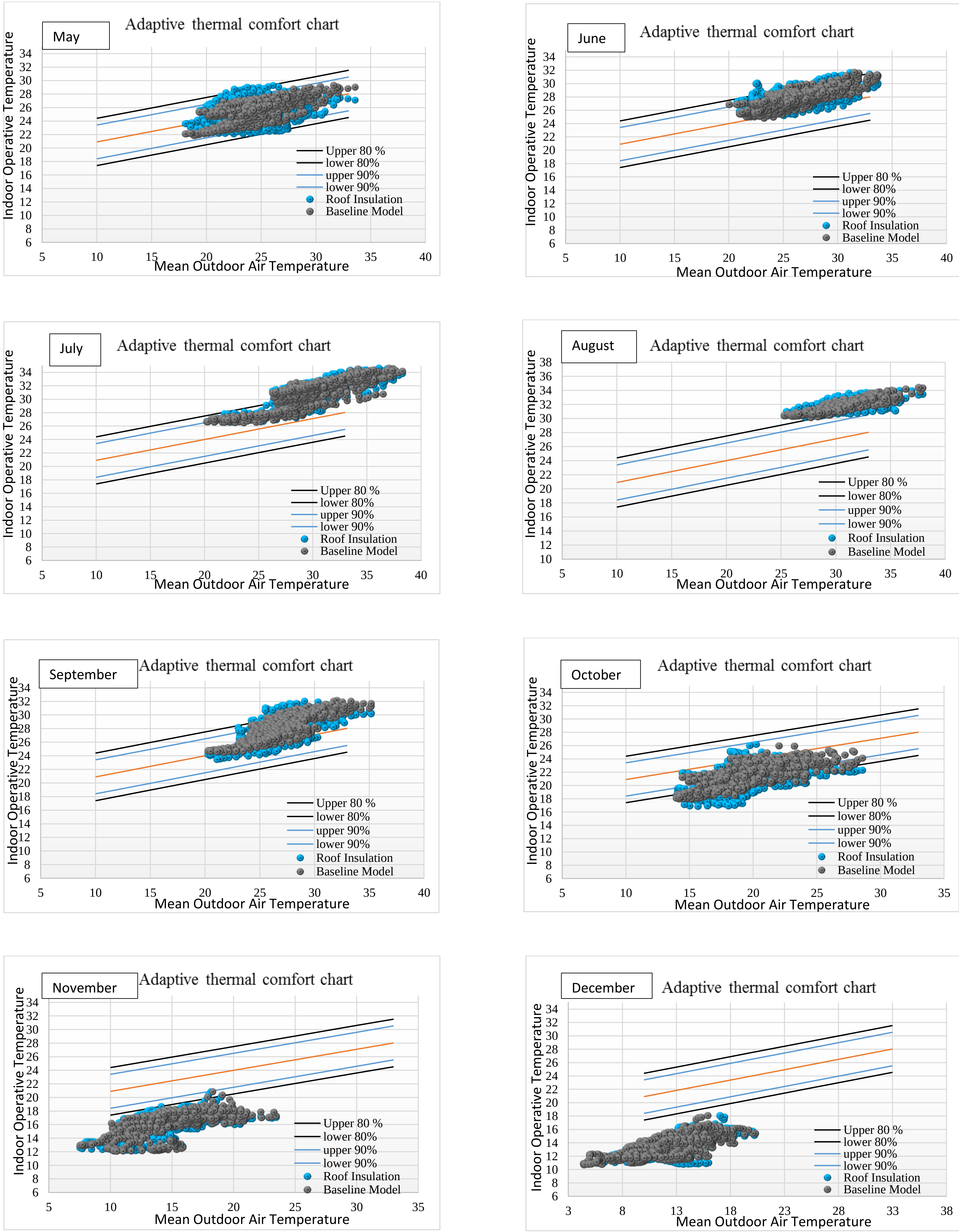

Figure A.4. Comparative between Baseline model with the Roof Insulation.

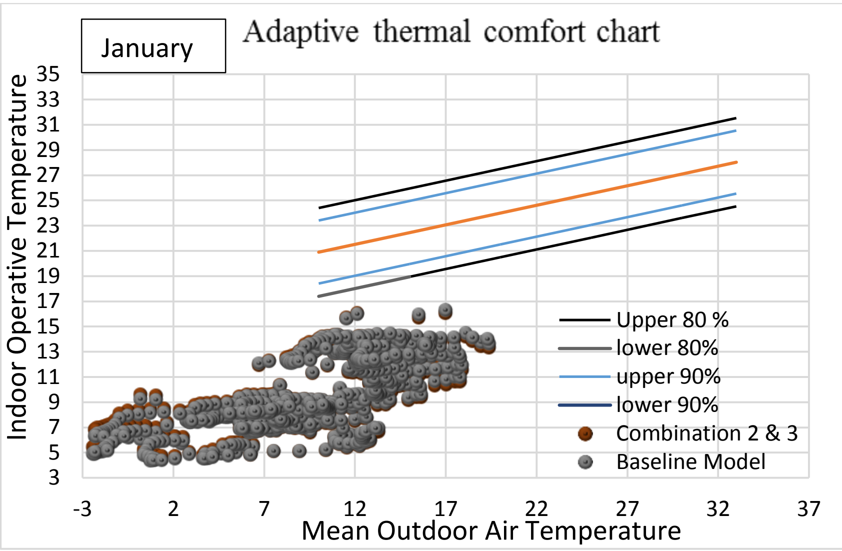
January
Adaptive thermal comfort chart
Indoor Operative Temperature
Mean Outdoor Air Temperature
Upper 80 %
lower 80%
upper 90%
lower 90%
Combination 2 & 3
Baseline Model

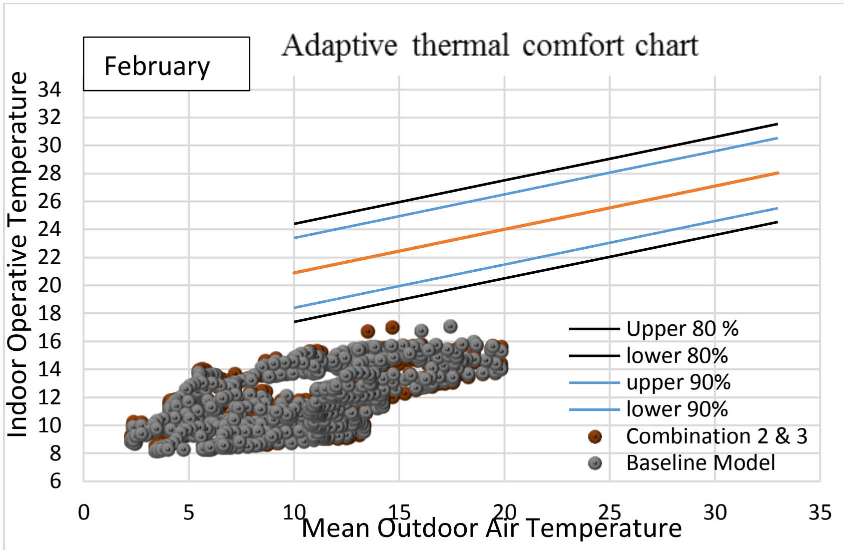
February
Adaptive thermal comfort chart
Indoor Operative Temperature
Mean Outdoor Air Temperature
Upper 80 %
lower 80%
upper 90%
lower 90%
Combination 2 & 3
Baseline Model

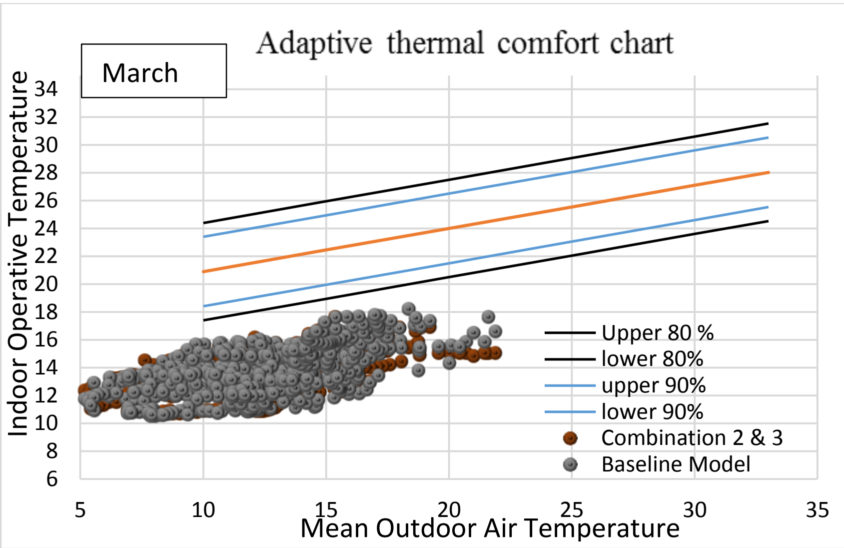
March
Adaptive thermal comfort chart
Indoor Operative Temperature
Mean Outdoor Air Temperature
Upper 80 %
lower 80%
upper 90%
lower 90%
Combination 2 & 3
Baseline Model

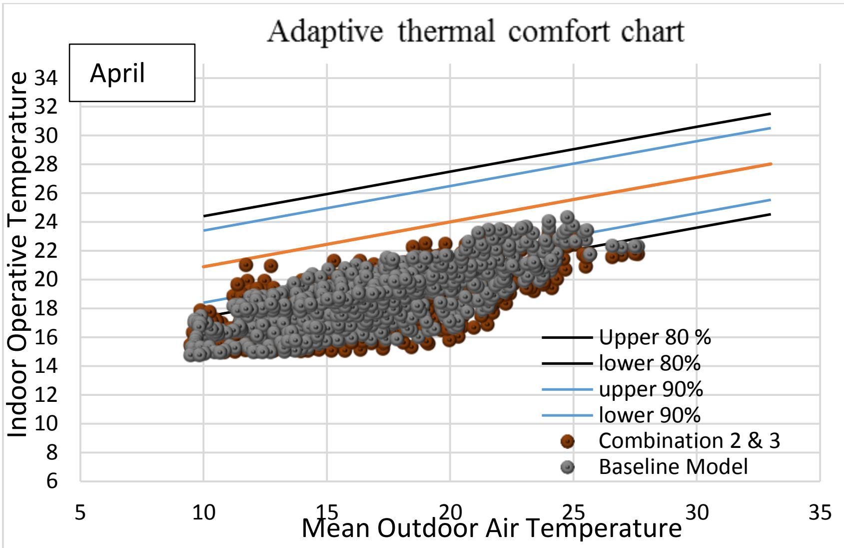
April
Adaptive thermal comfort chart
Indoor Operative Temperature
Mean Outdoor Air Temperature
Upper 80 %
lower 80%
upper 90%
lower 90%
Combination 2 & 3
Baseline Model

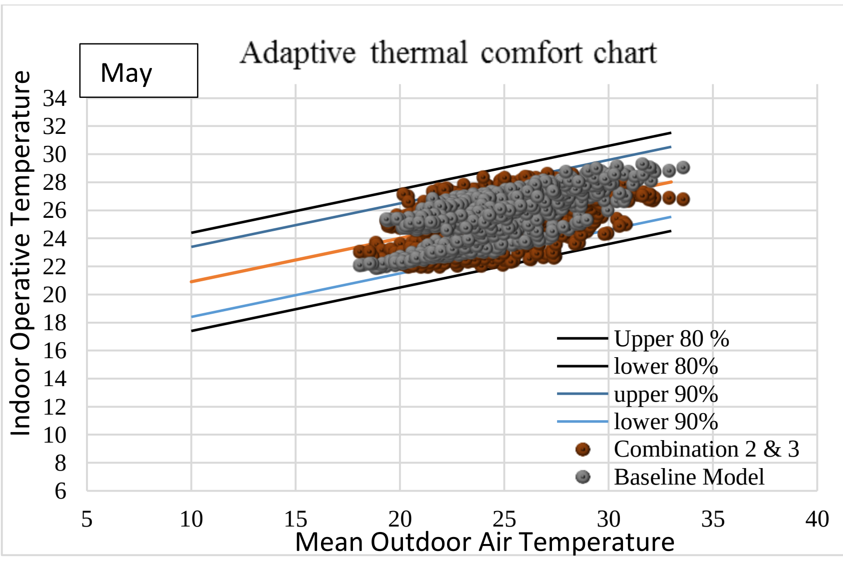
May
Adaptive thermal comfort chart
Indoor Operative Temperature
Mean Outdoor Air Temperature
Upper 80 %
lower 80%
upper 90%
lower 90%
Combination 2 & 3
Baseline Model

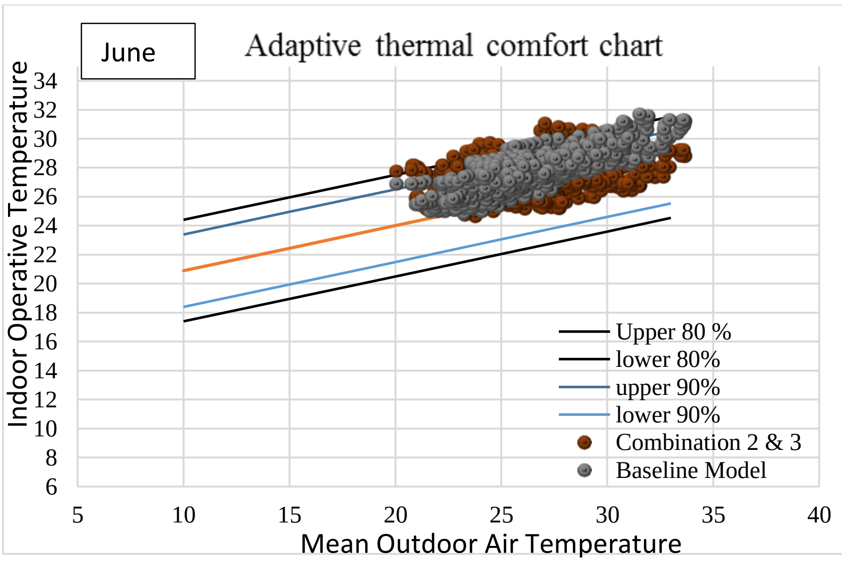
June
Adaptive thermal comfort chart
Indoor Operative Temperature
Mean Outdoor Air Temperature
Upper 80 %
lower 80%
upper 90%
lower 90%
Combination 2 & 3
Baseline Model

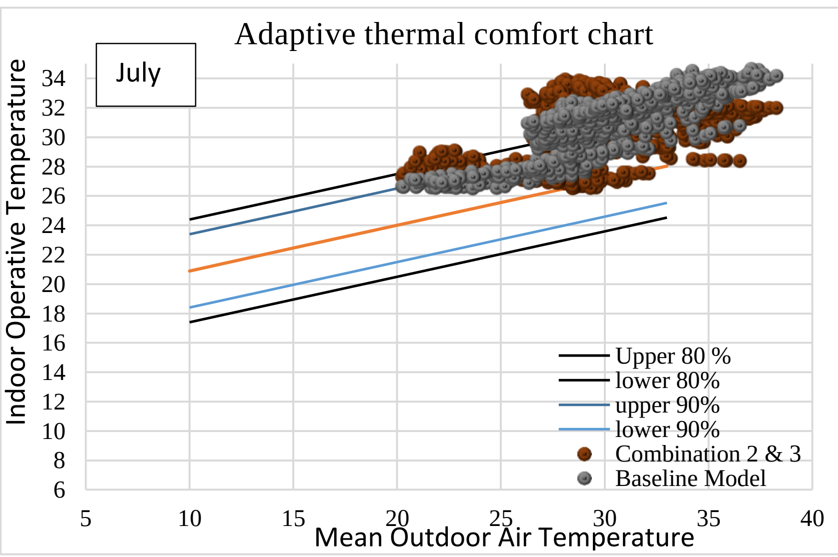
July
Adaptive thermal comfort chart
Indoor Operative Temperature
Mean Outdoor Air Temperature
Upper 80 %
lower 80%
upper 90%
lower 90%
Combination 2 & 3
Baseline Model

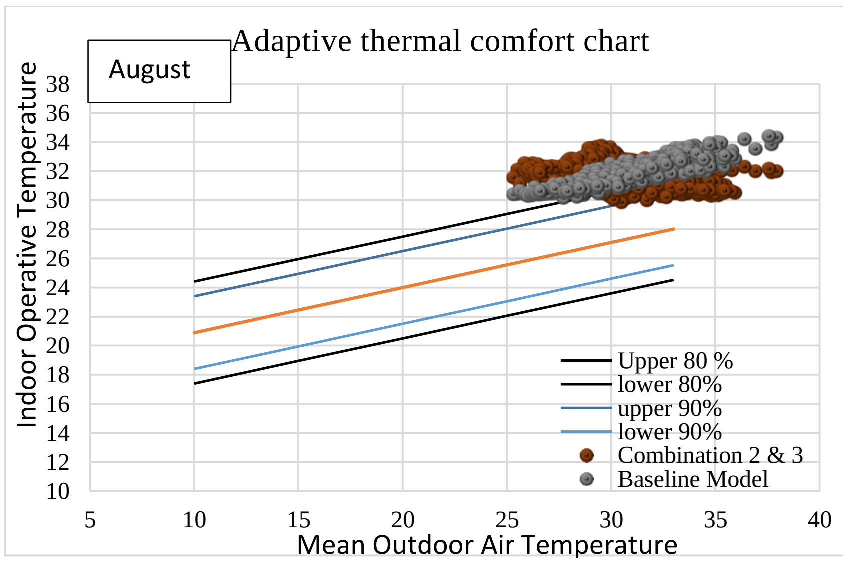
August
Adaptive thermal comfort chart
Indoor Operative Temperature
Mean Outdoor Air Temperature
Upper 80 %
lower 80%
upper 90%
lower 90%
Combination 2 & 3
Baseline Model

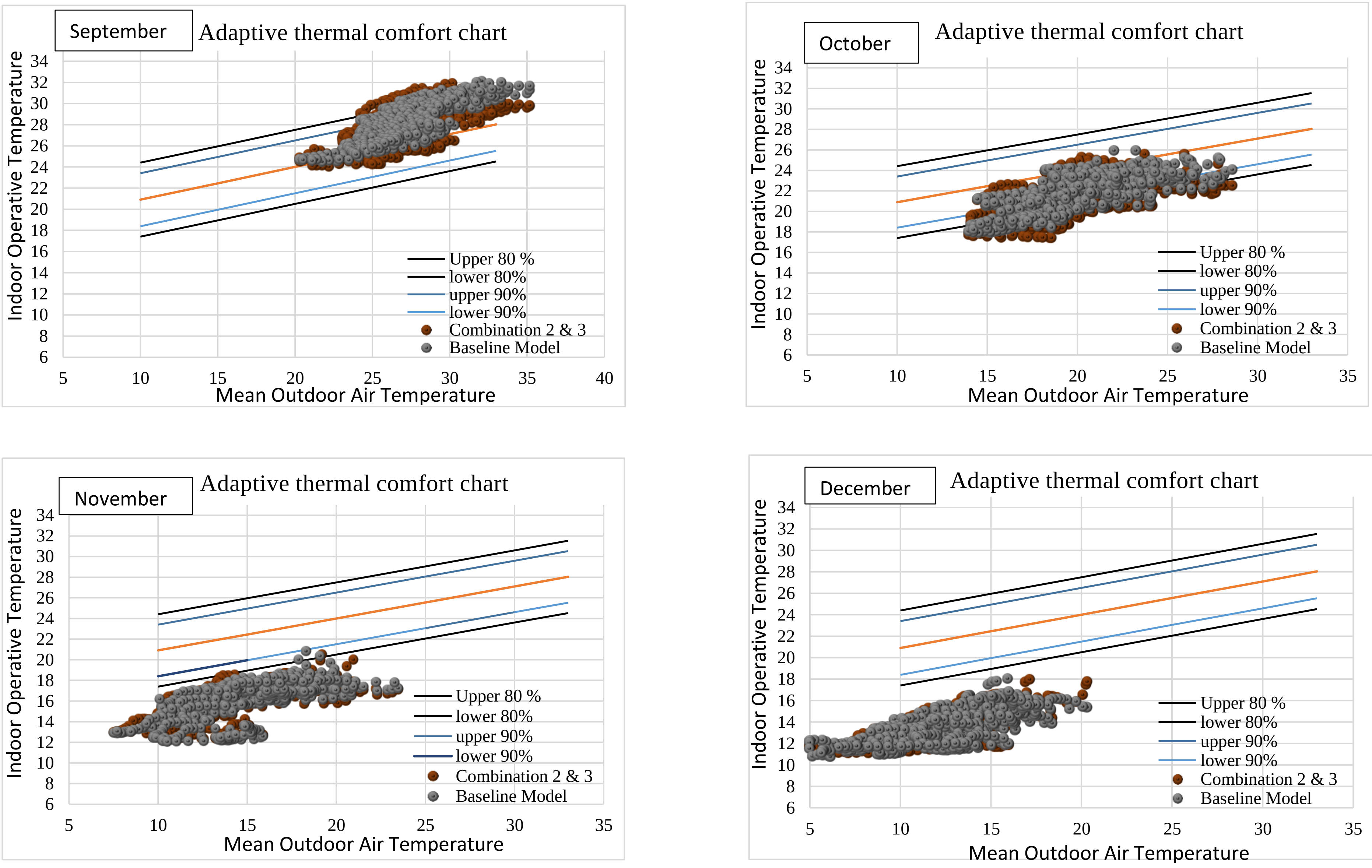

Figure A.5. Comparative between Baseline model with combination of Double Glasses with low-Emissivity and Roof Insulation.

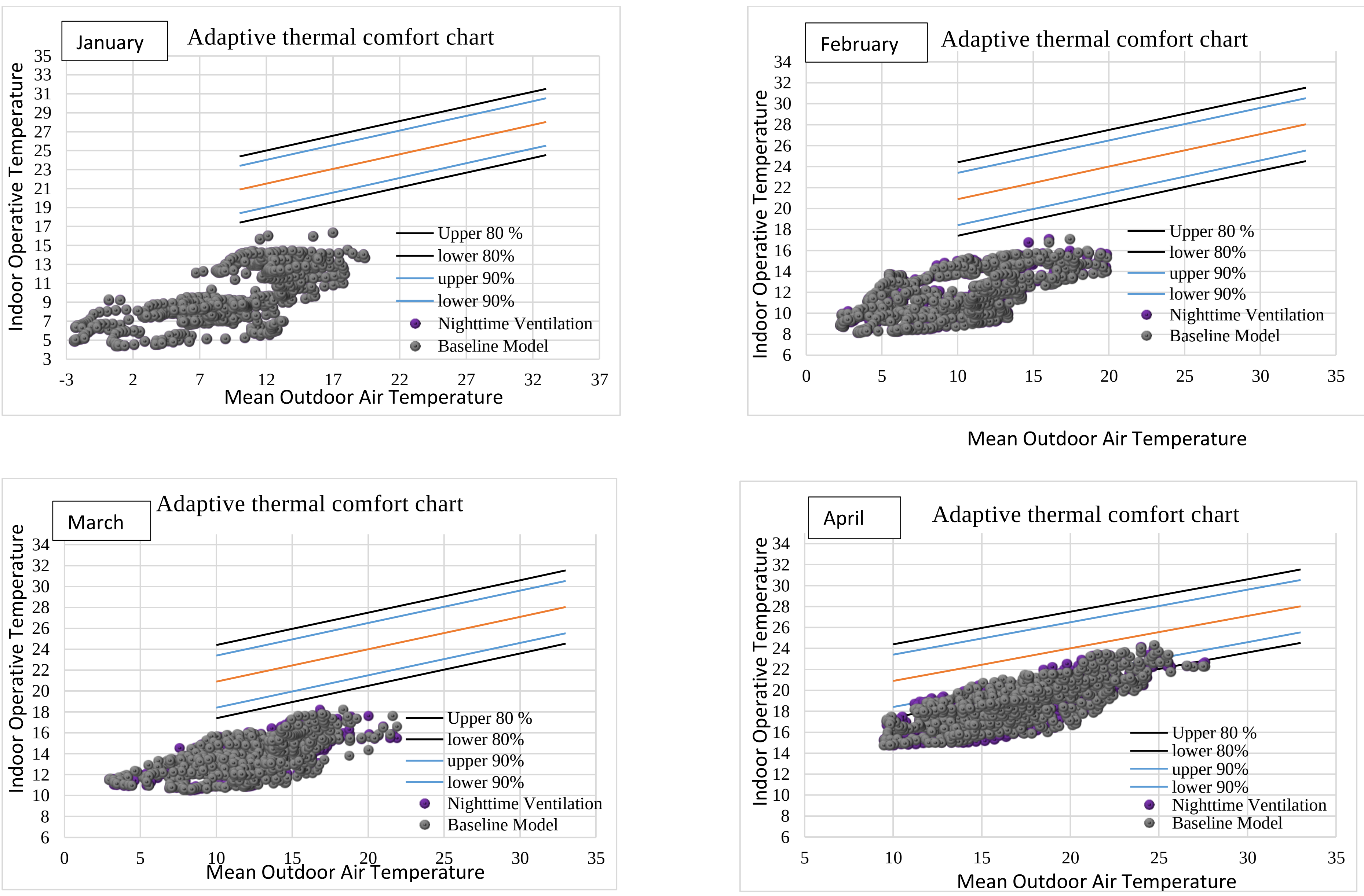

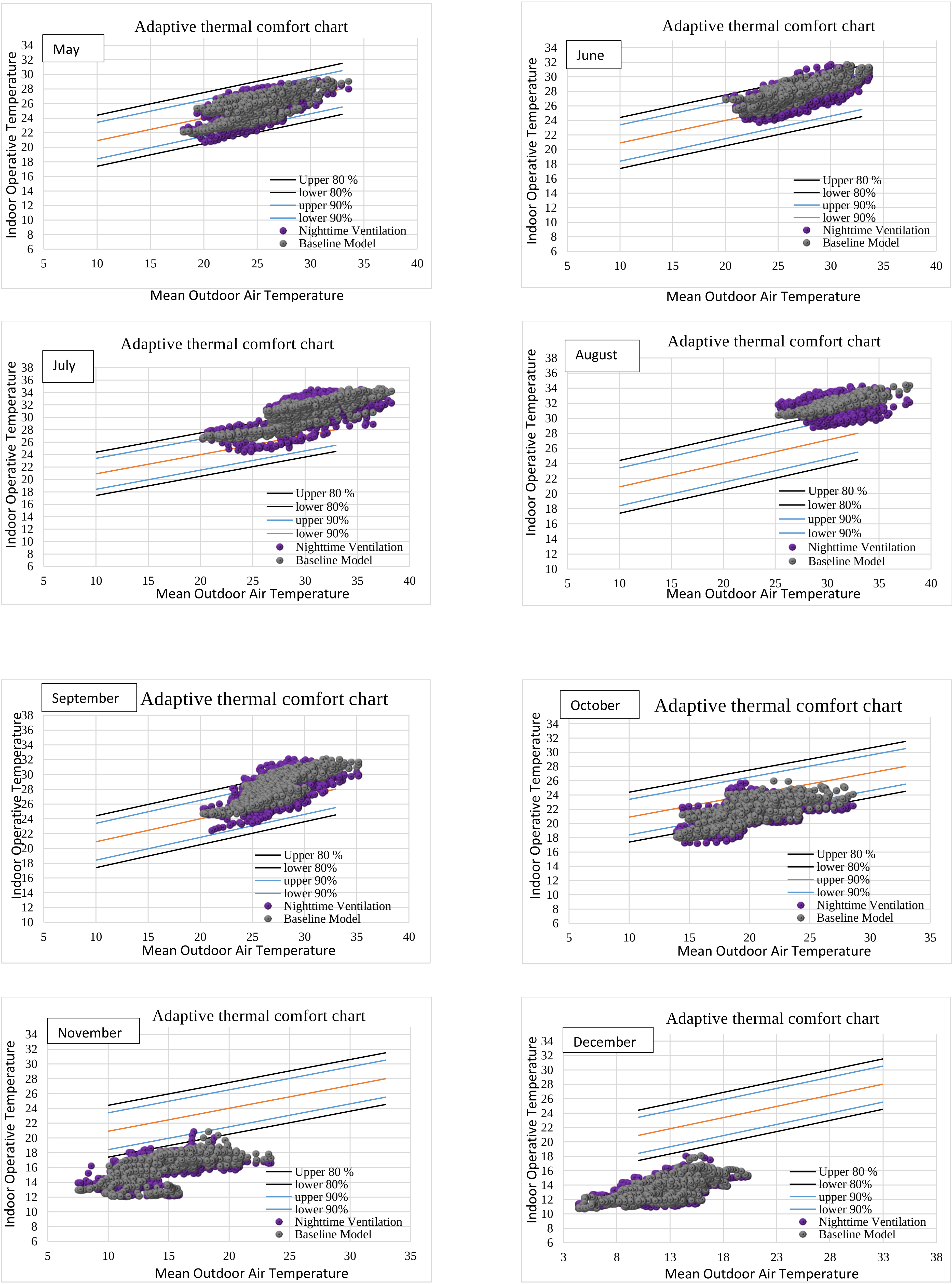

Figure A.6. Comparative between Baseline model with Nighttime Ventilation.

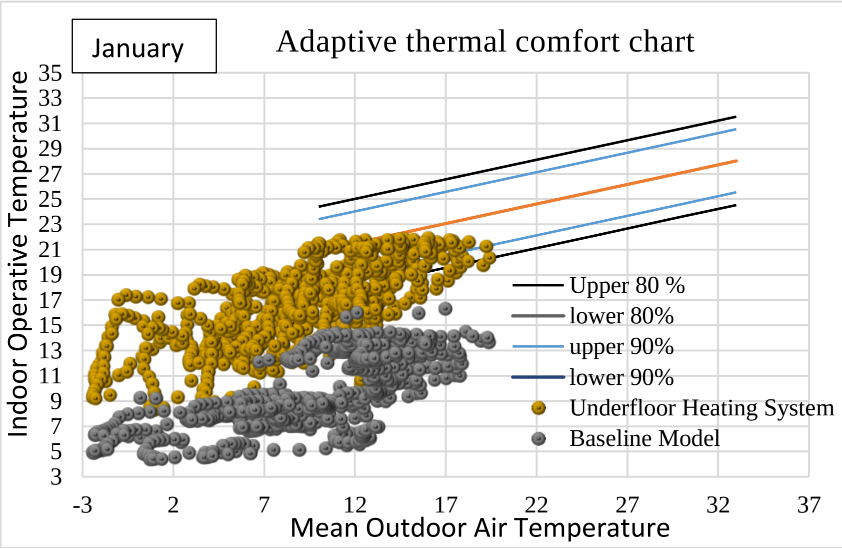
January
Adaptive thermal comfort chart
Indoor Operative Temperature
Mean Outdoor Air Temperature
Upper 80 %
lower 80%
upper 90%
lower 90%
Underfloor Heating System
Baseline Model

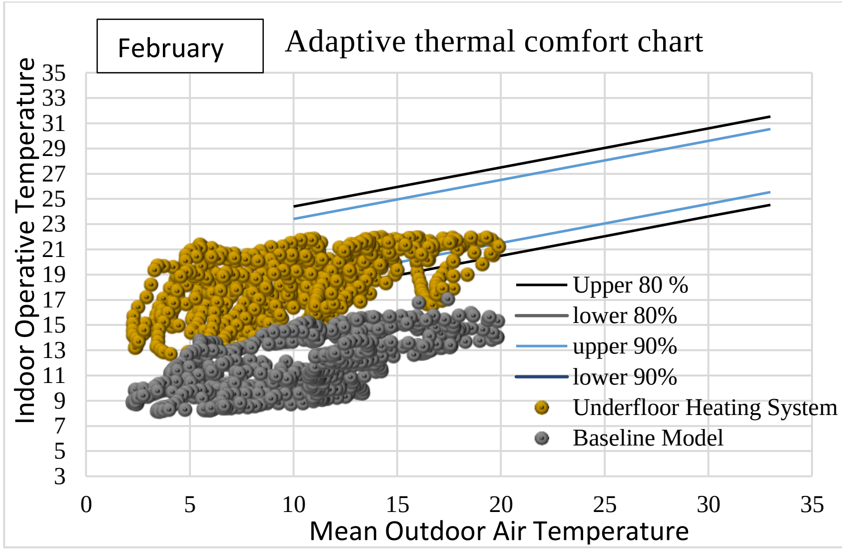
February
Adaptive thermal comfort chart
Indoor Operative Temperature
Mean Outdoor Air Temperature
Upper 80 %
lower 80%
upper 90%
lower 90%
Underfloor Heating System
Baseline Model

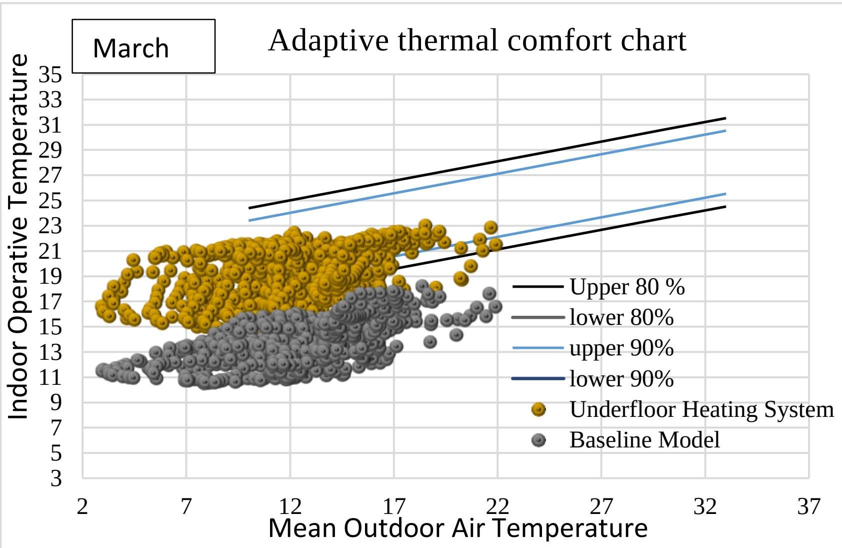
March
Adaptive thermal comfort chart
Indoor Operative Temperature
Mean Outdoor Air Temperature
Upper 80 %
lower 80%
upper 90%
lower 90%
Underfloor Heating System
Baseline Model

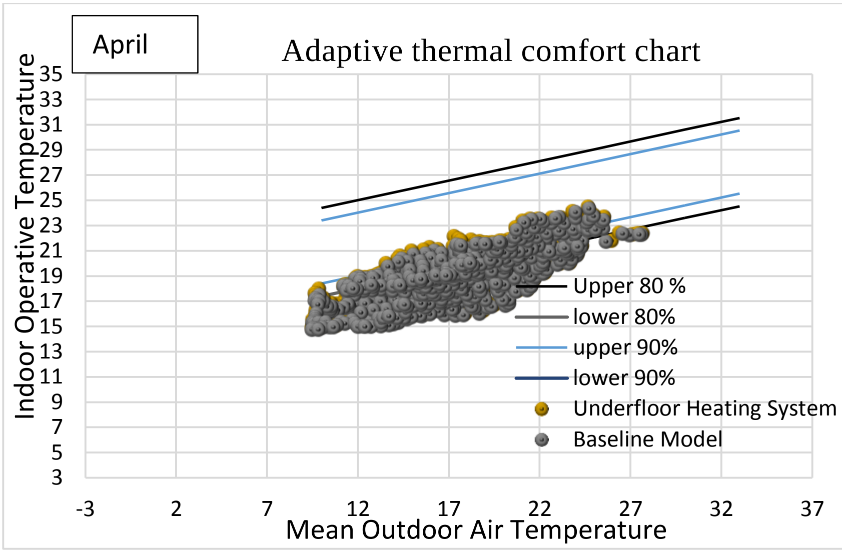
April
Adaptive thermal comfort chart
Indoor Operative Temperature
Mean Outdoor Air Temperature
Upper 80 %
lower 80%
upper 90%
lower 90%
Underfloor Heating System
Baseline Model

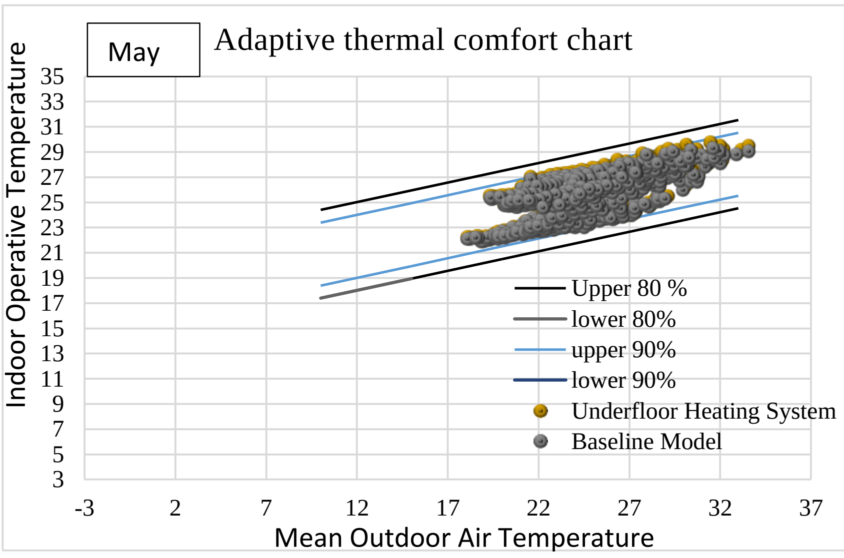
May
Adaptive thermal comfort chart
Indoor Operative Temperature
Mean Outdoor Air Temperature
Upper 80 %
lower 80%
upper 90%
lower 90%
Underfloor Heating System
Baseline Model

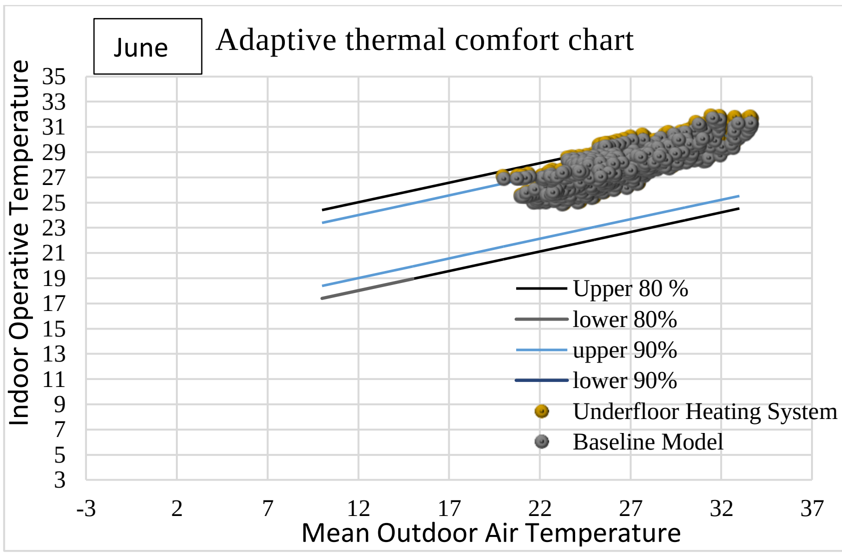
June
Adaptive thermal comfort chart
Indoor Operative Temperature
Mean Outdoor Air Temperature
Upper 80 %
lower 80%
upper 90%
lower 90%
Underfloor Heating System
Baseline Model

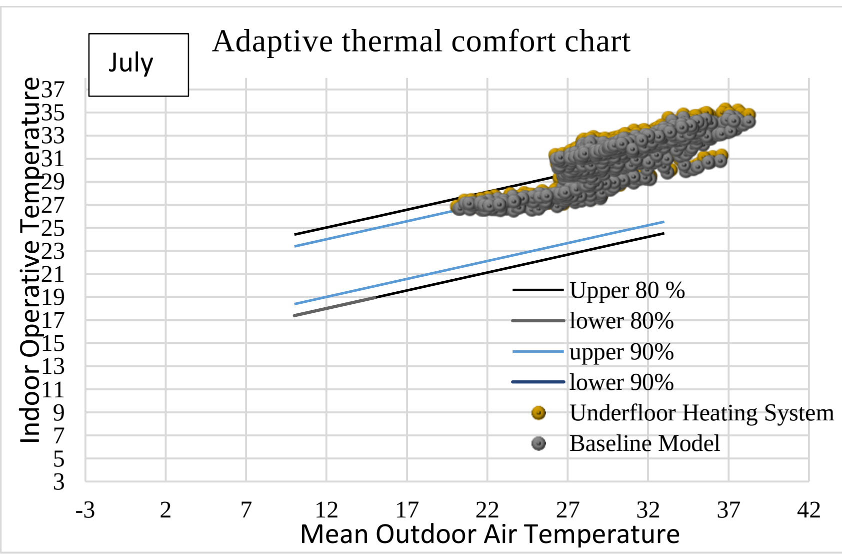
July
Adaptive thermal comfort chart
Indoor Operative Temperature
Mean Outdoor Air Temperature
Upper 80 %
lower 80%
upper 90%
lower 90%
Underfloor Heating System
Baseline Model

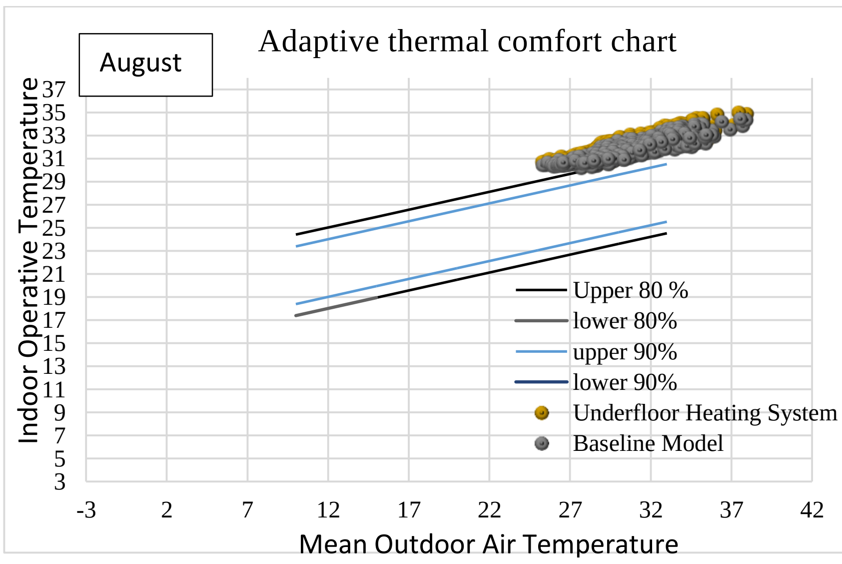
August
Adaptive thermal comfort chart
Indoor Operative Temperature
Mean Outdoor Air Temperature
Upper 80 %
lower 80%
upper 90%
lower 90%
Underfloor Heating System
Baseline Model

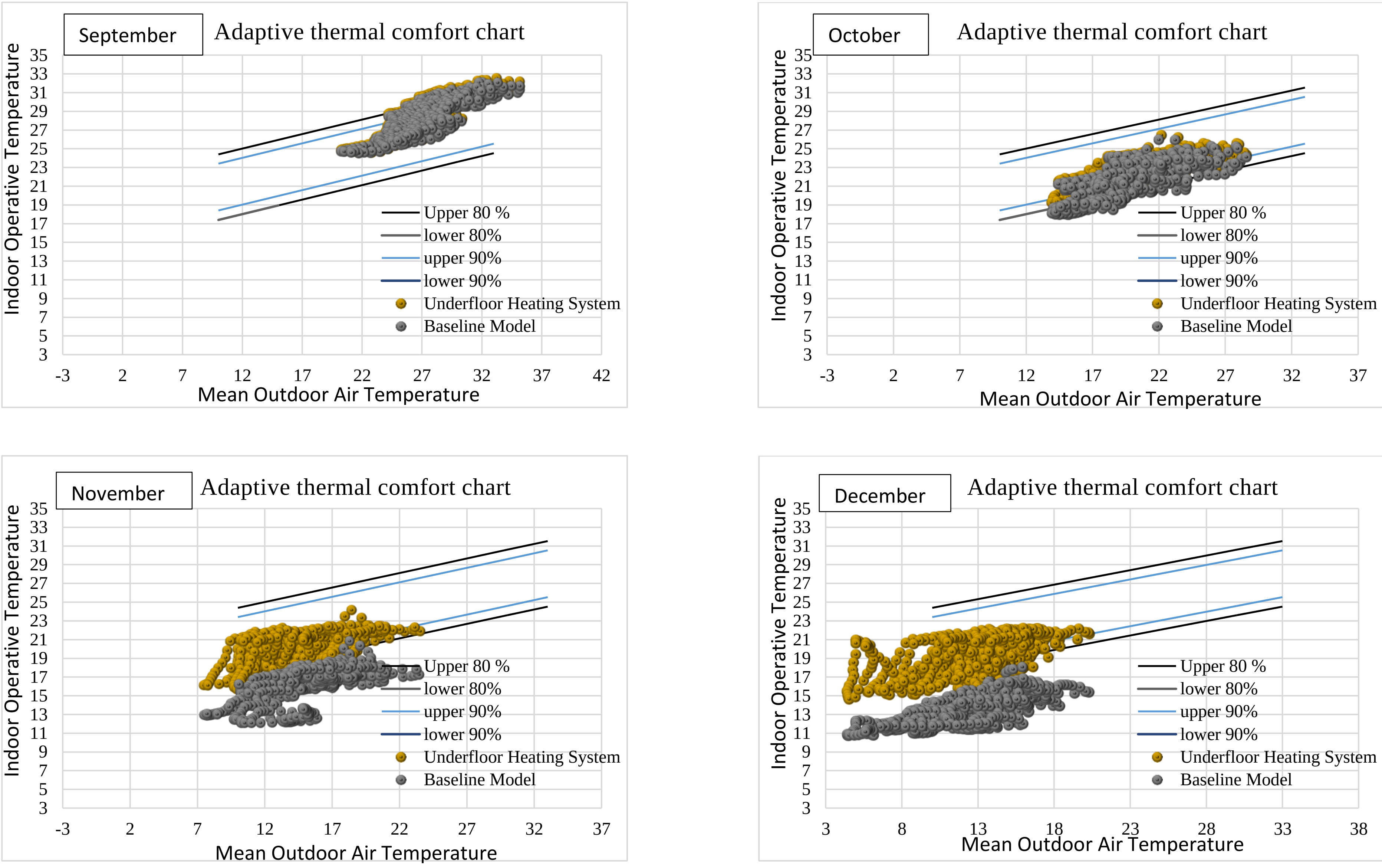

Figure A.7. Comparative between Baseline model with underfloor heating system.

APPENDIX B

MONTHLY AVERAGE, MINIMUM AND MAXIMUM INDOOR TEMPERATURES AND RELATIVE HUMIDITY

In this section instant maximum, instant minimum and monthly average temperatures and relative humidity, are listed on Table B.1 and B.2. These values are strained from the data sheets.

Table B.1. Maximum, minimum and average values of the indoor temperature of the zones.

Main Prayer Area			
Month	Max	Min	Ava
October	28.77	18.94	23.46
November	23.66	14.05	18.37
December	19.54	10.06	15.24
January	18.84	4.90	11.29
February	19.36	7.80	12.36
March	20.81	12.28	14.86
April	22.66	13.61	18.11
May	29.79	22.08	25.84
June	32.02	23.73	27.69
July	35.47	26.24	31.07
August	35.94	27.73	31.61
September	34.15	24.17	28.66

Corridor First Floor			
Month	Max	Min	Ava
October	26.47	18.09	22.25
November	21.36	12.98	17.19
December	19.08	9.61	14.57
January	17.95	3.38	10.37
February	18.58	6.75	11.61
March	19.84	11.15	14.15
April	24.05	13.12	17.91
May	30.73	20.86	25.37
June	32.25	23.63	26.91
July	36.53	26.32	30.65
August	35.81	28.22	31.32
September	33.71	24.16	28.15

Women prayer area			
Month	Max	Min	Ava
October	26.43	18.94	23.20
November	21.39	13.90	18.01
December	18.26	10.10	14.90
January	17.62	4.81	10.91
February	18.03	7.64	12.10
March	17.69	12.07	14.72
April	23.40	13.39	18.67
May	29.35	22.52	26.28
June	31.46	25.13	28.03
July	35.45	28.57	31.90
August	35.53	27.94	31.83
September	33.37	23.03	28.27

Sub-Main Prayer Area			
Month	Max	Min	Ava
October	25.26	20.68	23.65
November	20.85	16.82	19.31
December	19.22	12.97	16.56
January	15.75	8.56	11.99
February	16.87	10.61	12.87
March	19.62	13.38	15.07
April	20.44	15.21	17.60
May	25.38	20.32	23.61
June	28.09	23.69	26.24
July	32.23	28.49	30.11
August	31.88	29.40	30.67
September	31.18	25.63	28.69

Corridor Basement			
Month	Max	Min	Ava
October	25.04	19.06	22.68
November	20.23	15.64	18.40
December	18.61	11.54	16.11
January	16.56	7.61	11.80
February	17.01	9.31	12.50
March	18.35	12.42	14.64
April	21.00	14.15	17.08
May	26.56	19.63	23.05
June	28.26	22.94	25.66
July	32.08	28.04	29.68
August	32.13	28.31	30.15
September	30.75	24.20	27.84

Table B.2. Maximum, minimum and average values of the relative humidity of the zones.

Main Prayer Area			
Month	Max	Min	Ava
October	64.15	33.36	53.26
November	72.55	41.44	58.41
December	80.28	51.60	69.37
January	81.19	40.86	66.39
February	77.18	46.80	63.38
March	83.03	41.67	65.32
April	73.05	30.52	53.70
May	63.69	18.85	46.14
June	65.86	34.78	50.84
July	62.48	23.03	43.96
August	63.45	20.34	48.59
September	66.47	29.24	53.79

Corridor First Floor			
Month	Max	Min	Ava
October	67.33	39.66	56.81
November	73.87	47.55	61.04
December	82.25	54.28	69.29
January	87.57	45.75	66.85
February	79.75	45.27	63.41
March	76.25	46.02	64.90
April	72.22	32.47	53.81
May	65.36	24.51	49.40
June	67.25	39.48	54.23
July	64.62	29.56	47.43
August	62.11	27.53	51.85
September	68.78	34.95	56.85

Women Prayer Area			
Month	Max	Min	Ava
October	66.31	37.29	54.77
November	78.51	47.54	60.32
December	84.35	55.14	71.50
January	84.10	48.59	68.75
February	79.04	50.24	65.42
March	79.36	45.16	68.81
April	73.24	30.16	54.11
May	62.38	19.61	47.24
June	64.68	35.51	52.12
July	61.44	23.57	44.37
August	62.84	25.35	50.63
September	70.06	34.39	51.53

Sub-Main Prayer Area			
Month	Max	Min	Ava
October	65.40	36.25	54.12
November	71.22	41.56	57.40
December	80.99	47.01	65.41
January	77.42	34.84	61.80
February	79.39	39.91	60.55
March	77.77	41.89	64.19
April	74.31	40.27	55.43
May	67.38	37.86	55.20
June	66.15	42.76	57.70
July	62.23	31.14	49.37
August	61.70	31.54	48.14
September	65.21	42.26	54.59

Corridor Basement			
Month	Max	Min	Ava
October	68.57	35.53	57.54
November	76.75	43.56	60.73
December	82.89	44.09	68.18
January	86.64	34.62	64.96
February	83.11	36.79	63.60
March	80.98	42.33	66.58
April	78.47	32.35	57.64
May	73.40	37.23	57.92
June	75.60	42.66	60.69
July	66.26	29.81	51.72
August	65.30	28.26	55.26
September	70.52	42.97	58.35